

## Response to the review by S. D. Schery

*We wish to thank Stephen Schery for his insightful comments and suggestions and have revised our manuscript as explained below:*

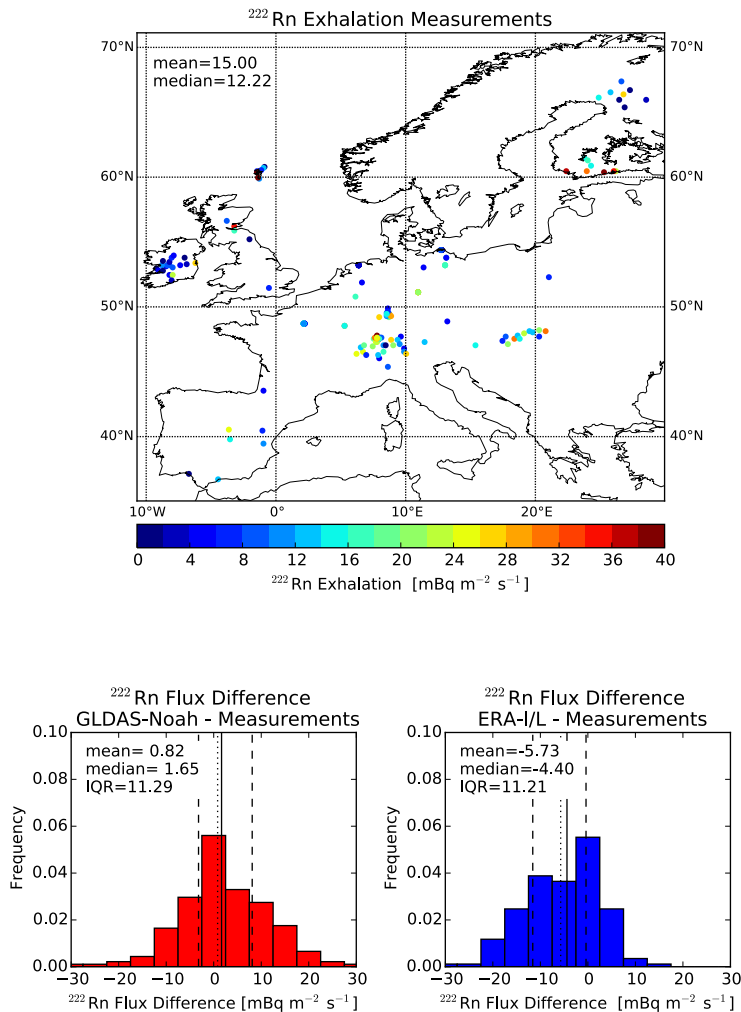
### GENERAL COMMENTS

This is a major new effort modelling radon ( $^{222}\text{Rn}$ ) flux from the soils of Europe. The model incorporates a dependence on such soil properties as radium (uranium) content, moisture content, soil texture, and the depth of the water table. Using geochemical datasets and other strategies to deduce these soil properties, the model is able to make predictions of radon exhalation as a function of position and time period for Europe. Radon exhalation maps for Europe are presented at a resolution of  $0.083^\circ \times 0.083^\circ$  for various periods. Comparisons are made with two previous flux map models (Szegvary et al., Lopez-Coto et al.) plus with actual field point measurements at selected locations. Results seem reasonable and more detailed in time and place than previous efforts. Given the well-recognized need for more complete and accurate maps of radon flux density from the earth's surface it would be difficult to argue against publication of any carefully thought out effort that offers new predictions for Europe using plausible modeling refinements. The present manuscript appears to meet these requirements although there are a few details discussed in my later specific comments that could use some attention. In terms of the "big picture" of modelling radon flux from the earth's surface, if I was forced to point out a limitation of the present manuscript it would be along the following lines. The paper does a fairly good job of presenting various modeling options that are worthy of consideration, including two different models of soil moisture plus those assumptions involved in the production of two previously published modeling predictions by Szegvary et al. and Lopez-Coto et al. However, in the end, due to the lack of suitable, calibrated measurement data for a wide enough area and time period for Europe, the authors, and readers, are left at a little bit of a loss as to which formulation is actually superior for use, for example, in something like global atmospheric transport models. Accurate overall normalization remains a major issue. We are able to make careful comparisons of one model to another, but not between a region-wide model and actual measurement data for the same region. I don't want to single this paper out. This comment applies to much of the published radon flux modeling literature including some of my own! My overall assessment is that this is a valuable paper that should be published after consideration of the comments that follows.

*We agree that in the submitted manuscript we failed to give guidance to the reader, which soil moisture model we think would be best suited to estimate accurate  $^{222}\text{Rn}$  fluxes for Europe. As the reviewer states, the main reason for this is the lack of sufficient representative measurements available for validation of our flux estimates. But in our Figure 7 we could show that for those sites where the soil moisture model was adequately reproducing measured soil moisture, also the Rn flux estimates compared very well to the measured fluxes (e.g. for the Gebesee station). Moreover, we showed in the previous Table 1 of the Supplementary Material that biases between soil model results and observations, on average, have been larger for the ERA-I/L model than for the GDLAS-Noah model. From this finding alone, one could conclude that the GDLAS-Noah-based Rn fluxes are most probably more accurate than those based on the ERA-I/L model.*

*In order to better quantify the effect of soil moisture biases on the agreement between measured and modelled Rn fluxes, we decided to change Figure 8 in the revised manuscript. Although being aware of the fact that many of the available measurements may not be representative for the whole pixel in the map where they are located, we now present in Figure 8 (see revised version below) the differences between monthly modelled and measured Rn fluxes. The number of available (monthly) measurements is limited to a total of ca. 170 data points. We nevertheless clearly see from the*

distribution of the differences that the mean bias between GLDAS-Noah-modelled and measured fluxed is close to zero, while there is a large mean bias between ERA-I/L-modelled and measured fluxes (> 70%). The inter-quartile ranges of differences for both models are similar and large. However, this may be mainly due to the lack of representativeness of the point measurement on the pixel scale, besides the fact that the measurements stem from different laboratories, which may cause additional variability. We find no geographical dependency of the differences (not shown). Based on this comparison, in the revised manuscript we now make the statement that the GLDAS-Noah-based flux estimates seem to be generally more accurate than those based on the ERA-I/L model.



Revised Figure 8: Map of episodic <sup>222</sup>Rn flux observations in Europe (upper panel) and frequency distribution of model-data differences at sites where co-located data exist (GLDAS-Noah: red histogram, ERA-I/L: blue histogram). All measurement data are provided in the Supplement (Table S1).

#### SPECIFIC COMMENTS

Page 5, equation 5. The authors use the symbol P in equation 5 for the proportionality constant in Fick's Law and call that symbol "permeability". As far as I am aware, the term "permeability" is reserved for something quite different in the porous media transport literature. Permeability, often characterized by the symbol k or K, is the proportionality constant (Darcy's constant) in Darcy's law

relating flux density to a PRESSURE gradient not a CONCENTRATION gradient. The proportionality constant in Fick's law, often represented by the symbol  $D$  or something similar, is usually called something like "diffusion coefficient", "diffusivity," or "effective diffusion coefficient." In fact, on page eight, line 26, the authors comment: ". . . the permeability  $P$ , i.e., on the diffusion coefficient of  $^{222}\text{Rn}$  in the soil air . . ." Any of their references I checked used terminology like "diffusion coefficient." In the mks system, the diffusion coefficient has units of  $\text{m}^2\text{sec}^{-1}$  whereas permeability has units of  $\text{m}^2$ . To avoid serious confusion for readers used to conventional usage on this subject matter, unless the authors can present a strong argument to the contrary, I think they should strike use of the term "permeability" and use the term diffusion coefficient or one of its related variants. They might consider using a different symbol than " $P$ " for the diffusion coefficient, which is often reserved for pressure. However, the exact symbol used is not so important as long as it is not called "permeability."

*We agree with the reviewer that the term "Permeability ( $P$ )" can be misleading and changed the expression into "effective diffusion coefficient or diffusivity ( $D_e$ )", throughout the text, also to be conform to Schery et al., 1989 (JGR 94, D6, 8567-8576) and other follow-up publications.*

Section 2.3 on the effect of water table depth. Study of a water table effect (or more generally a transporting soil layer of finite depth) is a good idea and good feature of this paper. However, I had a little trouble following and evaluating the approximate "first order budget approach." I may be missing something but it seems to me there is an exact correction that could be used. Given a boundary condition of zero concentration at the surface and zero flux (zero derivative of the concentration) at some depth  $zG$ , I think there is an exact correction to equation 8 by a factor that goes something like  $[1 - \exp(-2zG/zbar)]/[1 + \exp(-2zG/zbar)]$ . Why was this result not used instead of that given by equation 8a?. The underlying data that must be provided to evaluate the effect,  $zG$  and  $zbar$ , remain the same.

*We thank the reviewer for his suggestion and revised section 2.3 accordingly.*

Section 3, Validation of the theoretical concepts to estimate  $^{222}\text{Rn}$  fluxes. If the authors have not already done so, they might take a look at the paper by D. J. Holford et al., "Modeling Radon Transport in Dry, Cracked Soil", Journal of Geophysical Research, vol. 98, B1, pages 567-580, 1993. Using a numerical calculation with a fundamental porous media transport model similar to, but more elaborate than, the authors equation 6a, and incorporating the effects of the water table depth and varying atmospheric pressure, Holford was able to provide a detailed prediction of the time dependence of the radon flux at the soil's surface at one field site that matched well time-dependent measurement data.

This prediction was done using measurements of the underlying fundamental soil properties with no free (adjustable) parameters. To my mind, this calculation indicates that the fundamental physical science of radon transport in porous media is well understood. The problem is to try to deduce the fundamental underlying parameters, or surrogates for them, from global and geochemical data sets for the earth's surface which contain estimates of less direct properties averaged over a larger scale. Alternately, an attempt can be made to use the fundamental models for guidance in producing an approximate parameterization of a flux density model using the type of properties available in the global and geochemical data sets with some adjustable parameters to match field measurements of radon. Unfortunately, for the case Holford modeled, the soil moisture was small and constant, so validation of a particular moisture dependence in her model would be difficult to make. In her model, tortuosity (which depends in part on porosity), not porosity itself, is a key soil property.

Another important point about these fundamental models and calculations is that they probably could be used to gain more insight into subjects such as snow cover, frozen soil, and ice layers. Generally as long as a layer remains porous, much of the radon gets through. It takes a solid layer of ice, or saturated frozen soil, to strongly block radon transport. However, future calculations would be helpful to fully quantify these statements.

*It is correct that a more elaborate model like the one developed by Holford et al. (1993) that also includes advective fluxes would be better suited to e.g. investigate short-term variability of radon exhalation at individual sites; and indeed, in reality radon fluxes are probably much more variable than what we can derive from our basic estimate that essentially provides a climatology of large scale (average) fluxes. It is true that the fundamental physical science of radon transport in porous media is well understood. However, there are two parameters required for transport modelling that are not well characterized: One is the model or parameterization of how to estimate the effective diffusion coefficient  $D_e$  from bulk soil properties (i.e. porosity, soil moisture) and the second is how to estimate the one governing variable parameter, namely soil moisture. While the different models and parametrizations available to estimate  $D_e$ , e.g. by Millington and Quirk (1960; 1961) or Moldrup et al. (1996; 1999) had already been tested by the authors, in our work we focus on measured radon soil profiles (as shown in our Figure 1) to decide on the most appropriate (and simple) way to estimate  $D_e$ . The error of  $D_e$  for some cases can still be up to 100% (Table 1), leading to potentially large uncertainties in the estimated radon fluxes. Still, we cannot see how a more fundamental model like the one by Holford et al. (1993) may help us to reduce this uncertainty (e.g. by parameter adjustment) for all relevant cases we have to deal with on the scale of our Europe-wide Rn flux map. In fact, and that has also been pointed out by the reviewer, a big advantage of our simple approach is that we can use existing gridded information on all soil properties needed for our  $^{222}\text{Rn}$  flux estimate and that we can use our measurements and those from the literature for an independent model validation, rather than for parameter adjustment. Similar arguments hold for quantifying the effect of frozen soil or snow cover, where we have to deal with highly variable unknown porosity.*

Section 6. Conclusions and Perspectives. The authors state: "It would be extremely helpful to apply our approach to other areas of the world. However, this is hampered by the un-availability of a systematic  $^{238}\text{U}$  or  $^{226}\text{Ra}$  survey in other regions and continents." I agree with the first sentence but not the second. For starters, there is detailed gamma-ray-based aerial survey data for the entire United States of America for uranium (NURE, mrddata.usgs.gov), radium soil survey data exists for China (Shurong et al., Chin. J. Radiol. Med. Prot. 8, 1988, see Hirao et al.), and Griffiths et al. 2010 discuss a radiometric map of Australia they used for surface radium for Australia. It's probably a subject for a new paper but it would be interesting to see how the present authors' model works in one of these other geographical locations if a methodology could be worked out for the other geochemical parameters that may not be available in the same form as used for Europe.

*We agree with the reviewer that we should re-formulate this concluding sentence. What we originally wanted to state is that for other regions of the world it would not have been straight-forward to use exactly the same approach as for Europe, mainly because in many regions direct  $^{226}\text{Radium}$  or  $^{238}\text{Uranium}$  concentration measurements in the soil are lacking. Already extrapolating our map to Eastern Europe where no direct  $^{238}\text{Uranium}$  measurements exist introduced additional uncertainty on the estimated fluxes. We therefore decided to postpone development of a global radon flux map to future work.*

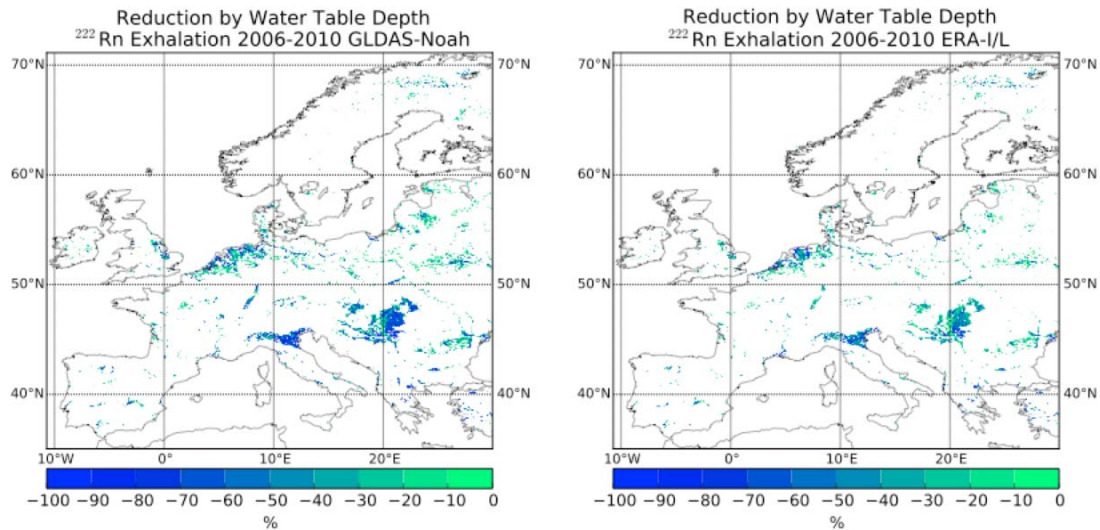
Sections 5.2, 5.4, 5.5 and elsewhere -- Validation of predictions and comparison with other flux maps.

After all the work done by the authors with what looks like a more thorough consideration of various possible radon transport effects (water table, porosity models, moisture models, snow cover, etc.) and use of more comprehensive and up-to-date geochemical data I was hoping for some more definitive conclusions. For example, the authors were even unable to conclude which of their two major moisture models was superior. The accuracy and importance of the water table correction is unclear. I understand the problem. There just is not enough measurement data over a wide enough geographical region and for different seasons of the year to either carefully calibrate a model or unequivocally establish its performance relative to other models. Still, is it possible their evaluation could be pushed a little further?

The authors' major comparison is with Szegvary et al. and Lopez-Coto et al. Would it be possible to go outside the Europe-only predictions and gain some useful information? Here's an example of what I mean. Both Zhang et al. (Atmos. Chem. Phys. 11, 7817-7838, 2011) and Hirao et al. (Jpn. J. Health Phys., 45, 2010) present global maps of radon flux density. I realize the difficulty with details of these predictions (possible unavailability of their grided numbers, what countries do they classify as in Europe?, what statistical conventions are they using -- means, medians, other?, what exact time periods are their maps applicable to?, etc.) so their papers would have to be studied carefully. Nevertheless, hopefully their modelling and normalization would be independent so that calibration at some other part of the world could be used to project normalization for Europe. Hirao et al. quote a number of 18.3 mBqm<sup>-2</sup>s<sup>-1</sup> for Europe while Zhang et al quote a value for Europe of 13.0 mBqm<sup>-2</sup>s<sup>-1</sup> for their preferred "merged" model. Further, it looks like support for the Zhang model comes in part from atmospheric measurements of radon gas (responding to larger regions of soil flux), measurements of a type different and independent from that used in the present paper by Karstens et al. Could the results of Hirao and Zhang be used as evidence that perhaps the present GLDAS moisture formulation is superior? I don't mean to make that conclusion myself but just point out the type of reasoning that might enable the authors to make some stronger statements than presently exist. There may be other maps or flux density data that could be useful along these lines. Another avenue might be for the authors to apply their model to other countries, continents, and regions for which independent flux density maps are available (Australia, China, other?) and check, at least, the overall normalization. In any case, additional evaluation using a broader comparison with existing maps and models may be possible, or at least reasons given why this is not possible. I understand that any major new data analysis effort might best be left for a later paper.

*1. We are very grateful for the suggestion of the reviewer to "push the evaluation of our results a little further". In the revised manuscript and based on the model-data comparison from section 5.5 and our new evaluation presented in Figure 8 (see above), we therefore now make a statement, which of the two soil moisture models most probably provides on average the more accurate radon flux estimates (see reply to the General Comments). We hesitated to do so in the first place because of the (potential) lack of representativeness of the available measurements for the entire model grid box they are located in. Unfortunately, due to lack of detailed soil parameter information at the radon flux measurement sites, we are not able to select only measurement sites where the soil represents the parameters of the map pixels. Therefore, we decided to use all data, which probably leads to the large inter-quartile-range of the differences presented in the new Figure 8 of our revised manuscript.*

*2. We have also revised our Supplementary Figure S4, now showing the percent change of fluxes for areas with water table restriction.*



*Revised Figure S4: Influence of elevated water table on  $^{222}\text{Rn}$  flux as percent change in individual pixels: left, based on the GLDAS-Noah soil moisture model, right, based on the ERA-I/L soil moisture model.*

3. Our emphasis in the current manuscript was to develop an accurate and high-resolution (in space and time) estimate of radon fluxes for Europe. There is an urgent need for such a map in the European modelling community and also when applying the Radon-Tracer-Method (e.g. Levin et al., 1999) for preliminary greenhouse gases flux estimates. Our comparison with other flux maps was restricted to the only two existing maps recently developed for Europe because they had a similar spatial and temporal resolution as our flux map but used different approaches and parameters for flux estimation. The Zhang et al. (2011) map is identical to the Szegvary et al. (2007) map for its European parts (see their Figure 2d) and will thus not provide new insights. The Hirao et al. (2010) map used only a very broad resolution of  $^{226}\text{Ra}$  in soils (based on the country-by-country data from UNSCEAR 2000, if available). We, therefore, do not feel that comparison with these two estimates could provide new insights in terms of validation of our approach.

#### PROOFREADING AND EDITING COMMENTS

Entire paper. Delete usage of terminology “permeability” and use more conventional terminology such as “diffusion coefficient”, “effective diffusion coefficient”, or “diffusivity”. Restrict usage of terminology “permeability” to situations involving flux density in response to a pressure gradient, a subject apparently not brought up in this paper. Optional: consider a different symbol than “P”, such as “D” or “D” with qualifying subscripts.

*We have changed the term “permeability” to “effective diffusion coefficient or diffusivity”.*

p.18, Lopez-Coto citation, Is not the correct date 2013, not 2011?

*We have corrected the wrong date of López-Coto et al. in the reference list to 2013.*



p. 2, Abstract, “The average . . .10 . . . or 15 . . . “ I had trouble tracing this presumably major conclusion back to the text. It looks like it apparently comes from figure 4 where the term “mean” is used. Perhaps use the term “mean” in the abstract and add more detail such as the period of time covered (five years)?

*We have clarified the origin of the numbers “10 or 15 ...” in the Abstract and revised it according to our new evaluation of data-model differences.*

Overall scope and organization. I assume this paper is to be published in an electronic form with essentially no page limit. If this is the case, then the present format and organization is acceptable. However, if there was a length restriction, it would be possible to present the authors’ main points in a more tightly worded document with less presentation of certain details that are not essential or not resolved. The paper would focus on 1) why we did what we did 2) what we did 3) what were our results, and 4) what we learned from our effort. On a subject as complex as radon flux from soil, I think there is little chance that any specific modelling formulation will be the last word, so spending too much time discussing all the options may be a futile effort. For example, the influence of moisture based on climate-like data sets could be entering in a number of different ways: effect on diffusivity, effect on emanation coefficient, relation to water table, a breakdown of the homogeneous soil properties with depth assumption, etc. So in the end you must just chose a certain approach and see how it works. A lot of time is spent comparing spatially averaged model predictions to limited point measurements (for example, Figure 7). It comes as no surprise that agreement is very mixed at best. I would be happy with a shorter summary of this effort with all the details left to, say, an appendix. On the other hand, a little more time might be spent synthesizing what was learned from the study (many issues were brought up in the model development sections) and strengthening conclusions.

*We fully agree with the reviewer that our manuscript is a bit lengthy and may benefit from re-organization. But as we have no page limitation we decided to keep the contents of the main manuscript as is. We do disagree, however, that the discussion of e.g. Figure 7 is unnecessarily detailed. In fact, we think that a detailed comparison/validation with measurements is a particular strength of our work. For example, we find it very important to elaborate on the good agreement of the large seasonality between our modelled and observed fluxes. This feature is almost totally missing in the Szegvary et al. (2009) map, and it also seems to be too small in the López-Coto et al. (2013) approach. Comparison of modelled and measured radon fluxes in Australia (Griffith et al., 2010) seems not conclusive with respect to the seasonal amplitude, while Hirao et al. (2010) model a global amplitude of the radon fluxes of only +/-10%. Although we cannot directly compare the seasonal amplitude of the mean global flux with our results, we want to stress here that for Europe at many sites it exceeds the +/-10% level.*

*As suggested by the reviewer, we tried to strengthen our conclusions, again emphasizing the importance of accurate soil moisture data and more measurements to properly validate the <sup>222</sup>Rn fluxes. Based on our new evaluation we now make the recommendation to use the GLDAS-Noah-based radon fluxes.*

## **Response to the review by R. Fujiyoshi**

The reviewer thinks this manuscript is to be accepted as its form.

*We wish to thank R. Fujiyoshi for her review and her favourable opinion on the manuscript.*



## List of relevant changes made in the manuscript:

### Abstract

- Mean values and seasonal variations were adjusted due to the new correction for shallow water table depth.
- The use of GLDAS-Noah-based  $^{222}\text{Rn}$  fluxes is now recommended.

### 2. Theoretical considerations

- The term “permeability (P)” was changed to “effective diffusion coefficient” or “diffusivity  $D_e$ ” throughout the manuscript.
- Sect.2.3: The approximation of  $^{222}\text{Rn}$  fluxes at sites with shallow water table depth (Eq. 8a) was revised according to the suggestions of S. D. Schery.

### 4 Input data for estimation of the $^{222}\text{Rn}$ fluxes from soils in Europe

#### 4.3.1 Soil moisture

- The results of the comparison of both soil moisture data sets with observations are now summarized in the manuscript itself instead of (previous) Table S1 of the supplement.

### 5. Results and discussion

- All results were re-computed using the new correction for shallow water table depth (Eq. 8a).

#### 5.1 Distribution of European $^{222}\text{Rn}$ fluxes

- Median values and IQR were adjusted due to the new correction for shallow water table depth (Eq. 8a).
- Mean values and seasonal variation for the period 2006-2010 are listed.

#### 5.5 Comparison with published episodic $^{222}\text{Rn}$ flux observations

- The evaluation focuses now on quantifying the effect of soil moisture biases on the agreement between measured and modelled  $^{222}\text{Rn}$  fluxes.
- The revised Fig. 8 now presents the difference between monthly modelled and measured fluxes instead of the modelled fluxes (previous Fig. 8).

#### 5.6 Discussion of uncertainties

- The uncertainty of each component in our approach was estimated separately.
- A section discussing the combined uncertainty of our approach and the resulting  $^{222}\text{Rn}$  flux map was added (Sect. 5.6.8).

### 6 Conclusion and perspectives

- The conclusions were re-formulated to reflect that we now recommend the use of the GLDAS-Noah-based  $^{222}\text{Rn}$  fluxes.

## Supplement

- Figure S4 now shows the influence of elevated water table on  $^{222}\text{Rn}$  flux instead of water table depth itself.
- Table S1 (comparison of modelled and observed soil moisture) and references therein were removed.

1 **A process-based <sup>222</sup>Radon flux map for Europe and its**  
2 **comparison to long-term observations**

3

4 **U. Karstens<sup>1,+</sup>, C. Schwingshackl<sup>2,\*</sup>, D. Schmithüsen<sup>2</sup>, and I. Levin<sup>2</sup>**

5 [1]{Max-Planck-Institut für Biogeochemie, Jena, Germany }

6 [2]{Institut für Umweltphysik, Heidelberg University, Heidelberg, Germany }

7 [+]{now at: ICOS Carbon Portal, Lund University, Lund, Sweden }

8 [\*]{now at: Institute for Atmospheric and Climate Science, ETH Zürich, Switzerland }

9 Correspondence to: U. Karstens (~~ukarst@bge-jena.mpg.de~~[ukarst@bge-jena.mpg.de](mailto:ukarst@bge-jena.mpg.de), [deute.karstens@nateko.lu.se](mailto:deute.karstens@nateko.lu.se))

10

11

## 1 Abstract

2 Detailed <sup>222</sup>Radon (<sup>222</sup>Rn) flux maps are an essential pre-requisite for the use of radon in  
3 atmospheric transport studies. Here we present a high-resolution <sup>222</sup>Rn flux map for Europe,  
4 based on a parameterization of <sup>222</sup>Rn production and transport in the soil. The <sup>222</sup>Rn  
5 exhalation rate is parameterized based on soil properties, uranium content, and modelled soil  
6 moisture from two different land-surface reanalysis data sets. Spatial variations in exhalation  
7 rates are primarily determined by the uranium content of the soil, but also influenced by soil  
8 texture and local water table depth. Temporal variations are related to soil moisture variations  
9 as the molecular diffusion in the unsaturated soil zone depends on available air-filled pore  
10 space. The implemented diffusion parameterization was tested against campaign-based <sup>222</sup>Rn  
11 soil profile measurements. Monthly <sup>222</sup>Rn exhalation rates from European soils were  
12 calculated with a nominal spatial resolution of 0.083° x 0.083° and compared to long-term  
13 direct measurements of <sup>222</sup>Rn exhalation rates in different areas of Europe. The two  
14 realizations of the <sup>222</sup>Rn flux map, based on the different soil moisture data sets, both  
15 realistically reproduce the observed seasonality in the fluxes but yield considerable  
16 differences for absolute flux values. The ~~average-mean~~ <sup>222</sup>Rn flux from soils in Europe is  
17 estimated to be 10 mBq m<sup>-2</sup> s<sup>-1</sup> (ERA I/L soil moisture) or 15 mBq m<sup>-2</sup> s<sup>-1</sup>, ~~depending on the~~  
18 ~~soil moisture data set, and the~~ (GLDAS-Noah soil moisture) for the period 2006-2010. The  
19 ~~corresponding~~ seasonal variations ~~with low fluxes in winter and high fluxes in summer range~~  
20 ~~in the two realisations range from ca. 7.1 mBq m<sup>-2</sup> s<sup>-1</sup> to ca. 14 mBq m<sup>-2</sup> s<sup>-1</sup> in February to~~  
21 ~~13.9 and from ca. 11 mBq m<sup>-2</sup> s<sup>-1</sup> in August and from 10.8 to ca. 20 mBq m<sup>-2</sup> s<sup>-1</sup> in March to~~  
22 ~~19.7 mBq m<sup>-2</sup> s<sup>-1</sup> in July~~, respectively. These systematic differences highlight the importance  
23 of realistic soil moisture data for a reliable estimation of <sup>222</sup>Rn exhalation rates. Comparison  
24 with observations suggests that the flux estimates based on the GLDAS-Noah soil moisture  
25 model on average better represent observed fluxes.

26

27

# 1 1 Introduction

2 One of the limiting factors for applying atmospheric  $^{222}\text{Rn}$  measurements for transport model  
3 validation is a reliable, high-resolution  $^{222}\text{Rn}$  flux map for the global continents, but also on  
4 the regional scale for Europe. It has been shown earlier that the assumption of a constant  
5 exhalation rate of  $1 \text{ atom cm}^{-2} \text{ s}^{-1}$  for continental areas, as was proposed by Jacob and Prather  
6 (1990) as an intermediate value from data reported by Wilkening et al. (1972) and Turekian et  
7 al. (1977), is an over-simplification of the true conditions, in particular for Europe (Dörr and  
8 Münnich, 1990; Schüßler, 1996; Conen and Robertson, 2002). Nevertheless, this assumption  
9 was used, for simplicity, in different transport model estimates and model inter-comparison  
10 studies (Rasch et al., 2000; Chevillard et al., 2002; Taguchi et al., 2011). Only in the last  
11 decade, a number of attempts have been made to develop high-resolution maps of the  
12 variability of  $^{222}\text{Rn}$  exhalation from continental soils (Schery and Wasiolek, 1998; Sun et al.,  
13 2004; Zhuo et al., 2008; Szegvary et al., 2009; Griffith et al., 2010; Hirao et al., 2010; López-  
14 Coto et al., 2013). We present here a high-resolution  $^{222}\text{Rn}$  flux map for Europe, based on a  
15 parameterization of  $^{222}\text{Rn}$  production and transport in the soil.

16  $^{222}\text{Rn}$  is a progeny of  $^{238}\text{Uranium}$  ( $^{238}\text{U}$ ), a trace element in natural soils. Since  $^{222}\text{Rn}$  is the  
17 first gaseous element in the  $^{238}\text{U}$  decay chain, [which can escape from the soil](#), all daughter  
18 nuclides from  $^{238}\text{U}$  up to  $^{226}\text{Radium}$  ( $^{226}\text{Ra}$ ), the mother nuclide of  $^{222}\text{Rn}$ , are often assumed to  
19 be in equilibrium in the soil. Besides the  $^{226}\text{Ra}$  content,  $^{222}\text{Rn}$  exhalation rates also strongly  
20 depend on soil properties ([Nazaroff, 1992](#)). Therefore, not only the  $^{238}\text{U}$  content but also the  
21 parameters influencing diffusive transport characteristics of the soil need to be known to  
22 properly estimate the variability of  $^{222}\text{Rn}$  exhalation rates (Schüßler, 1996). Taking these into  
23 account, Griffith et al. (2010) developed a high-resolution  $^{222}\text{Rn}$  flux map for Australian land  
24 surfaces. They used a transport model for the unsaturated upper soil layers, national  $\gamma$ -ray  
25 surveys, maps of soil properties, such as porosity and bulk density, as well as modelled soil  
26 moisture to estimate monthly  $^{222}\text{Rn}$  exhalation rates at  $0.05^\circ$  spatial resolution. Likewise,  
27 López-Coto et al. (2013) published a  $^{222}\text{Rn}$  flux map for Europe that also uses numerical  
28 modelling of  $^{222}\text{Rn}$  transport in the upper soil layers. Their input parameters were measured  
29  $^{238}\text{U}$  activity concentrations from the Geochemical Atlas of Europe (Salminen, 2005) and  
30 other soil properties as well as modelled soil temperature and moisture data. Based on these  
31 parameters, they estimated average monthly  $^{222}\text{Rn}$  exhalation rates for the time period of  
32 1957-2002 at a spatial resolution of 1 km. Szegvary et al. (2007b) found an empirical relation

1 between  $^{222}\text{Rn}$  exhalation rate and  $\gamma$ -dose rate. Following this finding, Szegvary et al. (2009)  
2 published a  $^{222}\text{Rn}$  flux map for Europe that solely uses  $\gamma$ -dose rate as a proxy for  $^{222}\text{Rn}$   
3 exhalation rate.

4 In the present work, we use a similar approach as Griffith et al. (2010) for Australia and  
5 López-Coto et al. (2013) for Europe. We estimate the  $^{222}\text{Rn}$  exhalation rate from European  
6 land surface based on the measured distribution of  $^{238}\text{U}$  in the upper soil layers (Salminen,  
7 2005), the soil texture class distribution (Reynolds et al., 2000) as well as model estimates of  
8 the soil moisture, which largely governs molecular diffusion in the unsaturated soil. For the  
9 period of 2006 to 2010, we test two different soil moisture reanalysis data sets, i.e. (1) from  
10 the Noah Land Surface Model in the Global Land Data Assimilation System (GLDAS-Noah,  
11 Rodell et al., 2004), and (2) from the ERA-Interim/Land reanalysis (Balsamo et al., 2015).  
12 Soil moisture-dependent molecular diffusive transport in the upper meter of the soil is  
13 calculated based on the Millington and Quirk (1960) model. The validity of our diffusion  
14 model approach is tested at different soil moisture regimes, using systematic  $^{222}\text{Rn}$  soil profile  
15 measurements at our observational site close to Heidelberg, Germany. The European flux  
16 maps are further compared to direct spot and long-term measurements of  $^{222}\text{Rn}$  exhalation  
17 rates in different areas across Europe.

18

## 19 **2 Theoretical considerations**

### 20 **2.1 Basic equations for $^{222}\text{Rn}$ production, decay and diffusion in soils**

21 The derivations below essentially follow those presented in Dörr and Münnich (1990), Born  
22 et al. (1990), Schüßler (1996), and Griffiths et al. (2010). They are valid for an infinitely deep  
23 unsaturated homogeneous soil and we consider only changes of concentration  $c(z, t)$ , flux  $j(z,$   
24  $t)$  as well as source  $Q(z, t)$  or sink strength  $S(z, t)$  in the vertical direction  $z$  (with the  $z$ -  
25 coordinate defined as positive downwards and  $z=0$  at the soil-atmosphere interface).

26 In this case the equation of continuity in the soil air can be reduced to one spatial dimension,  
27 namely

$$28 \quad \frac{dc(z,t)}{dt} + \frac{\partial j(z,t)}{\partial z} = Q(z,t) + S(z,t). \quad (1)$$

1 We further assume that, at any depth in the soil, the only sink process is radioactive decay,  
2 which is described by

$$3 \quad S(z,t) = -\lambda c(z,t) \quad (2)$$

4 with the decay constant  $\lambda(^{222}\text{Rn}) = 2.0974 \cdot 10^{-6} \text{ s}^{-1}$ .

5 The source term Q, i.e. the production rate of  $^{222}\text{Rn}$  gas in the soil, is calculated according to  
6 Schüßler (1996) from

$$7 \quad Q(z) = \lambda \rho_b(z) c_{\text{Ra}}(z) \varepsilon(z) \quad (3)$$

8 with  $\rho_b$  the dry bulk density of the soil ( $\text{kg m}^{-3}$ ),  $c_{\text{Ra}}$  the  $^{226}\text{Ra}$  activity concentration in the soil  
9 material ( $\text{Bq kg}^{-1}$ ), and  $\varepsilon$  the  $^{222}\text{Rn}$  emanation coefficient, which is defined as the probability  
10 that a  $^{222}\text{Rn}$  atom produced in a soil grain can actually escape into the soil air.

11 If we consider steady state conditions, i.e. no explicit dependence on time, Eq. (1) simplifies  
12 to

$$13 \quad 0 = -\frac{\partial j(z)}{\partial z} + Q(z) + S(z) = -\frac{\partial j(z)}{\partial z} + Q(z) - \lambda c(z) \text{ or}$$

$$14 \quad \frac{\partial j(z)}{\partial z} = Q(z) - \lambda c(z). \quad (4)$$

15 Taking into account only molecular diffusion of the trace gas in the soil air ~~with P, the~~  
16 ~~permeability of the soil, assumed here to be constant with depth,~~ we can apply Fick's first law

$$17 \quad j(z) = -D_e \frac{\partial c(z)}{\partial z}, \quad (5)$$

18 where  $D_e$  is the effective diffusion coefficient of the trace gas in the soil air (hereafter also  
19 named effective diffusivity or simply diffusivity).  $D_e$  is assumed to be constant with depth.

20 Note that in Eq. (5)  $j(z)$  is the flux per unit area of the bulk soil. This is not immediately  
21 obvious and in the respective Eq. (1) in Griffith et al. (2010), and also in Sun et al. (2004)  $j(z)$

22 is multiplied with  $\theta_p$ , the porosity of the soil to yield the flux density per bulk unit area.

23 However, they also use a different expression to calculate the source strength Q in the soil  
24 (Eq. (3) in Griffith et al. (2010)) where they divide our Eq. (3) by  $\theta_p$ .

25 Combining Eqs. (4) and (5) yields



$$1 \quad \frac{\partial^2 c(z)}{\partial z^2} - \frac{\lambda}{D_e} c(z) = -\frac{Q(z)}{D_e}. \quad (6)$$

2 If we further assume that the  $^{226}\text{Ra}$  activity concentration in the soil particles, the  $^{222}\text{Rn}$   
3 emanation coefficient, and the soil bulk density are constant with depth, we obtain a depth-  
4 independent source strength, i.e.  $Q(z) = Q$ , and Eq. (6) becomes

$$5 \quad D_e \frac{\partial^2 c(z)}{\partial z^2} - \lambda c(z) + Q = 0. \quad (6a)$$

## 6 **2.2 The $^{222}\text{Rn}$ soil air profile and its exhalation rate at the soil surface**

7 The general solution of the inhomogeneous differential equation Eq. (6a) is

$$8 \quad c(z) = c_\infty \left(1 - e^{-\frac{z}{\bar{z}}}\right),$$

9 where  $c_\infty$  is the asymptotic concentration at large depths and  $\bar{z}$  the relaxation depth.

10 With the boundary conditions that (1) at the soil-air interface the  $^{222}\text{Rn}$  activity concentration  
11 approaches zero and (2) at large depths there is no change of the concentration with depth, i.e.  
12 equilibrium between  $^{222}\text{Rn}$  production and decay,

$$13 \quad c(z=0) = 0 \quad \text{and} \quad \frac{dc}{dz}(z=\infty) = 0,$$

14 the solution of Eq. (6a) gets

$$15 \quad c(z) = c_\infty \left(1 - e^{-\frac{z}{\bar{z}}}\right) = \frac{Q}{\lambda} \left(1 - e^{-\sqrt{\frac{\lambda}{D_e}} z}\right) \quad (7)$$

$$16 \quad \text{i.e.} \quad c_\infty = \frac{Q}{\lambda} \quad \text{and} \quad \bar{z} = \sqrt{\frac{D_e}{\lambda}}. \quad (7a)$$

17 Introducing solution (7) into the diffusion equation (5) we can calculate the  $^{222}\text{Rn}$  flux at the  
18 soil surface

$$19 \quad j(z=0) = -D_e \left. \frac{\partial c(z)}{\partial z} \right|_{z=0} = -D_e \frac{c_\infty}{\bar{z}} = -\bar{z} c_\infty \lambda = -Q \sqrt{\frac{D_e}{\lambda}} = -\rho_b c_{Ra} \varepsilon \sqrt{D_e \lambda}. \quad (8)$$

1 Note that the last term in Eq. (8), which allows calculating the  $^{222}\text{Rn}$  flux density per unit bulk  
2 surface of the soil from “bottom-up” parameters and the [effective diffusivity](#) in the soil, is  
3 now identical to Eq. (4) in Griffith et al. (2010).

### 4 **2.3 Approximation of $^{222}\text{Rn}$ fluxes at sites with shallow water table depth**

5 The solution of the differential equation (6a) given by Eqs. (7) and (7a) is only valid if we can  
6 assume an infinitely deep unsaturated soil. This assumption is not always fulfilled.  
7 Particularly in Northern Europe or in Siberian wetland areas the water table depth can be as  
8 close to the surface as 10 or 20 cm. In that case there is only a very shallow soil depth  
9 available for  $^{222}\text{Rn}$  production and exhalation into the atmosphere (if we consider that the  
10 molecular diffusion coefficient of  $^{222}\text{Rn}$  in water is lower by 2-3 orders of magnitude  
11 compared to air, and that there is only negligible  $^{222}\text{Rn}$  flux from ground water into the  
12 unsaturated soil zone). [With the boundary conditions of zero  \$^{222}\text{Rn}\$  activity concentration at  
13 the soil-air interface and zero  \$^{222}\text{Rn}\$  flux, i.e. zero concentration gradient, at water table depth  
14  \$z\_G\$](#)

$$15 \quad c(z=0) = 0 \quad \text{and} \quad \frac{dc}{dz}(z=z_G) = 0,$$

16 [the solution of the differential equation \(6\) gives the modified flux at the surface according to](#)

$$17 \quad j(z=0) = -Q \sqrt{\frac{D_e}{\lambda}} \tanh\left(\frac{z_G}{\bar{z}}\right). \quad (8a)$$

18 The solution Eq. (8a) has the same form as Eq. (8) and for  $z_G \gg \bar{z}$  it yields Eq. (8).

19 ~~[Note that the budget equation \(9\) is only an approximation of the real conditions in the  
20 unsaturated soil zone in situations when the water table is close to the soil surface because we  
21 assume that the concentration profile is the same as if the ground water table was at very large  
22 depths. However, it is still a good first approximation of the exhalation flux for areas with a  
23 shallow water table depth \(Sect. 3.2\).](#)~~

### 24 **2.4 The role of snow cover and frost on the $^{222}\text{Rn}$ exhalation rate from 25 continental soils**

26 The role of snow cover on the  $^{222}\text{Rn}$  exhalation rate is not yet fully understood. Robertson  
27 (2004) found in her measurements that a layer of snow had no significant influence on the

1 <sup>222</sup>Rn exhalation rate. However, when the top layer of the snow melted and froze again, a  
2 smaller <sup>222</sup>Rn exhalation rate was measured. This finding suggests that the physical properties  
3 of the snow, such as a thin ice layer on its top, determine the magnitude of the <sup>222</sup>Rn flux.  
4 However, most of the studies cited in Robertson (2004) found no or merely a small effect of  
5 snow cover on <sup>222</sup>Rn exhalation rate. Thus, although a shielding effect of snow cover has been  
6 included in the López-Coto et al. (2013) flux map, this effect is not taken into account in our  
7 <sup>222</sup>Rn flux estimates.

8 Another point concerning the <sup>222</sup>Rn exhalation rate in winter months is the influence of frozen  
9 soils on <sup>222</sup>Rn exhalation rates. While different authors e.g. cited by Robertson (2004) report a  
10 reduction in <sup>222</sup>Rn flux when the soil was frozen, Robertson (2004) found no evidence for a  
11 strong influence of frozen soils on <sup>222</sup>Rn emissions. However, particularly when soil moisture  
12 is high or when an ice layer forms on the ground, this might cause a substantial decrease in  
13 <sup>222</sup>Rn exhalation rates. Because no systematic analysis of the influence of soil freezing on the  
14 <sup>222</sup>Rn flux is available, our standard <sup>222</sup>Rn flux maps do not take into account any positive or  
15 negative effect of frozen soil on the exhalation rate. However, we will show one hypothetical  
16 scenario of the potential influence of frost on the exhalation rate with reduced fluxes, based  
17 on the number of ice days during winter months (Sect. 4.3).

## 18 **2.5 Estimating the effective diffusivity from soil properties**

19 From Eq. (8) we see that the <sup>222</sup>Rn flux at the soil surface not only depends on the production  
20 rate  $Q$  in the soil (see Eq. 3), but also on the effective diffusivity  $D_e$  of <sup>222</sup>Rn in the soil air.  
21 Estimating  $D_e$  in soil air is, however, not a trivial task. This parameter depends mostly on the  
22 percentage of soil air volume available for gas diffusion, but also on the grain size distribution  
23 of the soil, i.e. its texture. The unit volume of soil consists of the soil material fraction  $\theta_m$ , the  
24 fraction that is filled with water  $\theta_w$ , and the air-filled fraction  $\theta_a$  so that

$$25 \quad \theta_m + \theta_w + \theta_a = 1 \quad (10)$$

26 The porosity  $\theta_p$  of the soil is defined as

$$27 \quad \theta_p = 1 - \theta_m = \theta_a + \theta_w \quad (10a)$$

28 Different models were developed in the past to estimate  $D_e$  depending on soil properties and  
29 soil moisture. While the more recent models by Moldrup et al. (1996; 1999) require as input  
30 detailed parameters of the soil texture, i.e. percentages of clay, coarse sand and fine sand, the

1 earlier models by Millington and Quirk (1960; 1961) and also the parameterization reported  
 2 by Rogers and Nielson (1991) only require information on soil porosity and soil moisture.  
 3 The latter parameterization by Rogers and Nielson (1991) has been used by Zhuo et al.  
 4 (2008), Griffith et al. (2010) and López-Coto et al. (2013) in their  $^{222}\text{Rn}$  flux estimates.  
 5 However, Jin and Jury (1996) could show that the original estimate of the **effective diffusivity**  
 6 according to Millington and Quirk (1960), i.e.

$$7 \quad D_e = D_a \frac{\theta_a^2}{\theta_p^3} = D_a \frac{(\theta_p - \theta_w)^2}{\theta_p^3} \quad (11)$$

8 (where  $D_a=1.1 \cdot 10^{-5} \text{m}^2 \text{s}^{-1}$  is the diffusion coefficient of radon in air) yields excellent agreement  
 9 with a large set of available observational data of the **effective diffusivity**  $D_e$  for soils with  
 10 different texture obtained from different studies in the literature (Jin and Jury, 1996, and  
 11 references therein). Moreover, when comparing **diffusivity** calculated from the Millington and  
 12 Quirk (1960) model with that of Moldrup et al. (1996), both agree very well (and for a  
 13 hydraulic parameter  $b = 6$ , which corresponds to a typical soil with about 20% clay, they yield  
 14 identical values of  $D_e$  (see Fig. S1 of the Supplement)). More importantly, when comparing  
 15 measured  $^{222}\text{Rn}$  profile-based **diffusivity** values calculated from Eq. (7a) (see Sect. 3, Table 1)  
 16 with the model-estimated results, we find the best agreement with these two models  
 17 (Millington and Quirk, 1960 and Moldrup et al., 1996). The Rogers and Nielson (1991) model  
 18 seems to overestimate **diffusivity**, particularly during dry conditions, and the Moldrup et al.  
 19 (1999) model largely underestimates the measured **diffusivity**. Therefore, we decided to use  
 20 the Millington and Quirk (1960) model (Eq. 11), which is solely based on soil porosity and  
 21 soil moisture, to estimate **effective diffusivity**.

22 The temperature dependence of the **diffusivity** for the  $^{222}\text{Rn}$  flux map has been estimated  
 23 according to Schery and Wasiolek (1998):

$$24 \quad D_e(T) = D_{e0} \left( \frac{T}{273 \text{ K}} \right)^{\frac{3}{2}} \quad (12)$$

25 with T the mean soil temperature in Kelvin and  $D_{e0}$  the **effective diffusivity** at the reference  
 26 temperature 273 K.

27

### 1 3 Validation of the theoretical concepts to estimate <sup>222</sup>Rn fluxes

#### 2 3.1 Evaluation of measured <sup>222</sup>Rn soil profiles and diffusivity estimates

3 Schmithüsen (2012) measured the <sup>222</sup>Rn exhalation rate and corresponding vertical  
4 concentration profiles of <sup>222</sup>Rn in a loamy soil close to the Institut für Umweltphysik (IUP) in  
5 Heidelberg, Germany. These measurements provide a first validation of the theoretical  
6 concept described in Sect. 2, which is used for estimating the <sup>222</sup>Rn exhalation rates in Europe  
7 from bottom-up data. Measured concentration profiles were binned into mean profiles for dry  
8 (nominal  $\theta_w = 0.124$ , actual range 0.098-0.145), medium dry (nominal  $\theta_w = 0.199$ , actual  
9 range 0.160-0.239), and wet (nominal  $\theta_w = 0.311$ , actual range 0.264-0.345) soil moisture  
10 conditions (Fig. 1). The ranges of the soil moisture classes resulted from a roughly equal  
11 distribution of all measured soil moistures (in the upper 20 cm of the soil) during the course  
12 of one year. From fitting a curve according to Eq. (7) to the mean profile data one obtains the  
13 parameters  $\bar{z}$  and  $c_\infty$  as well as values for the <sup>222</sup>Rn source strength  $Q$  and the **effective**  
14 **diffusivity**  $D_{e, \text{exp}}$  (Table 1). The values for  $Q$ , which should be the same for all three moisture  
15 situations (wet, medium, dry), indeed agree rather well (i.e. to within  $\pm 25\%$ ). The <sup>222</sup>Rn  
16 exhalation rate at the soil surface ( $j_{\text{profile}}$ ) calculated according to Eq. (8) from the parameters  
17 fitted to the measured profiles as well as the mean exhalation rates  $j_{\text{chamber}}$  independently  
18 measured using accumulation chambers are also listed in Table 1. They agree within a factor  
19 of two for all three soil moisture regimes and within 15% for the annual mean flux.

20 For comparison with the measured profile-based **diffusivity**, we can calculate  $D_e$  with the  
21 Millington and Quirk (1960) model  $D_{e, \text{M\&Q}}$  from measured porosity ( $\theta_p = 0.368$ ) and  
22 measured mean soil moistures according to Eq. (11). The **diffusivity** was adjusted to the mean  
23 soil temperatures during the measurement dates for wet, medium and dry conditions  
24 according to Eq. (12). Likewise, we use the Rogers and Nielson (1991) model (their Eq. 19)  
25 to estimate  $D_{e, \text{R\&N}}$ . The numbers of  $D_{e, \text{M\&Q}}$  and  $D_{e, \text{R\&N}}$  are given in the last two columns of  
26 Table 1. At our Heidelberg IUP sampling site the Millington and Quirk (1960) model  
27 underestimates **diffusivity** during wet and dry conditions by up to 25% while it overestimates  
28 **diffusivity** during medium dry conditions by about a factor of two. However, the  
29 discrepancies between the **diffusivity** calculated with the Rogers and Nielson (1991) model  
30 and the experimental results are larger at wet and medium dry conditions, while they fit very  
31 well at dry conditions ( $\theta_w < 0.15$ ). Using an average  $Q = 23.6 \text{ mBq m}^{-3} \text{ s}^{-1}$  from the measured

1 profiles and the respective  $D_{e,i}$  from Table 1, we also estimated Millington and Quirk- and  
2 Rogers and Nielson-based soil profiles according to Eq. (7) and (7a). These profiles are  
3 plotted in Fig. 1 for comparison to the observations. Again the Millington and Quirk model  
4 fits the observations better than the Rogers and Nielson model. Hence, we favour the  
5 Millington and Quirk (1960) model (i.e. Eq. 11) for estimating moisture-dependent  
6 diffusivities for all European soils.

### 7 **3.2 Evaluation of the concept to estimate flux restriction by water table depth**

8 As mentioned in Sect. 2.3, water table depth can be of huge importance limiting the  $^{222}\text{Rn}$   
9 exhalation when it rises to levels that are of the same order as  $\bar{z}$ . These situations are quite  
10 frequent in coastal areas, e.g. of Northern Germany or the Netherlands, or in wetland regions.  
11 Measurements of co-located  $^{222}\text{Rn}$  exhalation rates and shallow water table depths are  
12 available from a field site in Federovskoye, Western Russia (Levin et al., 2002). Thus, we can  
13 test the validity of Eq. (8a) and compare the solution with the measurements from the  
14 Federovskoye transect measurements from Levin et al. (2002, their Fig. 3). The solid lines in  
15 Fig. 2 are estimates of the  $^{222}\text{Rn}$  exhalation rate for a soil with a mean source strength  $Q = 12$   
16  $\text{mBq m}^{-3} \text{ s}^{-1}$  and relaxation depths  $\bar{z}$  of 0.2 m, 0.35 m and 0.5 m (roughly corresponding to  
17 wet, medium and dry soil moisture conditions). The parameterization with the water table  
18 limitation reproduces the observed relation reasonably well and was thus applied to all areas  
19 with shallow water table.

20

## 21 **4 Input data for estimation of the $^{222}\text{Rn}$ fluxes from soils in Europe**

22 Estimation of bottom-up  $^{222}\text{Rn}$  fluxes for the whole of Europe according to Eq. (8) or Eq. (8a)  
23 requires high-resolution data of the following parameters: (1)  $^{226}\text{Ra}$  content in the upper soil  
24 layers, (2) the distribution of soil types and porosity in the unsaturated soil zone, (3) the  
25 emanation coefficient of  $^{222}\text{Rn}$  from the soil grains into the soil air, and (4) soil moisture and  
26 temperature as well as information on frozen soil. Finally, (5) the water table depth should be  
27 known, at least for areas where it is less than 2-3 meters below surface. The respective input  
28 data used in our high-resolution  $^{222}\text{Rn}$  exhalation map are described in the following sections.  
29 If available, we compare with independently measured data to have some quantitative  
30 evaluation of our input data fields (e.g. for soil moisture).

#### 1 4.1 <sup>226</sup>Ra content in the soil

2 The <sup>226</sup>Ra activity concentration in soils is the governing parameter for the <sup>222</sup>Rn flux at the  
3 soil surface. It scales linearly with the exhalation rate. The Geochemical Atlas of Europe  
4 (Salminen, 2005) summarises results of a European-wide effort within the FOREGS (Forum  
5 of European Geological Surveys) Geochemical Baseline Mapping Programme to provide high  
6 quality environmental geochemical baseline data for European stream waters, sediments and  
7 soils. Besides many other elements and trace constituents, the uranium content was also  
8 measured in regularly distributed topsoil and subsoil samples from 26 European countries.  
9 Topsoil samples were collected at 0-25 cm depth (with a potential overlying humus layer  
10 being removed), while subsoil samples were collected from another 25 cm layer located  
11 between 50 and 200 cm depth. Uranium content was measured on residual soil samples (from  
12 the <2 mm grain fraction, with Total Organic Matter (TOC) being removed from these  
13 samples) and is reported in mg Uranium per kg residual soil. As total uranium in soil material  
14 consists of ca. 99% of <sup>238</sup>U, the values given in the Geochemical Atlas (Salminen, 2005) can  
15 be directly transferred into <sup>226</sup>Ra activity concentrations, when assuming secular equilibrium  
16 between <sup>238</sup>U and its daughter <sup>226</sup>Ra. The conversion factor from Uranium concentration to  
17 <sup>238</sup>U activity concentration was taken from IAEA (1989), i.e. 12.35 Bq kg<sup>-1</sup> per mg kg<sup>-1</sup>  
18 uranium.

19 The equally distributed 843 individual topsoil uranium measurements (median ± standard  
20 deviation: 2.03±2.35 mg kg<sup>-1</sup>) and the 792 subsoil uranium measurements (median ± standard  
21 deviation: 2.00±2.34 mg kg<sup>-1</sup>) were interpolated by ordinary kriging (e. g. Wackernagel,  
22 2003) for both layers to the 0.083° x 0.083° grid of our map (see Fig. S2 of the Supplement).  
23 The resolution of our basic map is restricted in its spatial resolution by that of the global soil  
24 texture map of Reynolds et al. (2000), which we used to determine soil texture parameters  
25 (see Sect. 4.2). As the uranium content was measured on residual soil samples with total  
26 organic carbon being removed, we corrected the activity concentrations for “dilution” with  
27 organic carbon, using the TOC data that have also been reported in the Geochemical Atlas of  
28 Europe (Salminen, 2005). This correction is small with typical TOC values in topsoil between  
29 0 and 6 % (median ± standard deviation: 1.73 ± 3.18%) and in subsoil between 0 and 3%  
30 (median ± standard deviation: 0.40 ± 2.86%).

31 For calculating the <sup>222</sup>Rn exhalation rates for each pixel, we used the mean values of topsoil  
32 and subsoil from the TOC-corrected interpolated <sup>226</sup>Ra activity concentrations (i.e.  $c_{Ra}$  of Eq.



1 3). Assuming a depth-constant  $c_{Ra}$  seems to be well justified in view of the very good  
2 agreement between topsoil and subsoil uranium concentrations reported in the Geochemical  
3 Atlas of Europe (Salminen, 2005).

4 For those regions of our map, for which the uranium content was not available in the  
5 Geochemical Atlas (e.g. Belarus, Ukraine), we estimated the  $^{226}Ra$  activity concentration  
6 based on geological information available from the high-resolution global lithological map  
7 GLiM (Hartmann and Moosdorf, 2012). First, a median  $^{226}Ra$  activity concentration was  
8 computed for each lithological class in GLiM using the measured uranium content at all  
9 sampling sites together with co-located GLiM data. The resulting relation was then used to  
10 extrapolate the  $^{226}Ra$  activity concentration map to the regions not covered by the  
11 Geochemical Atlas. Due to this very indirect approach, the resulting  $^{222}Rn$  exhalation rates  
12 will have a much higher uncertainty in these regions (hatched area in Fig. S2 of the  
13 Supplement).

#### 14 **4.2 Distribution of soil types and estimate of emanation coefficients**

15 Soil texture, i.e. the percentages of sand (0.5-2 mm), silt (0.002-0.5 mm) and clay (<0.002  
16 mm) for our  $^{222}Rn$  exhalation map have been taken from Reynolds et al. (2000), a soil  
17 database that is frequently used in modelling studies of similar problems. Porosity and soil  
18 bulk density were computed from soil texture according to Saxton et al. (1986). The data are  
19 given at a horizontal resolution of  $0.083^\circ \times 0.083^\circ$  and for two different depth intervals (from  
20 0-30 cm and from 30-100 cm). Here we use weighted mean values for 0-100 cm depth for all  
21 parameters. As has been shown by Zhuo et al. (2006; 2008), the emanation coefficient  $\epsilon$ , i.e.  
22 the likelihood of a newly formed  $^{222}Rn$  atom to escape the grain and reach the air-filled soil  
23 volume, depends on the soil type and on soil moisture. The soil moisture dependency is,  
24 however, only relevant at very small moisture content below 15% water saturation (i.e. at  $\theta_w$   
25  $< 0.06$  for a typical porosity of  $\theta_p = 0.4$ ). Outside this range  $\epsilon$  was shown to be largely  
26 constant (Zhuo et al., 2006). For simplicity and because water contents below 15% saturation  
27 are very rare in European soils, we used constant (saturation) values for each texture class.  
28 We also neglected the temperature dependence of  $\epsilon$ , as it changes by only a few percent  
29 within a temperature range of 0-20°C (Iskandar et al., 2004). The numbers to calculate  $\epsilon_{sat}$  for  
30 sand, silt and clay are given in Zhuo et al. (2008) in their Table 2. The values must, however,  
31 be exchanged, as was noted by Griffith et al. (2010) and confirmed by W. Zhuo (pers. comm.

1 2013). From this we estimated  $\epsilon_{\text{sat}} = 0.285$  for sand,  $\epsilon_{\text{sat}} = 0.382$  for silt and  $\epsilon_{\text{sat}} = 0.455$  for  
2 clay. These numbers are well in accordance with emanation coefficients determined by  
3 Schüßler (1996) from measured  $^{222}\text{Rn}$  profiles and known  $^{226}\text{Ra}$  contents in different soils of  
4 the surroundings of Heidelberg (M1-M5, see Sect. 5.3 and Table 2). We used weighted mean  
5 values for the different texture classes to estimate the emanation coefficients for each pixel of  
6 our map.

## 7 **4.3 Determination of variable soil parameters: soil moisture, temperature, and** 8 **frost influence**

### 9 **4.3.1 Soil moisture**

10 Soil moisture has a strong impact on the [effective diffusivity  \$D\_e\$](#)  of the soil. Its high temporal  
11 and spatial variability makes it a crucial parameter for determining the  $^{222}\text{Rn}$  exhalation rate at  
12 individual sites. As is illustrated in Fig. 1 and listed in Table 1, the measured mean  $^{222}\text{Rn}$  flux  
13 from the loamy soil at the IUP sampling site changes by about a factor of six between wet ( $\theta_w$   
14  $\approx 0.31$ ) and dry ( $\theta_w \approx 0.12$ ) conditions. Systematic European-wide soil moisture  
15 measurements are still limited. Only few long-term in situ monitoring stations exist. Satellite-  
16 derived soil moisture, although providing relatively good spatial coverage, is only  
17 representative for the uppermost centimetres of the soil and hence not suited for our approach.  
18 Therefore, we use here soil moisture data simulated by soil models driven by numerical  
19 weather prediction models, i.e. these models have been specifically assimilated to determine  
20 soil moisture. Two estimates that provide data at high temporal resolution (3h or 6h) have  
21 been used: (1) Simulations from the Land Surface Model Noah (driven by NCEP-GDAS  
22 meteorological reanalysis), which are part of the Global Land Data Assimilation System  
23 GLDAS (Rodell et al., 2004). The spatial resolution of these estimates is  $0.25^\circ \times 0.25^\circ$  with  
24 depth intervals of 0-10 cm, 10-40 cm, 40-100 cm and 100-200 cm; data for the period of  
25 2006-2012 were used. (2) Simulations from the ERA-Interim/Land reanalysis using the latest  
26 version of the ECMWF land surface model driven by ERA-Interim atmospheric reanalysis  
27 (Balsamo et al., 2015) [were applied as alternative soil moisture model](#). From this model we  
28 used a data set with a horizontal resolution of  $0.75^\circ \times 0.75^\circ$ ; it has a depth resolution with  
29 simulated values for 0-7 cm, 7-28 cm, 28-100 cm and 100-289 cm and is available until 2010.  
30 From both soil moisture models, we calculated vertical means from 0-100 cm depth to cover  
31 the same depth interval as the other input parameters. Note that with a relaxation depth of the

1 <sup>222</sup>Rn activity concentration profile in the soil of typically 20-100 cm (Table 1), soil  
2 parameters of the first 100 cm of the soil are most relevant to describe diffusive transport and  
3 the related flux at the soil surface. We further assume here that all parameters do not change  
4 with depth and are valid also below 100 cm.

5 Both soil moisture data sets were compared to observations from the International Soil  
6 Moisture Network (ISMN; <http://ismn.geo.tuwien.ac.at/>; Dorigo et al., 2011 [and references](#)  
7 [therein](#)). In addition, data from two German sites, Grenzhof near Heidelberg (Wollschläger et  
8 al., 2009) and Gebesee, located in North Eastern Germany (O. Kolle, pers. comm. 2013), as  
9 well as soil moisture data from Binningen, Switzerland (Szegvary et al., 2007b) were used for  
10 comparison (see also Fig. 7). ~~The performance of the land surface models is summarized in~~  
11 ~~Table S1 of the Supplement.~~ Soil moisture contents of the second and third model layer (10-  
12 40 cm and 40-100 cm for GLDAS-Noah, 7-28 cm and 28-100 cm for ERA-I/L) were  
13 compared to measurements at corresponding depths. ~~This preliminary model-observation~~  
14 ~~comparison at European sites yielded an overall mean~~ ~~correlations and mean model data~~  
15 ~~differences are given for each European network~~ ~~bias in ISMN as well as for the additional~~  
16 ~~sites. Both volumetric soil moisture estimates correlate well with of GLDAS-Noah –~~  
17 ~~observations (with a median correlation coefficient of = -0.79 for GLDAS Noah-01 m<sup>3</sup> m<sup>-3</sup>~~  
18 ~~(relative bias = -5%), while the bias between ERA-I/L and observations is +0.82 for ERA-~~  
19 ~~I/L), indicating that the temporal variations in monthly mean values are reasonably well~~  
20 ~~captured by the models. On the other hand, substantial differences between modelled and~~  
21 ~~observed mean values exist for some sites and networks (ranging from an underestimation by~~  
22 ~~60% to an overestimation by 15407 m<sup>3</sup> m<sup>-3</sup> (relative bias = +32%). This underlines that soil~~  
23 ~~moisture simulated by land surface models is a highly model-specific quantity, which often~~  
24 ~~represents the time variations much better than the absolute magnitude (Koster et al., 2009).~~  
25 ~~For the German sites, as well as for many ISMN sites in Central Europe, the ERA-~~  
26 ~~Interim/Land model estimates higher mean soil moisture for the upper 100 cm than the~~  
27 ~~GLDAS-Noah model. This~~ The tendency of ERA-I/L to estimate relatively high soil moisture  
28 is also confirmed by the study of Balsamo et al. (2015), who found an overestimation of  
29 surface soil moisture at the European ISMN sites. ~~Generally, measured soil moisture data fall~~  
30 ~~somewhere in between the two model estimates. Therefore, with all available observations,~~  
31 ~~we cannot per se decide if one or the other model provides more realistic soil moisture~~  
32 ~~estimates.~~

### 4.3.2 Spatial resolution and adjustment of soil moisture estimates to grid/pixel porosities

Soil moisture estimates are only available at lower spatial resolution than the other (constant) soil parameters described above. In order to apply internally consistent data sets for the flux estimates, based on the two different soil moisture models, we use the porosities originally applied in the respective land surface model to calculate [effective diffusivity](#) according to Eq. (11). Consequently, the different flux maps shown in Figs. 3 and 4 have different spatial resolutions. For flux estimates at higher spatial resolution, i.e.  $0.083^\circ \times 0.083^\circ$ , it will be necessary to make an adjustment of the model estimated soil moisture ( $\theta_{w(\text{model})}$ ) to the porosity of the pixel ( $\theta_{p(\text{pixel})}$ ) to make sure the same free pore space is available for diffusion according to

$$\theta_{w(\text{pixel})} = \frac{\theta_{w(\text{model})}}{\theta_{p(\text{model})}} \theta_{p(\text{pixel})} \quad (13)$$

In Eq. (13)  $\theta_{w(\text{pixel})}$  is the adjusted soil moisture and  $\theta_{p(\text{model})}$  is the original porosity used in the soil moisture model. However, in the present paper, we do not show any flux estimates at higher resolution than given by the soil moisture model estimates, but Eq. (13) is used here to adjust modelled soil moisture to the porosities measured at M1-M5 shown in Sect. 5.3 and Fig. 6.

### 4.3.3 Soil temperature

Soil temperature estimates are available from both soil models that provide soil moisture for the different depths. For respective flux estimates, we thus used these values to calculate the temperature dependence of [diffusivity](#) according to Eq. (12).

### 4.3.4 Frost

While the reduction of the  $^{222}\text{Rn}$  exhalation rate through snow cover is assumed as only minor according to Robertson (2004), the influence of frozen soil on the  $^{222}\text{Rn}$  flux may not always be negligible. In order to test its potential impact, we introduced a restriction of the exhalation rate based on atmospheric temperature. A very simple parameterization was used here for comparison with our standard estimates without frost restriction: For each month we have summed up the number of days with maximum air temperature below  $0^\circ\text{C}$  (ice days) and then reduced, for these days, the  $^{222}\text{Rn}$  exhalation rate by 50%. The monthly mean exhalation rate

1 was then calculated as the weighted mean for all days during this month with and without  
2 frost. With this parameterization, we implicitly include also some potential effect of snow  
3 cover that may be present during ice days. The effect of frost restriction on the flux, compared  
4 to our standard estimates where no frost restriction is assumed, is shown in Fig. S3 in the  
5 Supplement.

#### 6 **4.4 Water table depth**

7 As in the case of soil moisture, systematic European-wide measurements of water table depth  
8 that could be used as input for our  $^{222}\text{Rn}$  exhalation map are not existing. Hence, we use data  
9 from a hydrological model simulation by Miguez-Macho et al. (2008). **Supplementary Figure**  
10 **S4 shows the distribution influence of low water table depth on  $^{222}\text{Rn}$  fluxes for Europe,**  
11 **marking large. Large areas of the Netherlands, Northern Italy and Hungary with water table**  
12 **above 2 meters are affected.** For these areas, the  $^{222}\text{Rn}$  exhalation rate was reduced according  
13 to our **approximation estimation** described in Sect. 2.3.

14

### 15 **5 Results and discussion**

16 In this section, we first present results for a typical year (2006) of our two  $^{222}\text{Rn}$  flux maps,  
17 using the two different soil moisture model estimates described in Sect. 4.3.1. Subsequently,  
18 we compare the annual mean  $^{222}\text{Rn}$  flux of our two European maps for the period 2006-2010  
19 with the earlier published maps of Szegvary et al. (2009) and López-Coto et al. (2013). Before  
20 comparing time series of map pixels with observations, the representativeness issue is  
21 discussed for the Heidelberg pixel, where Schüßler (1996) performed long-term  
22 measurements at locations with different soil types. Finally, we show a comparison of  
23 episodic flux measurements with the results of our map and discuss **the potential biases and**  
24 **uncertainties of our approach.**

#### 25 **5.1 Distribution of European $^{222}\text{Rn}$ fluxes**

26 Figure 3 shows the maps and frequency distributions of European  $^{222}\text{Rn}$  fluxes as estimated  
27 with the model parameters described in Sect. 4, applying the two different soil moisture  
28 model estimates (GLDAS-Noah (left panels) and ERA-Interim/Land (central panels)) for  
29 January (top panels) and July 2006 (middle panels). Both maps show some areas of very high  
30  $^{222}\text{Rn}$  exhalations rates, most pronounced in July, which coincide with the areas in Europe

1 where the  $^{226}\text{Ra}$  activity concentration in the upper soil layer is very high. These areas concern  
2 for example the Massif Central in Southern France, the Iberian Peninsula and areas in Central  
3 Italy (compare  $^{226}\text{Ra}$  distribution displayed in Fig. S2 of the Supplement).

4 For both soil moisture models, we find in many regions seasonal differences of the fluxes that  
5 are as large as a factor of two. As mentioned before, these differences originate from the large  
6 changes of soil moisture and thus soil **diffusivity** between the drier summer and the – in  
7 general – wetter winter conditions. The frequency distribution of  $^{222}\text{Rn}$  fluxes, displayed in  
8 the lower part of Fig. 3, is most confined during winter (January 2006) and when calculated  
9 with the ERA-Interim/Land soil moisture data; these fluxes also show a low median value of  
10 only ~~5.8183~~ **5.3638**  $\text{mBq m}^{-2} \text{ s}^{-1}$  (**Inter Quartile Range (IQR) = 5.3638**  $\text{mBq m}^{-2} \text{ s}^{-1}$ ). This is about half  
11 of the median flux estimated with the GLDAS-Noah soil moisture data set for January 2006  
12 (~~11.9912.08~~ **12.08**  $\text{mBq m}^{-2} \text{ s}^{-1}$ ). During summer (July 2006), both frequency distributions of fluxes  
13 are broader than during winter (IQR: ERA-I/L = **8.4939**  $\text{mBq m}^{-2} \text{ s}^{-1}$  and GLDAS-Noah =  
14 **11.5847**  $\text{mBq m}^{-2} \text{ s}^{-1}$ ). The median values are much larger than in January 2006, i.e. in the  
15 case of the ERA-I/L soil moisture more than a factor of two larger, while the difference of the  
16 medians in July 2006 between the two maps is much smaller **than in winter** (only about 30%).

17 As both maps use the same  $^{226}\text{Ra}$  distribution and also the same  $^{222}\text{Rn}$  emanation coefficient  
18 (i.e. the same  $^{222}\text{Rn}$  source term), differences of  $^{222}\text{Rn}$  flux of the two maps are solely due to  
19 the differences of **diffusivity**, which we calculate from modelled soil moisture using the  
20 individual soil porosity data from the two models (according to Eq. (11)). The right panels in  
21 Fig. 3 show the flux differences between the two maps for January and July 2006. In fact, the  
22 differences of fluxes between the two maps are not homogeneous all over Europe, but they  
23 show a distinct north to south gradient. While fluxes estimated with ERA-I/L soil moisture for  
24 January 2006 are slightly higher than those estimated based on GLDAS-Noah in Sweden,  
25 Denmark and some parts of Northern Germany and Poland, they are much smaller than  
26 GLDAS-Noah-based fluxes in Central and Southern Europe. The differences in soil porosity  
27 in the two models are only small (i.e. ERA-I/L uses about 10% smaller porosity in Northern  
28 than in Central Europe, while porosity is pretty homogeneous all over Europe in GLDAS-  
29 Noah and similar to ERA-I/L in Central Europe) but very distinct differences are found in the  
30 soil moisture distributions. Soil moisture is much lower in the GLDAS-Noah model estimates  
31 for Central and Southern Europe than in ERA-I/L. Only in some areas of Scandinavia and the  
32 northern coasts of Central Europe, ERA-I/L estimates lower soil moisture than GLDAS-

1 Noah. This directly translates into higher  $^{222}\text{Rn}$  fluxes in the mentioned regions of  
2 Scandinavia.

3 The mean  $^{222}\text{Rn}$  flux for the period 2006-2010 is estimated to be  $10 \text{ mBq m}^{-2} \text{ s}^{-1}$  (ERA I/L soil  
4 moisture) or  $15 \text{ mBq m}^{-2} \text{ s}^{-1}$  (GLDAS-Noah soil moisture) with mean seasonal variations  
5 ranging from  $7 \text{ mBq m}^{-2} \text{ s}^{-1}$  in February to  $14 \text{ mBq m}^{-2} \text{ s}^{-1}$  in August (ERA I/L soil moisture)  
6 and from  $11 \text{ mBq m}^{-2} \text{ s}^{-1}$  in March to  $20 \text{ mBq m}^{-2} \text{ s}^{-1}$  in August (GLDAS-Noah soil moisture).

7 The huge differences between the estimates with different soil moisture input data emphasize  
8 the importance of direct comparison of our process-based  $^{222}\text{Rn}$  flux estimates with measured  
9 fluxes, in order to find out, which soil moisture model would better fit real ambient  
10 conditions. This comparison is shown below in Sects. 5.4 and 5.5.

## 11 **5.2 Comparison of annual mean $^{222}\text{Rn}$ fluxes with those from other published** 12 **maps**

13 Before comparing with observations at individual sites, we compare the distribution of annual  
14 mean fluxes calculated here based on the two soil moisture models for 2006-2010 with the  
15 other published European maps of Szegvary et al. (2009) for 2006 and of López-Coto et al.  
16 (2013). The latter is shown as climatology for the years 1957 - 2002. The maps and  
17 normalized frequency distributions are displayed in Fig. 4. Zonal averages of  $1^\circ$  latitudinal  
18 bands are compared in Fig. 5. The general shape with higher  $^{222}\text{Rn}$  exhalation rates in regions  
19 of high  $^{238}\text{U}$  activity concentrations (e.g., on the Iberian Peninsula) is similar in all four maps.  
20 The difference between GLDAS-Noah- and ERA-I/L-based fluxes, with generally higher  
21 fluxes estimated based on the GLDAS-Noah soil moisture model (except for some areas in  
22 Northern Europe), was discussed before for January and July 2006 (Fig. 3) and is also visible  
23 in annual mean flux estimates. The annual median values for the 2006-2010 period differ by  
24 more than 50% (Fig. 4, lower four panels). There is relatively good agreement in the spatial  
25 pattern, in the annual medians and IQRs between the ERA-I/L and the López-Coto et al.  
26 (2013) map. This is because the basis of the López-Coto et al. (2013) map is also the  $^{238}\text{U}$   
27 distribution from the Geochemical Atlas of Europe (Salminen, 2005), and López-Coto et al.  
28 (2013) use a similar process-based soil transport model as described here, but the  
29 parameterization for diffusivity developed by Rogers and Nielson (1991). Soil moisture  
30 estimates in López-Coto et al. (2013) are from ERA-40 reanalyses, which are based on an  
31 earlier version of the land surface model than used in ERA-I/L. Soil moistures in ERA-40



1 show an overall smaller variability than the ERA-I/L model estimates (Balsamo et al., 2015)  
2 used in our study (compare also Sect. 5.4, which discusses time profiles in comparison to  
3 observations). The maps of differences between our study and the López-Coto et al. (2013)  
4 climatology are displayed in Fig. S5 in the Supplement. While our GLDAS-Noah-based  
5 estimates are higher than López-Coto et al. (2013) throughout Europe (with the exception of  
6 Northern Ireland and a few areas in Italy) the higher fluxes of our ERA-I/L-based estimates  
7 compared to López-Coto et al. (2013) are most prominent in Scandinavia. Differences in  
8 annual mean  $^{222}\text{Rn}$  fluxes between these two maps are small in Central Europe. The  
9 difference in annual fluxes in regions north of  $60^\circ\text{N}$  (Fig. 5) might, at least to some extent, be  
10 caused by the reduction of  $^{222}\text{Rn}$  fluxes in snow-covered regions, which is included in the flux  
11 map of López-Coto et al. (2013) but not in our standard estimates. Including a restriction  
12 during frozen soil conditions in our flux estimates (orange and cyan lines in Fig. 5) reduces  
13 the difference of the annual mean in this region, but they are still more than 50% higher than  
14 López-Coto et al. (2013). However, it is important to keep in mind that López-Coto et al.  
15 (2013) use a ca. 40% smaller emanation coefficient of 0.2 for all soils, compared to a median  
16 value of 0.35 in our study. This difference is responsible for a generally 40% lower  $^{222}\text{Rn}$   
17 exhalation rate in the López-Coto et al. (2013) map than estimated for our two maps.

18 The Szegvary et al. (2009) map has lower spatial resolution and less pronounced hot spots of  
19 exhalation rates, but the median of its annual mean exhalation rates lies between our GLDAS-  
20 Noah- and ERA-I/L-based estimates. However, as Szegvary et al. (2009) used  $\gamma$ -dose rate  
21 observations and an empirical correlation with measured  $^{222}\text{Rn}$  fluxes, their fluxes are  
22 significantly different in certain areas of Europe. In particular, the pronounced maximum in  
23 the French Massif Central, where high  $^{238}\text{U}$  concentrations are measured in the soils (Fig. S2)  
24 is only slightly visible in the Szegvary et al. (2009) map. A detailed picture of the differences  
25 between our maps and the Szegvary et al. (2009) estimate for 2006 is shown in the  
26 Supplement (Fig. S5). Largest differences are seen in Central Europe, where our GLDAS-  
27 Noah-based estimates are in many places larger than the Szegvary et al. (2009) estimates by a  
28 factor of two, while ERA-I/L-based estimates are often about 50% smaller compared to the  
29 Szegvary et al. (2009) estimates. In Northern Scandinavia our two estimates are higher than  
30 the Szegvary et al. (2009) map. The reason might be the shielding effect of snow cover on the  
31 observed  $\gamma$ -dose rate (Szegvary et al., 2007a). Including the frost restriction in our flux

1 estimates reduces the difference of the annual mean in this region but leads to values lower  
2 than in the Szegvary et al. (2009) map in Southern Scandinavia (Fig. 5).

### 3 **5.3 Representativeness of local observations to validate the $^{222}\text{Rn}$ flux maps**

4 A large number of systematic direct  $^{222}\text{Rn}$  flux measurements using the accumulation  
5 chamber technique were carried out in the 1980s and 1990s at five sampling sites south of  
6 Heidelberg, Germany. Dörr and Münnich (1990) started these measurements in 1984 at a  
7 sandy soil site (M1) as well as at a clay-loam soil site (M4). Schüßler (1996), who sampled  
8 additional sites close to the earlier plots from Dörr and Münnich (1990) continued  
9 measurements on these plots. The soil parameters of the five sampling sites M1-M5 are listed  
10 in Table 2. For these sites we estimated the percentages of clay, silt and sand according to  
11 Cosby et al. (1984, Table 2) from the soil type descriptions given by Schüßler (1996). The  
12 soil properties of other IUP sampling sites studied by Schell (2004; Gebesee), Schmithüsen  
13 (2012; IUP) and Schwingshackl (2013; Gif-sur-Yvette (Gif)) at locations in Germany and  
14 France are also listed in Table 2. In addition, the soil parameter values of the  $0.083^\circ \times 0.083^\circ$   
15 pixels from the high-resolution soil parameter map, in which the measurement sites are  
16 located, are listed. From comparison, we can assess the representativeness of the  
17 measurement sites for their corresponding pixel of the map. While the Sandhausen sites M1-  
18 M3 are not at all representative for the corresponding map pixel, the soil texture and  $^{226}\text{Ra}$   
19 activity concentration of the loamy sites M4 and M5 as well as the IUP site, discussed already  
20 above (Sect. 3.1), are well comparable with the map pixel. The latter are thus suitable for  
21 validation of our maps and the transport model approach. For Gebesee in Northern Germany,  
22 actual site parameters agree well with the soil parameters of the map. Only the  $^{226}\text{Ra}$  content  
23 is about 20% lower in the map than measured by Schwingshackl (2013). Contrary, for Gif-  
24 sur-Yvette in France porosity, bulk density and  $^{226}\text{Ra}$  activity concentration are significantly  
25 different from the pixel values. This should be kept in mind when comparing our process-  
26 based maps with these observations.

27 Figure 6 shows the climatology of the monthly mean  $^{222}\text{Rn}$  exhalation rates measured at the  
28 Heidelberg M1-M5 stations over the periods of 1987-1995 (M1, M2, M4) and 1987-1998  
29 (M3, M5). Jutzi (2001) calculated these averages from the individual data of regular one - to  
30 two-weekly flux measurements reported by Schüßler (1996). The strong dependency of the  
31 mean exhalation rate on soil type is clearly visible. The clay or loamy soils (M4 and M5)  
32 show the highest fluxes with significant seasonal variations of the exhalation rate with up to a

1 factor of two larger values in July/August compared to January/February. In contrast, the  
2 seasonality at M1 and M3 is only very weak and fluxes at the sandy sites (M1-M3) are about  
3 three times lower than at M4 and M5.

4 Figure 6 also shows calculated exhalation rates (according to Eq. (8)) based on the measured  
5 soil parameters listed in Table 2 and the climatology of soil moisture for the Heidelberg pixel  
6 as calculated from the two soil moisture models for the years 2006-2010. Note that for these  
7 process-based calculations the GLDAS-Noah model used a porosity of  $\theta_p = 0.434$  in the map  
8 pixels while the ERA-Interim/Land model used  $\theta_p = 0.439$ , i.e. both significantly different  
9 from measured porosities, in particular at the sites with sandy soils (M1 and M3, Table 2). For  
10 our calculations, we thus individually adjusted the soil moistures for all sites M1-M5  
11 according to Eq. (13) to better approximate the pore volumes available for diffusion at the  
12 different sites. With these adjustments, the flux estimates based on GLDAS-Noah soil  
13 moisture agree very well with observations for the sites M1-M3, but are about 30% too high  
14 for the stations M4 and M5. When using modelled ERA-I/L soil moisture data, estimated  
15 mean seasonal  $^{222}\text{Rn}$  fluxes are always lower than observations, by up to a factor of three at  
16 M1 and M3 and by about a factor of two at the loamy and clay sites M2, M4 and M5. Without  
17 adjustment of modelled soil moisture to the site porosities, for all sites and both soil moisture  
18 estimates, modelled  $^{222}\text{Rn}$  fluxes would be underestimated by up to a factor of six (results not  
19 shown in Fig. 6). From this comparison of process-based estimates with long-term  
20 observations, we can conclude that (1) the agreement between estimates and observations  
21 strongly depends on the validity of soil texture parameters used in the map; (2) modelled soil  
22 moisture values need to be adjusted to the local porosity according to Eq. (13), if reliable flux  
23 estimates shall be calculated; (3) in the Heidelberg pixels associated to M1-M5, GLDAS-  
24 Noah-based  $^{222}\text{Rn}$  flux estimates agree rather well to existing observations while ERA-I/L-  
25 based estimates largely underestimate fluxes at all sites. This comparison also emphasizes that  
26 ~~proper quantitative validation of our  $^{222}\text{Rn}$  exhalation map is only feasible~~ can be misleading, if  
27 ~~the observations are representative for information on soil properties is missing at the pixels of~~  
28 ~~the map. In the case of the measurement sites discussed in Fig. 6, this is true only for sites M4~~  
29 ~~and M5.~~

## 5.4 Comparison of model-based $^{222}\text{Rn}$ flux estimates with measured time series and other flux maps

As demonstrated in the previous section, proper validation of our  $^{222}\text{Rn}$  flux estimates requires comparison with direct measurements carried out on soils representative for the respective pixel of the map. However, systematic  $^{222}\text{Rn}$  flux measurements in Europe are very sparse so that we include in this section all sites (except for M1-M4 that have already been discussed before, see Sect. 5.3), which have observations available to us over the course of at least four months. Figure 7 compares estimates from our  $^{222}\text{Rn}$  flux map based on the two soil moisture models GLDAS-Noah (red lines: standard, orange: with frost restriction), ERA-I/L (blue lines: standard, cyan: with frost restriction) with those from Szegvary et al. (2009: dark green lines), from López-Coto et al. (2013: light yellow-green lines) and with observations (black dots). Note that in case the observations do not fall into the modelled time span of 2006-2008 displayed here, the data points have been repeated as climatology for all years. If the dotted red and blue lines can be distinguished, they show the effect of shallow water table depth. Fluxes that are not restricted by the water table, contrary to those that are restricted, are then visible as dotted (red and blue) lines (relevant at Lutjewad and Gebesee where the water table is less than 2 m below the soil surface); otherwise, the solid and dotted lines fall onto each other. Figure 7 also shows the soil moisture estimates calculated by the two land surface models as well as direct soil moisture measurements in different depths, if available.

For most sites shown here, the ERA-Interim/Land-based  $^{222}\text{Rn}$  fluxes (plotted in blue and cyan) are significantly lower (often by more than a factor of two) than those estimated with the GLDAS-Noah soil moisture data (plotted in red and orange). Accordingly, ERA-I/L soil moisture estimates are significantly higher than those estimated by GLDAS-Noah at these sites; note that porosities do not differ very much in between models at these sites, with a maximum difference of 6% at Gebesee. Only at Lutjewad the two flux estimates are similar despite the high soil moisture in ERA-I/L; here also the porosity in the ERA-I/L model is by almost a factor of two higher than in GLDAS-Noah. At all sites except for Gif-sur-Yvette and Lutjewad, ERA-I/L-based fluxes are significantly lower than observed fluxes.

At Pallas station in Northern Finland no direct  $^{222}\text{Rn}$  flux measurements are available. For this reason, we use flux estimates derived from summer observations in the atmosphere and atmospheric transport modelling (Lallo et al., 2009). For this time of the year, the GLDAS-Noah-based  $^{222}\text{Rn}$  flux results compare best with the data. For the winter months, López-Coto

1 et al. (2013) predict very low fluxes at Pallas, and here the effect of frost restriction on  
2 GLDAS-Noah- and ERA-I/L-based estimates becomes visible (difference between red and  
3 orange resp. blue and cyan lines in Fig. 7a).

4 A station with very shallow water table is Lutjewad, located at the Netherland's North Sea  
5 coast. Not taking into account ground water table restriction in the modelled  $^{222}\text{Rn}$  exhalation  
6 rate (dotted lines in Fig. 7b) would largely overestimate the flux in both approaches by more  
7 than a factor of four. Here the Szegvary et al. (2009) and the López-Coto et al. (2013) models  
8 overestimate observed fluxes by more than a factor of two to three. Taking into account the  
9 restriction due to the shallow water table brings the modelled  $^{222}\text{Rn}$  exhalation rate closer to  
10 the observations but also reduces the amplitude of the seasonal variations. Note that ERA-I/L-  
11 based and GLDAS-Noah-based fluxes are almost identical under water table restriction and  
12 therefore hardly distinguishable in Fig. 7b.

13 At Gebesee, co-located soil moisture measurements are available. They agree very well with  
14 the GLDAS-Noah-based model estimates (Fig. 7c) and further, GLDAS-Noah-based  $^{222}\text{Rn}$   
15 fluxes fit the observations very well. Here again, the water table depth flux restriction turns  
16 out to be important: Estimated GLDAS-Noah-based fluxes not restricted by water table depth  
17 are significantly higher in early summer than observed fluxes (dotted red line in Fig. 7c), but  
18 those restricted by water table agree on average well with observations. At the end of the  
19 summer, local water table depth may be deeper than in winter and spring, which is why  
20 observations then seem to fall on the unrestricted GLDAS-Noah-based model estimates.

21 As has been indicated already in Fig. 6, the GLDAS-Noah-based estimates for M5-Nußloch  
22 are slightly higher than observations while the ERA-I/L-based estimates underestimate the  
23 observations by about a factor of two (Fig. 7d). Note, however, that in the current comparison,  
24 contrary to the results shown in Fig. 6, we use for both modelled fluxes all parameters,  
25 including  $^{226}\text{Ra}$  activity concentration and soil porosity, from our map and not from  
26 observations. Although absolute fluxes are not perfectly reproduced, both our models seem to  
27 capture much better the seasonal amplitude of observations than estimates by Szegvary et al.  
28 (2009) and López-Coto et al. (2013) models. The good agreement between GLDAS-Noah-  
29 based and observed  $^{222}\text{Rn}$  fluxes at M5 is accompanied by good agreement of GLDAS-Noah-  
30 modelled soil moisture and respective observations. Soil moisture data plotted for M5 do not  
31 exactly stem from the M5 site but are taken from a soil monitoring station north of Heidelberg  
32 at Grenzhof (Wollschläger et al., 2009). Modelled soil moistures as well as soil properties in

1 the grid cells corresponding to the location of M5 and Grenzhof are identical in GLDAS-  
2 Noah and very similar in ERA-I/L.

3 At Gif-sur-Yvette, all models except for GLDAS-Noah seem to reproduce well at least the  
4 annual mean observed fluxes (Fig. 7e). However, the seasonal amplitude seems to be best  
5 captured by the ERA-I/L-based and the GLDAS-Noah-based estimates, whereas the Szegvary  
6 et al. (2009) model for 2006, if also valid for other years, and the López-Coto et al. (2013)  
7 model underestimate the seasonal amplitude. GLDAS-Noah-based fluxes are larger than  
8 observations by about a factor of two. This is very surprising, because  $^{226}\text{Ra}$  activity  
9 concentration of the map pixel is a factor of two smaller than those measured by  
10 Schwingshackl (2013) (see Table 2). From this difference alone, we would expect an  
11 underestimation of Gif-sur-Yvette flux observations by both of our flux estimates. On the  
12 other hand, the shallow water table at the measurement site (Campoy et al., 2013) might  
13 restrict the  $^{222}\text{Rn}$  fluxes. This situation is not represented in our maps, where the water table is  
14 well below 10 m in this region.

15 At Binningen, Switzerland, which is the measurement station that Szegvary et al. (2009) also  
16 used for the empirical  $\gamma$ -dose rate-based estimates of their  $^{222}\text{Rn}$  flux map for 2006, their  
17 measured data fall in between our GLDAS-Noah- and ERA-I/L-based fluxes (Fig. 7f). Only  
18 in spring 2007 both our estimates are higher than the observed fluxes. Soil moisture estimates  
19 in both reanalysis are most of the time lower than the observations but capture the temporal  
20 variation rather well. In three summer months of 2006 Szegvary et al. (2009) model estimates  
21 are slightly lower than the observations, while the López-Coto et al. (2013) model results are  
22 considerably lower than all other model estimates and lower than the observations by at least  
23 a factor of two.

24 In summary, we conclude that at three out of six stations the (generally higher) GLDAS-Noah  
25 soil moisture-based  $^{222}\text{Rn}$  exhalation rates are in good agreement with observations. At two of  
26 these sites, where we have data available, this correlates with good agreement of model-  
27 calculated and observed soil moisture. Flux estimates based on ERA-Interim/Land soil  
28 moistures have the tendency to underestimate observed fluxes and only fit well at one of our  
29 comparison sites (Gif-sur-Yvette). The two published maps, in particular that developed by  
30 López-Coto et al. (2013), generally underestimate measured fluxes with the exception of the  
31 coastal site Lutjewad. There the shallow water table depth is not taken into account in these  
32 models, which leads to large over-estimation. Concerning the seasonal amplitude of fluxes,

1 the GLDAS-Noah-based estimates as well as those based on ERA-I/L soil moisture are in  
2 most cases very well in line with observations. Contrary, Szegvary et al. (2009) flux estimates  
3 largely underestimate seasonal amplitudes, at least in 2006. The same is true for the López-  
4 Coto et al. (2013) model estimates. As mentioned before, a large part of the general  
5 underestimation by López-Coto et al. (2013) may be due to the use of a too low emanation  
6 coefficient in their estimates. Based on available observations, the effect of frozen soils  
7 cannot be evaluated. However, restriction due to shallow water table turns out to be  
8 important, not only at the coastal site Lutjewad, but potentially also in river plains such as in  
9 the surroundings of the Gebesee site.

## 10 **5.5 Comparison with published episodic $^{222}\text{Rn}$ flux observations**

11 Since only very few systematic  $^{222}\text{Rn}$  flux measurements during different seasons are  
12 available in the literature, validation of our new  $^{222}\text{Rn}$  flux map is far from exhaustive. In  
13 order to better judge at least the reliability of the European-wide flux estimates, we have  
14 compiled here all published  $^{222}\text{Rn}$  flux measurements available to us, even if they are only  
15 based on episodic field campaigns (see Table S2S1 in the Supplement). Larger short-term  
16 data sets from a single site have been averaged to monthly values. ~~Figure 8 (left and included~~  
17 ~~in our model-data comparison in Fig. 8. The map in Fig. 8 (upper panel) shows the~~  
18 ~~geographical distribution of these episodic observations and their individual values colour-~~  
19 ~~coded. The frequency distribution of these distributions of the differences between modelled~~  
20 ~~and measured  $^{222}\text{Rn}$  fluxes are shown in Fig. 8 (right the lower part, black histogram) in~~  
21 ~~comparison to the frequency distributions of the respective monthly of Fig. 8. We find no~~  
22 ~~geographical dependency of the differences (not shown) but a large mean values estimated for~~  
23 ~~the corresponding pixels of the flux maps bias between ERA-I/L-based on the two soil~~  
24 ~~moisture data sets (red histogram) and measured fluxes. While the GLDAS-Noah, blue~~  
25 ~~histogram: ERA-I/L). While the observations differences yield a median mean value of~~  
26 ~~12.22 close to zero ( $0.82 \text{ mBq m}^{-2} \text{ s}^{-1}$  (with  $\text{IQR} = 13.49$   $11.29 \text{ mBq m}^{-2} \text{ s}^{-1}$ ), the GLDAS-~~  
27 ~~Noah-based model gives a median of  $15.03 \text{ Bq m}^{-2} \text{ s}^{-1}$  ( $\text{IQR} = 9.47 \text{ mBq m}^{-2} \text{ s}^{-1}$ ) and the ERA-~~  
28 ~~I/L-based estimates a median of  $7.43 \text{ Bq m}^{-2} \text{ s}^{-1}$  ( $\text{IQR} =$  are on average lower than observations~~  
29 ~~by  $5.61 \text{ mBq m}^{-2} \text{ s}^{-1}$ ). The median of observations is about 40% higher than the ERA-I/L-~~  
30 ~~based flux estimates while it is about 20% lower than the GLDAS-Noah-based estimates~~  
31  ~~$73 \text{ Bq m}^{-2} \text{ s}^{-1}$  ( $\text{IQR} = 11.21 \text{ mBq m}^{-2} \text{ s}^{-1}$ ). This is in accordance with the earlier comparison based~~  
32 ~~on the more systematic long-term results at fewer stations, discussed in Sect. 5.4, and gives a~~



1 strong hint that the GLDAS-Noah-based estimates on average provide the more accurate flux  
2 estimates than those based on ERA-I/L-soil moisture, which seem to be systematically too  
3 low. However, since IQR values of radon flux differences are large for both soil moisture  
4 models, a definitive decision, which soil moisture model to use is not yet possible. The large  
5 IQR values are most probably caused by the non-representativeness of many of our  
6 observations for the entire pixel and due to very similar uncertainties in the bottom-up  
7 information used for both flux estimates (see also Sec. 5.6).

## 8 **5.6 Discussion of uncertainties**

### 9 **5.6.1 Soil moisture**

10 Temporal and spatial variations of soil moisture have a huge influence on the **effective**  
11 **diffusivity** in the soil and thus on the  $^{222}\text{Rn}$  exhalation rate. This can clearly be seen when  
12 comparing the GLDAS-Noah-based and the ERA-I/L based  $^{222}\text{Rn}$  flux maps. Using our  
13 observations at the Heidelberg IUP site we find that the **diffusivity** differences during dry and  
14 wet conditions are as large as a factor of 20, leading to differences in the fluxes up to a factor  
15 of seven (Table 1). When comparing model estimated soil moisture values with respective  
16 observations it is not per se clear, if one or the other soil moisture model would generally  
17 provide more realistic values (see ~~Table S1 in the Supplement~~). ~~Likewise, comparison of Fig.~~  
18 ~~7). Comparison of~~  $^{222}\text{Rn}$  flux map results with **point** observations does ~~not allow~~  
19 ~~favouring~~ also not always favour one ~~or the other~~ soil moisture model. ~~While~~ However, on  
20 average over Europe, annual mean fluxes ~~may be over- or underestimated by one of the~~  
21 ~~models~~ are better reproduced with the GLDAS-Noah-based model. On the other hand, both  
22 ~~models~~ capture the seasonal amplitude of the fluxes very well. The same is true for the  
23 seasonal amplitudes of the soil moisture estimated by both models. ~~And, most important, in~~  
24 ~~cases where the soil moisture at a station is correctly captured by one of the models, we also~~  
25 ~~find good agreement between the modelled and measured~~  $^{222}\text{Rn}$  fluxes (e.g. GLDAS-Noah at  
26 Gebesee and M5/Grenzhof). This ~~indicates that there may be some systematic shortcomings~~  
27 ~~in the parameterization~~ underlines the importance of ~~the soil moisture models or a conceptual~~  
28 ~~difference in the meaning of the variable ‘soil moisture’ in the realistic soil moisture data for~~  
29  $^{222}\text{Rn}$  exhalation modelling. With currently available and frequently used soil moisture  
30 models (~~Koster et al., 2009~~). ~~In cases where the soil moisture at a station is correctly captured~~  
31 ~~by one of the models, we also find good agreement between the~~, biases in the mean European

1  $^{222}\text{Rn}$  flux ~~estimated by that model and the measured one (e.g. GLDAS Noah at Gebesee and~~  
2 ~~M5/Grenzhof)~~ of 50% can be introduced.

### 3 **5.6.2 Diffusivity model**

4 Even if we had good estimates of soil moisture, we need to keep in mind that the Millington-  
5 Quirk (1960) model used in this study does not necessarily describe *effective diffusivity* in the  
6 unsaturated soil zone correctly. Comparison of model-based *diffusivity with diffusivity*  
7 estimated from observed  $^{222}\text{Rn}$  soil profiles (Fig. 1) shows differences as large as a factor of  
8 two at medium dry conditions. This may translate into differences of the fluxes of up to 40%  
9 during these conditions. Therefore, also shortcomings in the parameterization of *diffusivity*  
10 may considerably contribute to the uncertainty of the  $^{222}\text{Rn}$  flux. However, using different  
11 parameterizations as e.g. the one of Rogers and Nielson (1991), as done by Griffiths et al.  
12 (2010) and López-Coto et al. (2013) does not improve the situation (see Table 1). *We*  
13 *estimate mean uncertainty of  $^{222}\text{Rn}$  fluxes to be on the order of 30% due to our choice of the*  
14 *diffusivity model.*

### 15 **5.6.3 $^{226}\text{Ra}$ content**

16 An important parameter determining the  $^{222}\text{Rn}$  flux from soils is the  $^{226}\text{Ra}$  content. In our  
17 study we have used an interpolated  $^{238}\text{U}$  distribution based on systematic measurements  
18 published in the European Geochemical Atlas (Salminen, 2005). Uncertainties in the soil  
19 sample analysis (Sandström et al., 2005) and the interpolation are both less than 10%. From  
20 the interpolated  $^{238}\text{U}$  distribution, we estimated  $^{226}\text{Ra}$  activity concentration by assuming  
21 secular equilibrium between  $^{238}\text{U}$  and its daughter  $^{226}\text{Ra}$ . This assumption may not always be  
22 fulfilled at all sites due to preferential leaching of  $^{234}\text{U}$  from the soil grains, so that our  $^{238}\text{U}$ -  
23 based equilibrium estimate of  $^{226}\text{Ra}$  must be seen as an upper limit of the true  $^{226}\text{Ra}$  values.  
24 However, when comparing the  $^{226}\text{Ra}$  values from the map with point measurements made at  
25 IUP Heidelberg, we find satisfactory agreement if other soil parameters, such as texture and  
26 bulk density, are similar, i.e. if the point measurement is representative for the pixel (data not  
27 shown). An example of obvious differences between the soil characteristics of our  
28 measurement site and the pixel of the map is Gif-sur-Yvette, France. Here we observe a factor  
29 of two higher  $^{226}\text{Ra}$  activity concentration in our measurement than assumed for the map  
30 pixel, but also bulk density and porosity show a large difference. *Therefore, the average*

1 uncertainty of our interpolated  $^{226}\text{Ra}$  activity concentration data is most probably less than  
2 15%.

### 3 **5.6.4 Emanation coefficient**

4 Besides the  $^{226}\text{Ra}$  activity concentration in the bulk soil material, the emanation coefficient is  
5 an essential parameter for correctly estimating the  $^{222}\text{Rn}$  exhalation rate. Only few  
6 measurements of the emanation coefficients for different soil types and environmental  
7 conditions exist and reported values span a wide range of 0.05 to 0.7 (Nazaroff, 1992). The  
8 emanation coefficient estimates of our study compare well with the observation-based  
9 estimates by Schüßler (1996) around the Heidelberg site. The averaged value used in our  
10 study (0.35) is, however, by 75% higher than the constant emanation coefficient of 0.2 used  
11 by López-Coto et al. (2013) for all soils. The underestimation of the  $^{222}\text{Rn}$  fluxes by the  
12 López-Coto et al. (2013) model at most sites indicates that an emanation coefficient of 0.2 is  
13 probably too small. More measurements of emanation coefficients and their dependence on  
14 soil texture would be helpful to reduce the uncertainty in this parameter. *Still, the uncertainty*  
15 *of our assumption of the texture-specific emanation coefficient as used for our maps is*  
16 *probably smaller than 20%.*

### 17 **5.6.5 Constancy of transport parameters with depth**

18 One basic assumption in our estimate is homogeneity of soil parameters with depth up to 1m.  
19 While the differences of  $^{238}\text{U}$  in the European Geochemical Atlas between upper and lower  
20 soil layers are only minor, other soil parameters such as porosity and texture may not be as  
21 homogeneous with depth. Porosity derived from the Reynolds et al. (2000) soil texture data  
22 set differs by ca. 3 % between the two soil layers, but this presumably underestimates vertical  
23 variability. The largest vertical inhomogeneity is most probably that of soil moisture. During  
24 summer months, at one of our sampling sites we observed that soil moisture differs by a  
25 factor of two between 30 and 90 cm depths (see Fig. 7 for M5 Nußloch). However, the  
26 differences between the two soil models, GLDAS-Noah and ERA-I/L can be even larger.  
27 Therefore, with the current reliability of soil moisture input data from the models, our  
28 simplification assuming homogeneous parameters throughout the unsaturated soil seems  
29 justified. In any case, except for dry summer conditions, more than three quarters of the total  
30  $^{222}\text{Rn}$  flux at the soil surface originate from the upper 50 cm of the soil; one should thus make  
31 sure that all parameters in this upper layer are determined as reliable as possible.

## 1 **5.6.6 Soil texture**

2 For consistency, we use in our European  $^{222}\text{Rn}$  flux estimations the same porosity as applied  
3 in the soil moisture simulations of the respective land surface model. In both models, the soil  
4 properties were derived from the FAO Digital Soil Map of the World (FAO DSMW), though  
5 from different versions (Reynolds et al., 2000; FAO, 2003), and indeed soil porosities in both  
6 models are very similar. Only parts of Northern Europe show differences of up to 10%. Soil  
7 databases are constantly improving as more soil information is collected and more detailed  
8 digital soil data sets are becoming available, like the Harmonized World Soil Database  
9 (HWSD, FAO/IIASA/ISRIC/ISSCAS/JRC, 2012) and the Global Soil Data set for use in  
10 Earth System Models (GSDE; Shangguan et al., 2014), which should reduce uncertainties  
11 associated with soil texture. However, the comparisons between soil properties in these new  
12 data sets (in Shangguan et al., 2014) also reveal maximum porosity differences of around 10%  
13 in Northern Europe.

## 14 **5.6.7 Frost**

15 In our sensitivity test with a very simple parameterization of frost and/or snow conditions,  
16  $^{222}\text{Rn}$  flux estimates in Scandinavia and Eastern Europe are reduced by 30-40% during winter  
17 and by 10% for annual mean fluxes in this region. However, due to the lack of systematic flux  
18 measurements during winter conditions, this parameterization could not be evaluated and can  
19 only give an estimate of the associated uncertainties. For more reliable estimations of  $^{222}\text{Rn}$   
20 fluxes in higher latitudes during winter, more investigations on the influence of frost and  
21 snow on  $^{222}\text{Rn}$  exhalation is desirable. [Uncertainties in annual mean  \$^{222}\text{Rn}\$  fluxes mainly in  
22 Northern Europe due to neglecting flux restriction by frozen soil may be of order 10-20%.](#)  
23 [However, we do not include this uncertainty in our overall uncertainty estimate below.](#)

## 24 **5.6.8 Combined uncertainty of the $^{222}\text{Rn}$ flux map**

25 [The overall uncertainty of  \$^{222}\text{Rn}\$  flux estimates for individual pixels, not taking into account  
26 systematic biases in the soil moisture models, can be roughly deduced from individual  
27 uncertainties of all parameters by error propagation. As discussed above, the two largest  
28 uncertainties stem from the uncertainty to determine effective diffusivity based on soil  
29 texture/porosity and soil moisture \(ca. 30%\). The uncertainty contribution of modelled soil  
30 moisture is probably also of order 30%, while the emanation coefficient is assumed to be  
31 known to about 25%. Other parameters are uncertain to about 10-15% on the pixel scale.](#)

1 Altogether, we therefore estimate the uncertainty of modelled fluxes for individual pixels to  
2 about 50%. In atmospheric applications, footprints are often covering several pixels and the  
3 relatively large uncertainty on the pixel scale may be reduced through averaging. At this  
4 larger multi-pixel scale, the uncertainty of our  $^{222}\text{Rn}$  fluxes is probably smaller than 20-30%.

5 Inspecting now our comparison between single measurements and modelled flux for the  
6 respective pixel (Fig. 8), the IQR of the differences were on the order of  $11 \text{ mBq m}^{-2} \text{ s}^{-2}$  or  
7 about 70-100% of the mean flux, depending on the soil moisture model. Standard deviations  
8 of these distributions are slightly larger than IQRs, in our case about 100%. With an estimated  
9 uncertainty of the modelled flux of about 50% this would imply that the contribution from  
10 non-representativeness and uncertainty of the measurements to the scatter is larger than 80%.  
11 This emphasises the importance of auxiliary measurements of soil properties that need to be  
12 performed in future  $^{222}\text{Rn}$  flux measurement campaigns if these data shall be useful for  
13 evaluation of bottom-up flux estimates.

## 15 6 Conclusions and Perspectives

16 A high-resolution  $^{222}\text{Rn}$  flux map for Europe was developed, based on a parameterization of  
17  $^{222}\text{Rn}$  production and transport in the soil. The approach includes a well-established  
18 parameterization of soil diffusivity (Millington and Quirk, 1960) and makes use of existing  
19 high-resolution data sets of soil properties, uranium content, model-derived soil moisture as  
20 well as model-derived water table depth. Comparisons with direct  $^{222}\text{Rn}$  flux measurements in  
21 different regions of Europe ~~indicate~~ show that the observed seasonality is realistically  
22 reproduced by our approach, which was not achieved by earlier studies for Europe, and  
23 confirms the validity of estimating diffusivity in soil air based on the Millington and Quirk  
24 (1960) model.

25 Using two different sets of soil moisture reanalyses ~~also reveals~~ underlines the strong  
26 dependence of ~~the reliability of our~~  $^{222}\text{Rn}$  flux estimates on realistic soil moisture values.  
27 ~~While both~~ Both model-based soil moisture estimates evaluated here ~~seem to reproduce~~  
28 ~~realistically~~, either from the GLDAS-Noah or the ERA-Interim/Land model, realistically  
29 reproduce observed seasonality in soil moisture, ~~which~~. This translates into a realistic  
30 seasonality of  $^{222}\text{Rn}$  exhalation rates in both realizations of our flux map; however, the overall  
31 magnitude of the  $^{222}\text{Rn}$  fluxes differs. ~~Soil moisture estimates could largely be~~  
32 ~~improved~~ Comparison of the two  $^{222}\text{Rn}$  flux maps with European-wide point observations

1 indicates better agreement of GLDAS-Noah-based flux estimates than of those calculated  
2 with ERA-I/L soil ~~models. Currently available models show large deviations~~moisture. While  
3 at a monthly time resolution the overall mean <sup>222</sup>Rn flux values from the GLDAS-Noah-based  
4 map show almost no bias to the overall mean of point observations in ~~their estimates;~~  
5 ~~however, comparison with observations from the soil moisture network does not allow any~~  
6 ~~univocal ranking.~~Europe (ca. 15 mBq m<sup>-2</sup> s<sup>-1</sup>), the ERA-I/L-based model underestimates mean  
7 fluxes by more than 60%. The variability of model-measurement differences is, however,  
8 large for both maps. Besides model uncertainties, which are estimated to contribute about  
9 50% to the scatter of the differences, limited representativeness of single point measurements  
10 for the entire pixel of the map contributes most.

11 The spatial resolution of the soil moisture models used here restricts spatial resolution of the  
12 two realizations of our European <sup>222</sup>Rn exhalation map. In many applications, such as the  
13 Radon-Tracer-Method (e.g. Levin et al., 1999), local estimates of <sup>222</sup>Rn fluxes ~~are~~  
14 ~~required~~would also be useful. In such cases, our theoretical approach could easily be applied  
15 e.g. by using local soil texture information and measured soil moisture data, which become  
16 more and more available at ecosystem sites in Europe or elsewhere (e.g. FLUXNET,  
17 Baldocchi et al., 2001). Also, in our study we restricted the temporal resolution to one month  
18 because (quasi-) continuous <sup>222</sup>Rn flux measurements were not available to us for comparison.  
19 However, extension of the temporal resolution to that of the soil moisture models ~~is~~(sub-  
20 daily) would be easily achievable.

21 Validation of our estimated <sup>222</sup>Rn fluxes was restricted in our study to ~~only~~relatively few not  
22 evenly distributed observational sites, most of them located in Central Europe. Many climate  
23 zones and soil types such as subarctic regions, wetlands and dry areas of Europe, could not be  
24 validated with observations. This includes quantification of the influence of snow cover or  
25 frozen soils. Hence, additional systematic <sup>222</sup>Rn flux measurements that are accompanied with  
26 ancillary data of soil properties and soil moisture would facilitate ~~a further~~and improve  
27 validation of the presented maps or may allow more reliable parameterisations, particularly  
28 for special regions and climatic situations.

29 It would ~~be extremely helpful~~also be interesting to apply our approach to other areas of the  
30 world.~~However,~~ which would allow comparison with maps developed for areas outside  
31 Europe and using different methodologies, e.g. of diffusivity estimation. We decided to leave  
32 this ~~is hampered by the~~uneffort to future work, also because of non-availability of a

1 systematic  $^{238}\text{U}$  or  $^{226}\text{Ra}$  survey in ~~other~~ a number of important regions and continents of the  
2 world (e.g. Russia, the Americas, and Africa). Empirical correlations between  $^{226}\text{Ra}$  activity  
3 concentrations and other soil parameters turned out to be only weak and do not allow for  
4 accurate evaluations of the  $^{222}\text{Rn}$  source ~~over large~~ in these regions.

5 The presented  $^{222}\text{Rn}$  flux maps for Europe are ~~directly~~ freely available e.g. for atmospheric  
6 transport model evaluations or comparable studies. ~~As~~ Feedback from such investigations that  
7 also integrate atmospheric observations could help improving our flux map, e.g. during  
8 afternoon when atmospheric model transport is more reliable.

9 ~~Although we cannot unambiguously identify which of the soil moisture reanalysis is more~~  
10 ~~reliable~~ currently favour the GLDAS-Noah-based  $^{222}\text{Rn}$  flux estimates for Europe, we ~~propose~~  
11 ~~to use an ‘ensemble mean’ of the two maps, thereby reducing the potential systematic effect~~  
12 ~~introduced by the soil models. Furthermore, emphasise that~~ in cases when soil moisture ~~is~~ data  
13 or reliable model estimates are directly available in the transport model (as is the case in most  
14 online transport models) our approach could also be applied using ~~th~~ these measured or  
15 model-generated soil moisture ~~s~~. This may improve local or regional  $^{222}\text{Rn}$  flux estimates.

16 Digital versions of the maps are available from the ~~authors upon request~~ ICOS-RI Carbon  
17 Portal at <https://www.icos-cp.eu/>.

18

## 19 **Acknowledgements**

20 The research leading to these results has received funding from the European Community’s  
21 Seventh Framework Programme (FP7/2007-2013) in the InGOS project under grant  
22 agreement n° 284274. ~~S. D. Schery is gratefully acknowledged for his insightful review and~~  
23 ~~comments, which helped to improve our paper.~~ We thank G. Miguez-Macho (Universidade de  
24 Santiago de Compostela, Spain) for providing the model-simulated water table depth data set,  
25 N. Manohar (Center for Isotope Research, University of Groningen, The Netherlands) for  
26 making available the  $^{222}\text{Rn}$  flux measurements at Lutjewad, and Felix Vogel (Laboratoire des  
27 Sciences du Climat et de l’Environnement, Gif-sur-Yvette, France) for helping with the flux  
28 measurement in Gif-sur-Yvette. We further thank O. Kolle (Max-Planck-Institute for  
29 Biogeochemistry, Jena, Germany) for providing soil moisture measurements at Gebesee and  
30 A. Gassama (Institut für Umweltphysik, Heidelberg University, Germany) for providing soil  
31 moisture measurements at Grenzhof. The GLDAS-Noah soil moisture data used in this study

1 were acquired as part of the mission of NASA's Earth Science Division and archived and  
2 distributed by the Goddard Earth Sciences (GES) Data and Information Services Center  
3 (DISC). ERA-Interim/Land soil moisture reanalysis data were obtained from the ECMWF  
4 Data Server.

5

6



## 1 **References**

- 2 Baldocchi, D., Falge, E., Gu, L., Olson, R., Hollinger, D., Running, S., Anthoni, P.,  
3 Bernhofer, C., Davis, K., and Evans, R.: FLUXNET: A new tool to study the temporal and  
4 spatial variability of ecosystem-scale carbon dioxide, water vapor, and energy flux densities,  
5 Bull. Amer. Meteor. Soc., 82, 2415-2434, 2001.
- 6 Balsamo, G., Albergel, C., Beljaars, A., Boussetta, S., Brun, E., Cloke, H., Dee, D., Dutra, E.,  
7 Muñoz-Sabater, J., Pappenberger, F., De Rosnay, P., Stockdale, T., and Vitart, F.: ERA-  
8 Interim/Land: a global land surface reanalysis data set, Hydrol. Earth Syst. Sci., 19, 389-407,  
9 doi:10.5194/hess-19-389-2015, 2015.
- 10 Born, M., Dörr, H., and Levin, I.: Methane consumption in aerated soils of the temperate  
11 zone, Tellus, 42B, 2-8, 1990.
- 12 Chevillard, A., Ciais, P., Karstens, U., Heimann, M., Schmidt, M., Levin, I., Jacob, D., and  
13 Podzun, R.: Transport of  $^{222}\text{Rn}$  using the on-line regional scale model REMO: A detailed  
14 comparison with measurements over Europe, Tellus, 54B, 850-871, 2002.
- 15 Campoy, A., Ducharne, A., Cheruy, F., Hourdin, F., Polcher, J., and Dupont, J. C.: Response  
16 of land surface fluxes and precipitation to different soil bottom hydrological conditions in a  
17 general circulation model, J. Geophys. Res. Atmos., 118, 10725-10739,  
18 doi:10.1002/jgrd.50627, 2013.
- 19 Conen, F. and Robertson, L.: Latitudinal distribution of radon-222 flux from continents,  
20 Tellus, 54B, 127–133, 2002.
- 21 Cosby, B. J., Hornberger, G. M., Clapp, B., and Ginn, T.R.: A Statistical Exploration of the  
22 Relationships of Soil Moisture Characteristics to the Physical Properties of Soils, Water  
23 Resour. Res., 20, 682-690, 1984.
- 24 Dorigo, W. A., Wagner, W., Hohensinn, R., Hahn, S., Paulik, C., Xaver, A., Gruber, A.,  
25 Drusch, M., Mecklenburg, S., van Oevelen, P., Robock, A., and Jackson, T.: The International  
26 Soil Moisture Network: a data hosting facility for global in situ soil moisture measurements,  
27 Hydrol. Earth Syst. Sci., 15, 1675–1698, doi:10.5194/hess-15-1675-2011, 2011.
- 28 Dörr, H. and Münnich, K. O.:  $^{222}\text{Rn}$  flux and soil air concentration profiles in West Germany.  
29 Soil  $^{222}\text{Rn}$  as tracer for gas transport in the unsaturated soil zone, Tellus, 42B, 20-28, 1990.

1 FAO: Digital soil map of the world and derived soil properties, Food and Agriculture  
2 Organization of the United Nations, Land and Water Digital Media Series, CD-ROM, Rome,  
3 Italy, 2003.

4 FAO/IIASA/ISRIC/ISSCAS/JRC: Harmonized World Soil Database (version 1.2), FAO,  
5 Rome, Italy, IIASA, Laxenburg, Austria, 2012.

6 Griffiths, A. D., Zahorowski, W., Element, A., and Werczynski, S.: A map of radon flux at  
7 the Australian land surface, *Atmos. Chem. Phys.*, 10, 8969-8982, doi:10.5194/acp-10-8969-  
8 2010, 2010.

9 Hartmann, J. and Moosdorf, N.: The new global lithological map database GLiM: A  
10 representation of rock properties at the Earth surface, *Geochem. Geophys. Geosyst.*, 13,  
11 Q12004, doi:10.1029/2012GC004370, 2012.

12 Hirao, S., Yamazawa, H., and Moriizumi, J.: Estimation of the global  $^{222}\text{Rn}$  flux density from  
13 the Earth's surface, *Jpn. J. Health Phys.*, 45, 161-171, 2010.

14 IAEA: Construction and Use of Calibration Facilities for Radiometric Field Equipment,  
15 International Atomic Energy Agency, Vienna, Austria, Technical Reports Series 309, 86 pp.,  
16 1989.

17 Iskandar, D., Yamazawa, H., and Iida, T.: Quantification of the dependency of radon  
18 emanation power on soil temperature, *Appl. Radiat. Isotopes*, 60, 971-973, 2004.

19 Jacob, D.J. and Prather, M. J.: Radon-222 as a test of convective transport in a general  
20 circulation model, *Tellus*, 42B, 118-134, 1990.

21 Jin, Y. and Jury, W. A.: Characterizing the Dependence of Gas Diffusion Coefficient on Soil  
22 Properties, *Soil Sci. Soc. Am. J.*, 60, 66-71. 1996.

23 Jutzi, S.: Verteilung der Boden-Radon Exhalation in Europa, Staatsexamensarbeit, Institut für  
24 Umweltphysik, Heidelberg University, Germany, 57pp., 2001.

25 Koster, R. D., Guo, Z., Yang, R., Dirmeyer, P. A., Mitchell, K., and Puma, M. J.: On the  
26 Nature of Soil Moisture in Land Surface Models, *J. Climate*, 22, 4322-4335,  
27 doi:10.1175/2009JCLI2832.1, 2009.

28 Lallo, M., Aalto, T., Hatakka, J., and Laurila, T.: Hydrogen soil deposition in the northern  
29 boreal zone, *Boreal Environ. Res.*, 14, 784-793, 2009.

1 Levin, I., Glatzel Mattheier, H., Marik, T., Cuntz, M., Schmidt, M. and Worthy, D. E.:  
2 Verification of German methane emission inventories and their recent changes based on  
3 atmospheric observations, *J. Geophys. Res.*, 104, 3447-3456, 1999.

4 Levin, I., Born, M., Cuntz, M., Langendörfer, U., Mantsch, S., Naegler, T., Schmidt, M.,  
5 Varlagin, A., Verclas, S., and Wagenbach, D.: Observations of atmospheric variability and  
6 soil exhalation rate of Radon-222 at a Russian forest site: Technical approach and deployment  
7 for boundary layer studies, *Tellus*, 54B, 462-475, 2002.

8 López-Coto, J., Mas, J. L., and Bolivar, J. P.: A 40-year retrospective European radon flux  
9 inventory including climatological variability, *Atmos. Environ.*, 73, 22-33, doi:  
10 10.1016/j.atmosenv.2013.02.043, [2014](https://doi.org/10.1016/j.atmosenv.2013.02.043).

11 Manohar, S. N., Meijer, H. A. J., Neubert, R. E. M., Kettner E., and Herber, M. A.: Radon  
12 flux measurements at atmospheric station Lutjewad – analysis of temporal trends and main  
13 drivers controlling the emissions, submitted, 2015.

14 Miguez-Macho, G., Li, H., and Fan, Y.: Simulated Water Table and Soil Moisture  
15 Climatology Over North America, *Bull. Amer. Meteor. Soc.*, 89, 663-672,  
16 doi:10.1175/BAMS-89-5-663, 2008.

17 Millington, R. J. and Quirk, J. P.: Transport in Porous media, *Proceedings of the 7th*  
18 *International Congress of soil Science*, Madison, Wisconsin, U.S.A., 97-106, 1960.

19 Millington, R. J. and Quirk, J. P.: Permeability of porous solids, *Trans. Faraday Soc.*, 57,  
20 1200-1207, 1961.

21 Moldrup, P., Kruse, C. W., Rolston, D. E., and Yamaguchi, T.: Modeling diffusion and  
22 reaction in soils: III. Predicting gas diffusivity from the Campbell soil-water retention model,  
23 *Soil Sci.*, 161, 366-375, 1996.

24 Moldrup, P., Olesen, T., Yamaguchi, T., Schjønning, P., and Rolston, D. E.: Modeling  
25 diffusion and reaction in soils: IX. The Buckingham-Burdine-Campbell Equation for gas  
26 diffusivity in undisturbed soil, *Soil Sci.*, 164, 542-551, 1999.

27 Nazaroff, W.: Radon transport from soil to air, *Reviews of Geophysics*, 30, 137-160, 1992.

28 Rasch, P. J., Feichter, J., Law, K., Mahowald, N. Benkovitz, C., Genthon, C.,  
29 Giannakopoulos, C., Kasibhatla, P., Koch, D., Levy, H., Maki, T., Prather, M., Roberts, D. L.,  
30 Roelofs, G.-J., Stevenson, D., Stockwell, Z., Taguchi, S., Kritz, M., Chipperfield, M.,

1 Baldocchi, D., McMurray, P., Barrie, L., Balkanski, Y., Chatfield, R., Kjellstrom, E.,  
2 Lawrence, M., Lee, H. N., Lelieveld, J., Noone, K. J., Seinfeld, J., Stenchikov, G., Schwartz,  
3 S., Walcek, C., and Williamson, D.: A comparison of scavenging and deposition processes in  
4 global models: results from the WCRP Cambridge Workshop of 1995, *Tellus*, 52B, 1025-  
5 1056, 2000.

6 Reynolds, C., Jackson, T., and Rawls, W.: Estimating soil water-holding capacities by linking  
7 the Food and Agriculture Organization soil map of the world with global pedon databases and  
8 continuous pedotransfer functions, *Water Resour. Res.*, 36, 3653-3662, 2000.

9 Robertson, L. B.: Radon Emissions to the Atmosphere and their use as Atmospheric Tracers,  
10 Ph.D. thesis, University of Edinburgh, United Kingdom, 237 pp., 2004.

11 Rodell, M., Houser, P. R., Jambor, U., Gottschalck, J., Mitchell, K., Meng, C.-J., Arsenault,  
12 K., Cosgrove, B., Radakovich, J., Bosilovich, M., Entin, J. K., Walker, J. P., Lohmann, D.,  
13 and Toll, D.: The Global Land Data Assimilation System, *B. Am. Meteor. Soc.*, 85, 381-394,  
14 doi:10.1175/BAMS-85-3-381, 2004.

15 Rogers, V.C. and Nielson, K. K.: Correlations for predicting air permeabilities and  $^{222}\text{Rn}$   
16 diffusion coefficients of soils, *Health Phys.*, 61, 225-230, 1991.

17 Salminen, R. (ed.): *Geochemical Atlas of Europe. Part 1: Background Information,*  
18 *Methodology and Maps*, Geological Survey of Finland, Espoo, Finland, 2005.

19 Sandström, H., Reeder, S., Bartha, A., Birke, M., Berge, F., Davidsen, B., Grimstvedt, A.,  
20 Hagel-Brunnström, M.-L., Kantor, W., Kallio, E., Klaver, G., Lucivjansky, P., Mackovych,  
21 D., Mjartanova, H., van Os, B., Paslawski, P., Popiolek, E., Siewers, U., Varga-Barna, Z.,  
22 van Vilsteren, E., and Ødegård, M.: Sample Preparation and Analysis, in: Salminen, R. (ed.):  
23 *Geochemical Atlas of Europe, Part 1: Background Information, Methodology and Maps,*  
24 *Geological Survey of Finland, Espoo, Finland, 2005.*

25 Saxton, K., Rawls, W. J., Romberger, J., and Papendick, R.: Estimating generalized soil-water  
26 characteristics from texture, *Soil Sci. Soc. Am. J.*, 50, 1031–1036, 1986.

27 Schell, S.:  $^{222}\text{Rn}$ -Profil-Messungen in Süd- und Ostdeutschland, Anwendung der Radon-  
28 Tracer-Methode zur Berechnung von  $\text{CO}_2$ - und  $\text{CH}_4$ -Flüssen, Diplomarbeit, Institut für  
29 Umweltphysik, Heidelberg University, Germany, 106 pp., 2004.

- 1 Schery, S. D. and Wasiolek, M. A.: Radon and Thoron in the Human Environment, chap.  
2 Modeling Radon Flux from the Earth's Surface, 207–217, World Scientific Publishing,  
3 Singapore, 1998.
- 4 Schmithüsen, D.: Atmospheric and soil flux radon measurements in Heidelberg,  
5 Diplomarbeit, Institut für Umweltp Physik, Heidelberg University, Germany, 66 pp. , 2012.
- 6 Schüßler, W.: Effektive Parameter zur Bestimmung des Gasaustauschs zwischen Boden und  
7 Atmosphäre, Ph.D. thesis, Heidelberg University, Germany, 1996.
- 8 Schwingshackl, C.: Experimental Validation of a Radon-222 Flux Map, Master Thesis,  
9 Institut für Umweltp Physik, Heidelberg University, Germany, 100 pp., 2013.
- 10 Shangguan, W., Dai, Y., Duan, Q., Liu, B., and Yuan, H.: A global soil data set for earth  
11 system modeling, *J. Adv. Model. Earth Syst.* 6, 249–263. doi:10.1002/2013MS000293, 2014.
- 12 Sun, K., Guo, Q, and Zhuo, W.: Feasibility for Mapping Radon Exhalation Rate from Soil in  
13 China, *J. Nucl. Sci. Technol.*, 41, 86-90, 2004.
- 14 Szegvary, T., Conen, F., Stöhlker, U., Dubois, G., Bossew, P. and de Vries, G.: Mapping  
15 terrestrial  $\gamma$ -dose rate in Europe based on routine monitoring data, *Radiat. Meas.*, 42, 1561-  
16 1572, doi:10.1016/j.radmeas.2007.09.002, 2007a.
- 17 Szegvary, T., Leuenberger, M. C., and Conen, F.: Predicting terrestrial  $^{222}\text{Rn}$  flux using  
18 gamma dose rate as a proxy, *Atmos. Chem. Phys.*, 7, 2789–2795, doi:10.5194/acp-7-2789-  
19 2007, 2007b.
- 20 Szegvary, T., Conen, F., and Ciais, P.: European  $^{222}\text{Rn}$  inventory for applied atmospheric  
21 studies. *Atmos. Environ.*, 43, 1536-1539, doi:10.1016/j.atmosenv.2008.11.025, 2009.
- 22 Taguchi, S., Law, R.M., Rödenbeck, C., Patra, P.K., Maksyutov, S., Zahorowski, W.,  
23 Sartorius, H., and Levin, I.: TransCom continuous experiment: comparison of  $^{222}\text{Rn}$  transport  
24 at hourly time scales at three stations in Germany, *Atmos. Chem. Phys.*, 11, 10071-10084,  
25 doi:10.5194/acp-11-10071-2011, 2011.
- 26 Turekian, K. K., Nozaki, Y., and Benninger L. K.: Geochemistry of atmospheric radon and  
27 radon products, *Ann. Rev. Earth Planer. Sci.*, 5, 227-255, 1977.
- 28 Wackernagel, H.: Multivariate geostatistics: an introduction with applications, Springer,  
29 Berlin, 2003.

- 1 Wilkening, M. H., Clements, W. E., and Stanley, D.: Radon-222 flux measurements in widely  
2 separated regions, in: *The Natural Radiation Environment* 11, J.A.S. Adams, W.M. Lowder  
3 and T. F. Gesell (Eds.), USAEC Report CONF-720805-P2 (National Technical Information  
4 Service), Springfield, VA, pp. 717, 1972.
- 5 Wollschläger, U., Pfaff, T., and Roth, K.: Field-scale apparent hydraulic parameterisation  
6 obtained from TDR time series and inverse modelling, *Hydrol. Earth Syst. Sci.*, 13, 1953-  
7 1966, doi:10.5194/hess-13-1953-2009, 2009.
- 8 Zhuo, W., Iida, T., and Furukawa, M.: Modeling radon flux density from the Earth's surface,  
9 *J. Nucl. Sci. Technol.*, 43, 479-482, 2006.
- 10 Zhuo, W., Guo, O., Chen, B., and Cheng, G.: Estimating the amount and distribution of radon  
11 flux density from the soil surface in China, *J. Environ. Radioactiv.*, 99, 1143-1148, 2008.  
12

1 Table 1. Parameters of the fit curves plotted in Figure 1, mean exhalation rates estimated from  
 2 the measured radon concentration profiles ( $j_{\text{profile}}$ ) and directly measured with flux chambers  
 3 ( $j_{\text{chambers}}$ ) at the same site as well as mean diffusivity as estimated from the experimental data  
 4 ( $D_{e, \text{exp}}$ ), from the Millington and Quirk (1960) model ( $D_{e, \text{M\&Q}}$ ) and from the Rogers and  
 5 Nielson (1991) model ( $D_{e, \text{R\&N}}$ ).

6

Profile	$c_{\infty}$ Bq m <sup>-3</sup>	Q mBq m <sup>-3</sup> s <sup>-1</sup>	$\bar{z}$ m	$j_{\text{profile}}$ mBq m <sup>-2</sup> s <sup>-1</sup>	$j_{\text{chamber}}$ mBq m <sup>-2</sup> s <sup>-1</sup>	$\theta_w$	$D_{e, \text{exp}}$ m <sup>2</sup> s <sup>-1</sup>	$D_{e, \text{M\&Q}}$ m <sup>2</sup> s <sup>-1</sup>	$D_{e, \text{R\&N}}$ m <sup>2</sup> s <sup>-1</sup>
wet	10000	21.0	0.20	4.3	6.8	0.311	$0.86 \cdot 10^{-7}$	$0.72 \cdot 10^{-7}$	$0.52 \cdot 10^{-7}$
medium	9900	20.8	0.38	7.8	13.5	0.199	$2.97 \cdot 10^{-7}$	$6.59 \cdot 10^{-7}$	$10.3 \cdot 10^{-7}$
dry	13800	29.0	0.97	28	14.7	0.124	$19.6 \cdot 10^{-7}$	$14.2 \cdot 10^{-7}$	$20.9 \cdot 10^{-7}$

7

8

1 Table 2. Characteristics of the long-term  $^{222}\text{Rn}$  flux sampling sites from IUP (compare Fig. 1  
2 and Table 1), M1-M5 close to Heidelberg as well as Gebesee, Northern Germany, and Gif-  
3 sur-Yvette, France. For M1-M5 the percentage of clay, silt and sand have been estimated  
4 from the soil type description of Schüßler (1996), according to mean percentages reported by  
5 Cosby et al. (1984, Table 2)); the  $^{226}\text{Ra}$  activity concentrations have been reported by  
6 Schüßler (1996). For IUP, Gebesee and Gif-sur-Yvette, these parameters were measured by  
7 Schwingshackl (2013). For comparison with measurements, we also list the data for the  
8 respective pixels from the high-resolution map of soil parameters (“pixel”) ( $\varepsilon$ : emanation  
9 coefficient,  $\theta_p$ : soil porosity,  $\rho_b$ : dry bulk density).

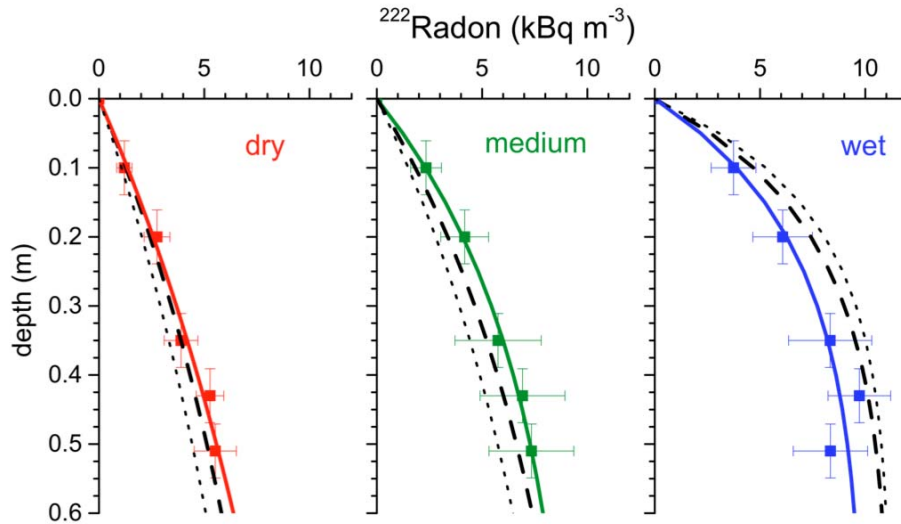
10

Site	Location	Measurement Period	Clay %	Silt %	Sand %	$\varepsilon$	$\theta_p$	$\rho_b$ kg m <sup>-3</sup>	$^{226}\text{Ra}$ Bq kg <sup>-1</sup>
M1: Sandhausen	49.35°N, 8.65°E	1987-1995	6	12	82	0.307	0.365	1540	9.4
M2: Sandhausen	49.35°N, 8.65°E	1987-1995	10	32	58	0.333	0.430	1510	14
M3: Sandhausen	49.35°N, 8.65°E	1987-1998	6	12	82	0.307	0.350	1630	8.4
M1-M3 pixel	49.38°N, 8.63°E	2006-2010	15	22	63	0.332	0.436	1495	37
M4: Nußloch	49.3°N, 8.72°E	1987-1995	27	15	58	0.346	0.425	1540	34
M5: Nußloch	49.3°N, 8.72°E	1987-1998	27	15	58	0.346	0.425	1540	38
M4, M5 pixel	49.29°N, 8.71°E	2006-2010	15	22	63	0.332	0.436	1495	38
IUP: Heidelberg	49.42°N, 8.68°E	2011-2012	19	37	44	0.353	0.368	1440	36
IUP pixel	49.46°N, 8.71°E	2006-2010	15	22	63	0.332	0.436	1495	37
Gebesee	51.10°N, 10.92°E	2003-2004	36	62	2	0.406	0.480	1370	38
Gebesee pixel	51.13°N, 10.96°E	2006-2010	28	39	34	0.369	0.491	1349	31
Gif	48.72°N, 2.17°E	2013	16	79	5	0.390	0.370	1650	40
Gif pixel	48.71°N, 2.13°E	2006-2010	28	39	33	0.371	0.493	1345	18

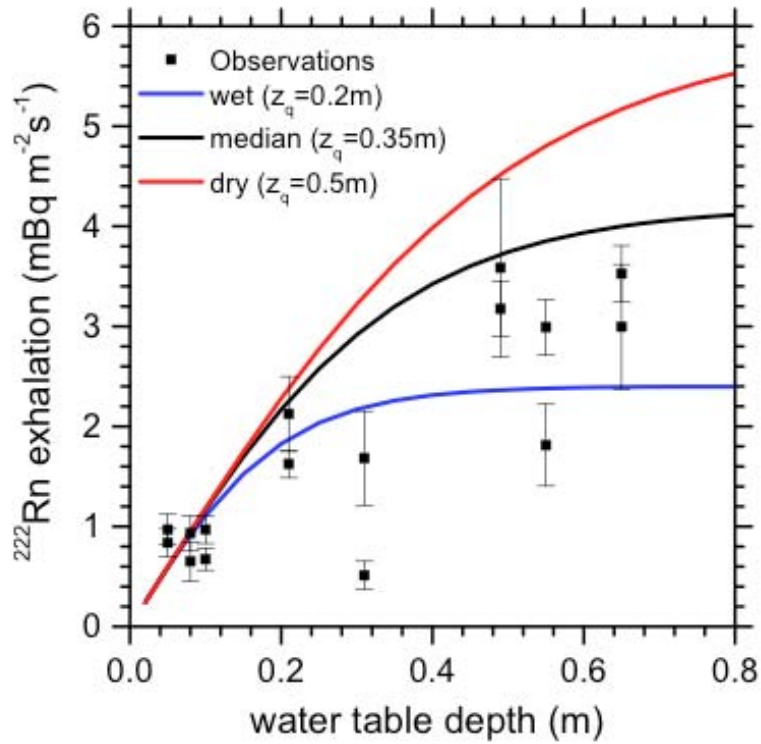
11

12





1  
2 Figure 1. Mean vertical profiles of the  $^{222}\text{Rn}$  activity concentrations measured in a soil in  
3 Heidelberg (IUP) averaged over dry (mean  $\theta_w = 0.124$ ), medium dry (mean  $\theta_w = 0.199$ ) and  
4 wet (mean  $\theta_w = 0.311$ ) soil moisture conditions in 2011-2012. The coloured lines are fitted  
5 curves through the data according to Eq. (7). The dashed lines are activity concentration  
6 profiles calculated with [diffusivity](#) estimated with the Millington and Quirk (1960) model,  
7 while dotted lines are respective profiles calculated with the [diffusivity](#) model from Rogers  
8 and Nielson (1991). Both estimates use the measured soil porosity ( $\theta_p=0.368$ ), mean  $\theta_w$  and  
9 soil temperature during the measurements as well as a mean source strength  $Q = 23.6 \text{ mBq m}^{-3}\text{s}^{-1}$ ,  
10 i.e. the mean from all measured profiles estimated according to Eq. (7a) (i.e. mean of  
11 Table 1, third column).  
12

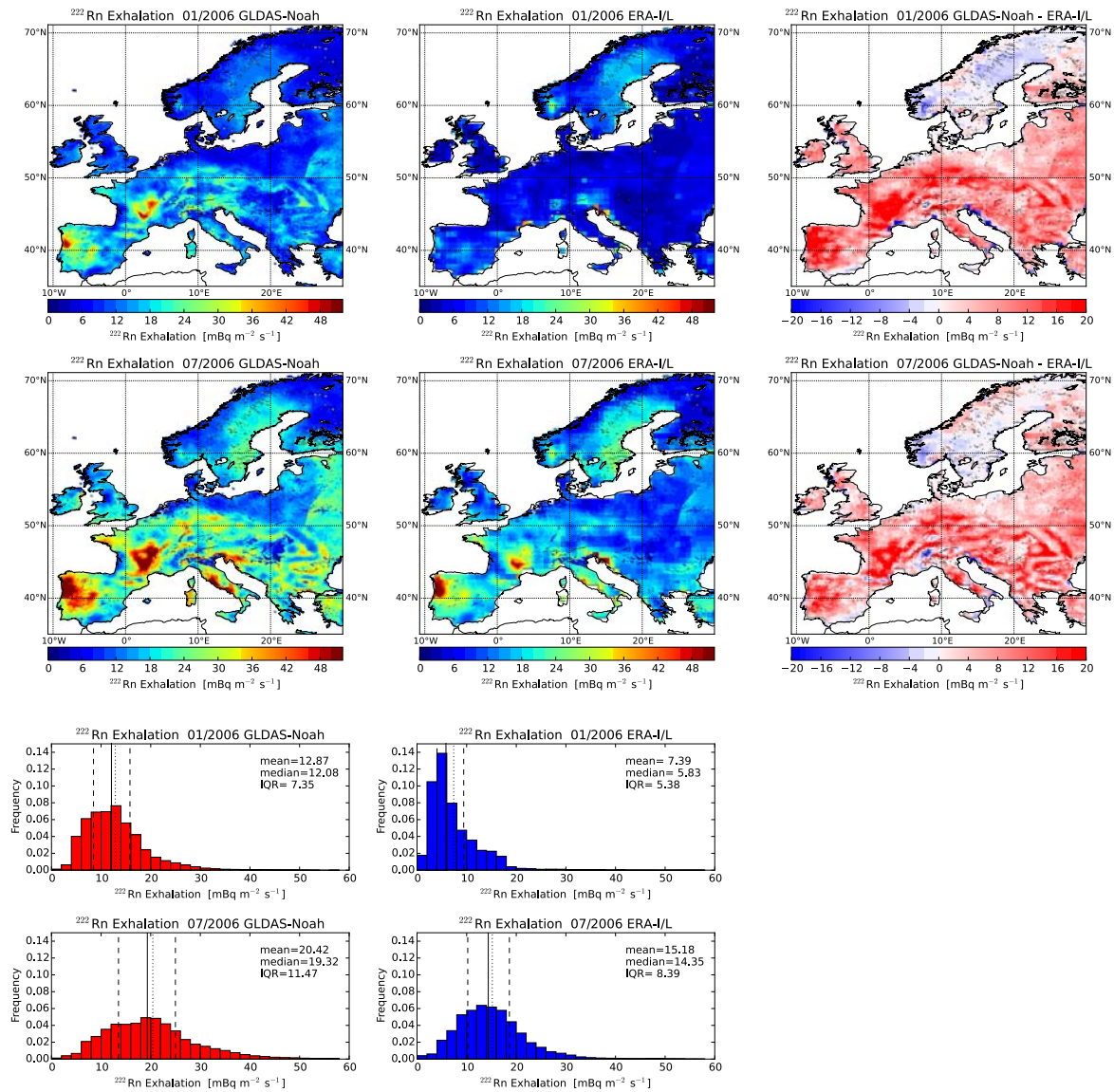


1

2

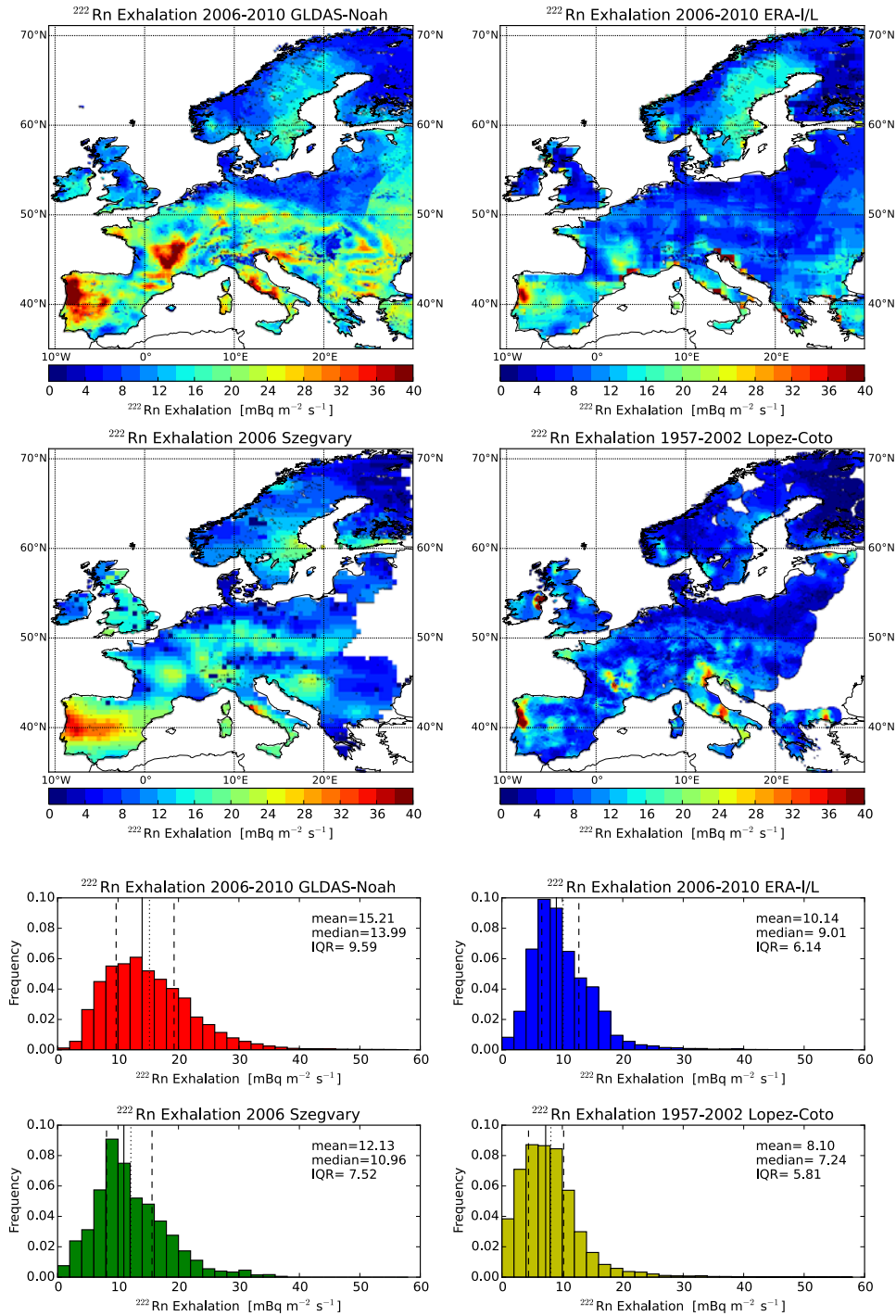
3 Figure 2. Dependency of the  $^{222}\text{Rn}$  exhalation rate on water table depth; the solid lines are  
 4 calculated according to Eq. (8a) with  $Q = 12 \text{ mBq m}^{-3} \text{ s}^{-1}$  and different **effective diffusivities**  
 5 resp. relaxation depths  $\bar{z} (=z_q)$ .

6



1  
 2 Figure 3.  $^{222}\text{Rn}$  exhalation rate maps of European soils, their differences and frequency  
 3 distributions for January and July 2006. The left panels show the flux maps and normalized  
 4 frequency distributions calculated with the monthly mean soil moisture estimates from the  
 5 GLDAS-Noah LSM for January and July 2006, while the middle panels show respective  
 6 estimates with the ERA-Interim/Land model. The mean values, median values and the Inter  
 7 Quartile Range (IQR) of the normalized frequency distributions of January and July 2006  
 8 fluxes (in  $\text{mBq m}^{-2} \text{s}^{-1}$ ) are also given. The right panels show the differences between  
 9 GLDAS-Noah- and ERA-Interim/Land-based fluxes.

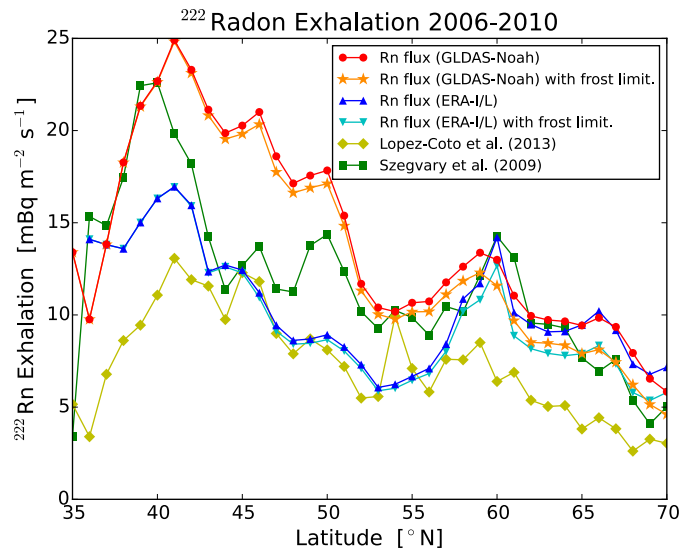
10



1

2 Figure 4. Annual mean  $^{222}\text{Rn}$  exhalation rates for 2006-2010 from this study in comparison  
 3 with published maps (Szegevary et al., 2009; Lopez-Coto et al., 2013). The upper four panels  
 4 show the geographical distributions, while the lower four panels display the normalised  
 5 frequency distributions of annual means from all pixels of the four maps.

6

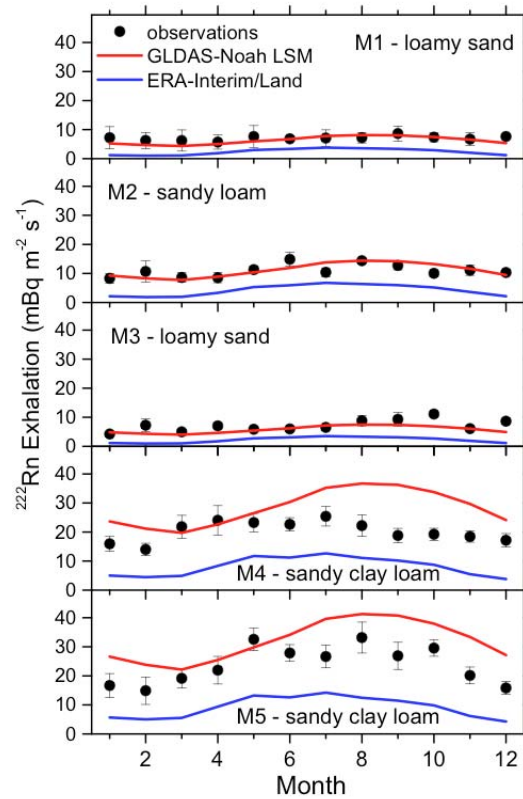


1

2 Figure 5. Latitudinal gradient of annual mean  $^{222}\text{Rn}$  exhalation rates for 2006-2010 from this  
 3 study in comparison with published maps (Szegvary et al., 2009; Lopez-Coto et al., 2013).

4 Zonal average land surface fluxes for  $1^\circ$  latitude bands are shown.

5

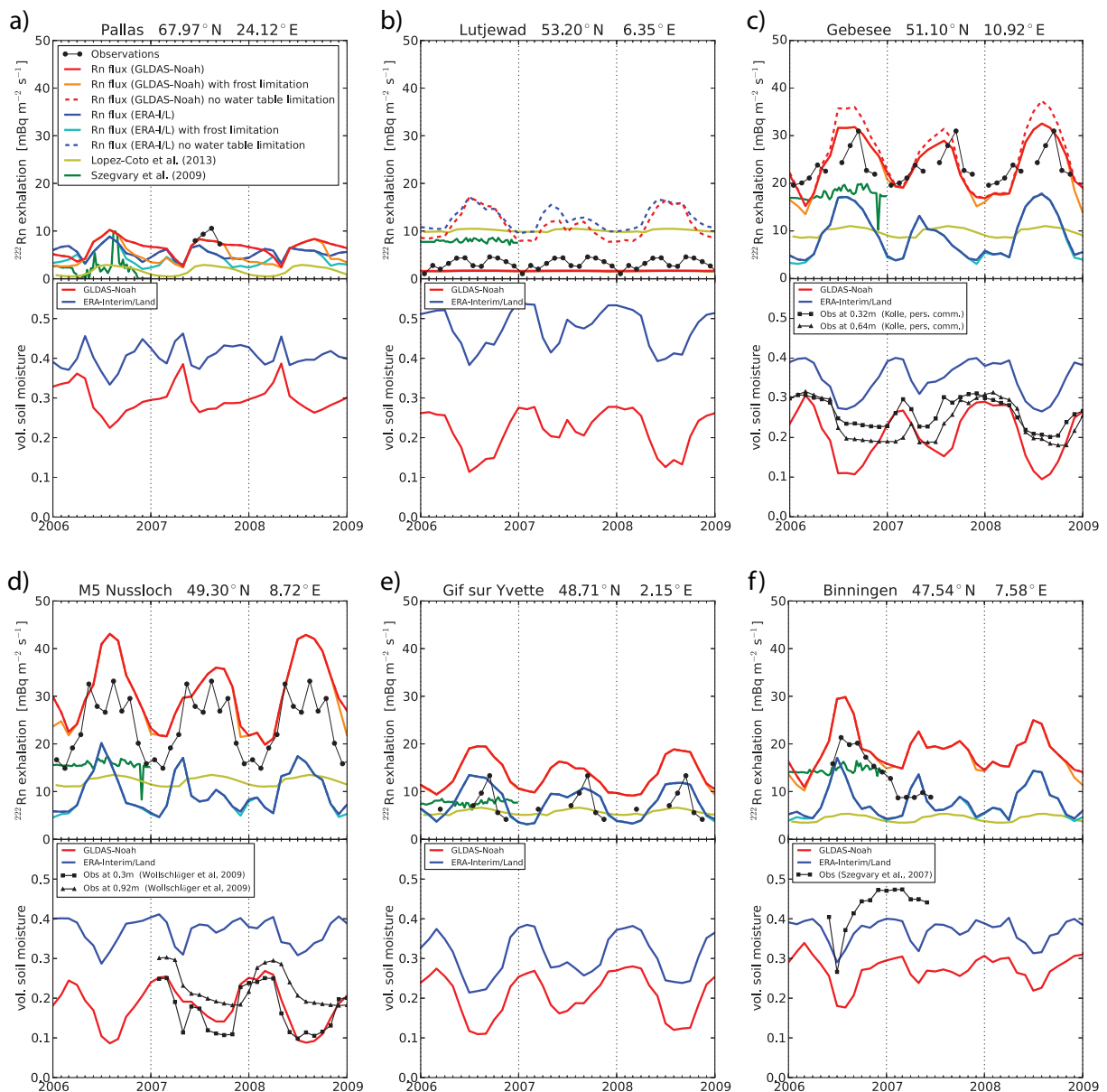


1

2 Figure 6. Comparison of the observed climatology of monthly  $^{222}\text{Rn}$  fluxes at the sampling  
 3 sites M1-M5 (symbols with error bars representing monthly mean observational data and their  
 4 standard error) with bottom-up estimates using the [diffusivity](#) estimate of Millington and  
 5 Quirk (1960). Soil moisture climatology is taken either from the GLDAS-Noah LSM (red  
 6 lines) or from the ERA-Interim/Land model (blue lines) for the respective pixels, averaged  
 7 over the period of 2006 – 2010. Note that the monthly soil moisture values have been adjusted  
 8 according to Eq. (13), i.e. taking into account the actual porosity at the measurement sites (see  
 9 text).

10

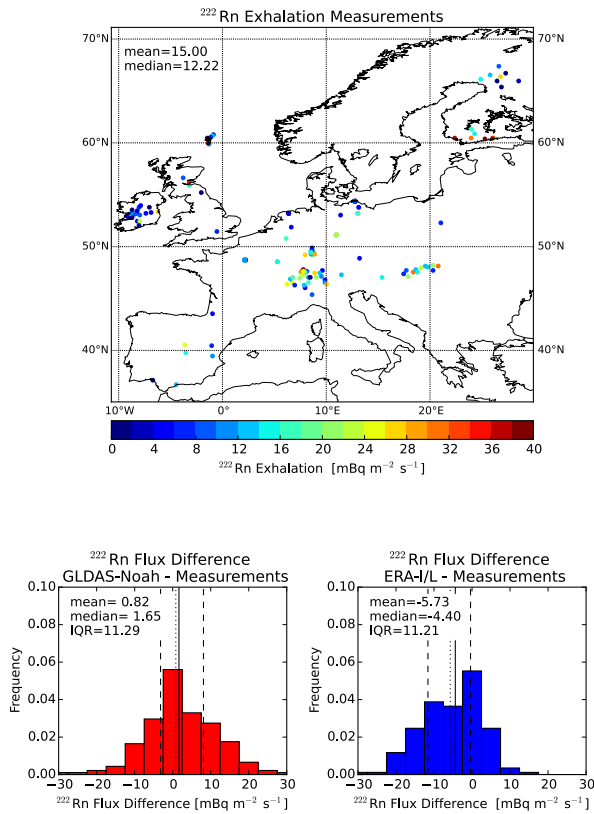




1  
2 Figure 7. Upper panels of each row: Comparison of estimated  $^{222}\text{Rn}$  fluxes (coloured lines)  
3 with monthly mean observations (solid black dots) at selected European sites. The flux data  
4 have been taken from the following publications: Pallas 2007 data: Lallo et al. (2009);  
5 Lutjewad multi-year mean data: Manohar et al. (2015); Gebesee 2003-2004 data: Schell  
6 (2004); M5 Nußloch 1985-1997 climatology: Jutzi (2001); Gif-sur-Yvette 2013 data:  
7 Schwingshackl (2013); Binningen 2006-2007 data: Szegvary et al. (2007b,  
8 <http://radon.unibas.ch>). Also included in the upper graphs of both rows are flux estimates  
9 from Szegvary et al. (2009) for the year 2006 and from López-Coto et al. (2013) for the years  
10 1957-2002 plotted as seasonal cycle climatology. Lower panels of each row: Comparison of  
11 GLDAS-Noah (red lines) and ERA-I/L (blue lines) estimated monthly mean soil moisture  
12 with observations. The soil moisture data were taken from the following publications:

- 1 Gebesee: data from O. Kolle (pers. comm. 2013); M5 Nußloch: Grenzhof data from
- 2 Wollschläger et al. (2009); Binningen: Szegvary et al. (2007b, <http://radon.unibas.ch>).
- 3





1

2 Figure 8. Map of episodic <sup>222</sup>Rn flux observations in Europe (left upper panel) and their  
 3 frequency distribution (black histogram) in comparison to those of monthly values of the  
 4 corresponding pixels of our two <sup>222</sup>Rn maps of model-data differences at sites where co-  
 5 located data exist (GLDAS-Noah-based fluxes: red histogram, ERA-I/L-based fluxes: blue  
 6 histogram). All measurement data are provided in the Supplement (Table S2-S1).

7

***Supplement of***

**A process-based <sup>222</sup>Radon flux map for Europe and its comparison to long-term observations**

**U. Karstens<sup>1,+</sup>, C. Schwingshackl<sup>2,\*</sup>, D. Schmithüsen<sup>2</sup>, and I. Levin<sup>2</sup>**

[1]{Max-Planck-Institut für Biogeochemie, Jena, Germany}

[2]{Institut für Umweltphysik, Heidelberg University, Heidelberg, Germany}

[+]{now at: ICOS Carbon Portal, Lund University, Lund, Sweden}

[\*]{now at: Institute for Atmospheric and Climate Science, ETH Zürich, Switzerland}

Correspondence to: U. Karstens (ute.karstens@nateko.lu.se)

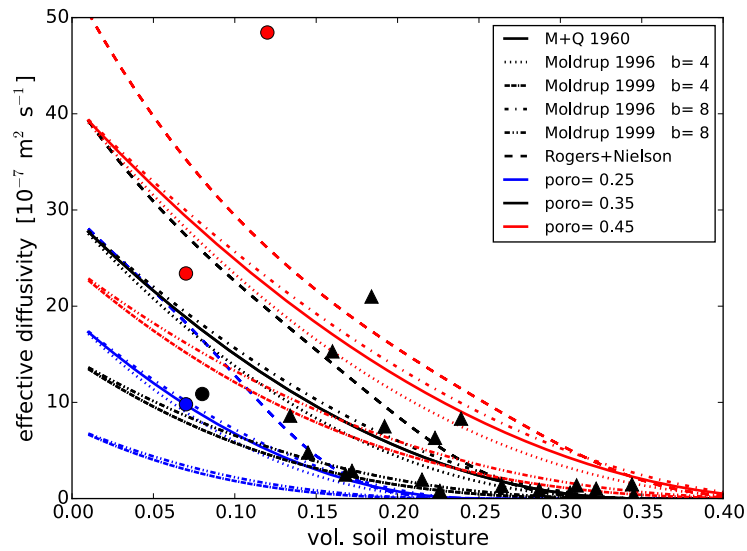


**Figure S1.** Dependency of soil **effective diffusivity** at 15°C on soil moisture as calculated with different models (Millington and Quirk, 1960; Rogers and Nielson, 1991; Moldrup et al., 1996; Moldrup et al., 1999) for different soil porosities together with measured values. Triangles correspond to individual estimates from the IUP site (Schmithüsen, 2012), while the filled circles were taken from locations close to Malaga from Dueñas et al. (1997). Colours of symbols and lines indicate mean porosity. The general shape of the Millington and Quirk (1960) and the Moldrup et al. (1996) models for typical hydraulic parameters of  $b=4$  (sandy soils) and  $b=8$  (clay soils) is very similar, with the curves being identical for  $b=6$ . Also included is the dependency for the Rogers and Nielson (1991) parameterization, which seems to overestimate **the effective diffusivity** at low soil moisture and underestimate at high soil moisture.

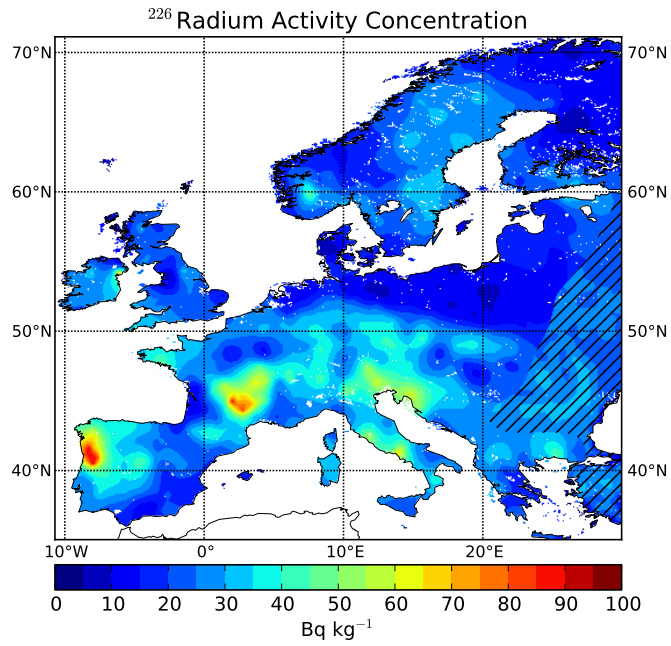


**Figure S2.** Distribution of the interpolated <sup>226</sup>Ra activity concentrations in the soil as derived from the Geochemical Atlas for Europe (Salminen, 2005) from their measured <sup>238</sup>U distributions at 0-0.25 m and 0.5-2.0 m of the soil. For the southeastern part of the model domain (not covered by the Geochemical Atlas), the <sup>226</sup>Ra activity concentration was extrapolated based on geological information from a global lithological map (Hartmann and Moosdorf, 2012), see Section 4.1 for more explanations.

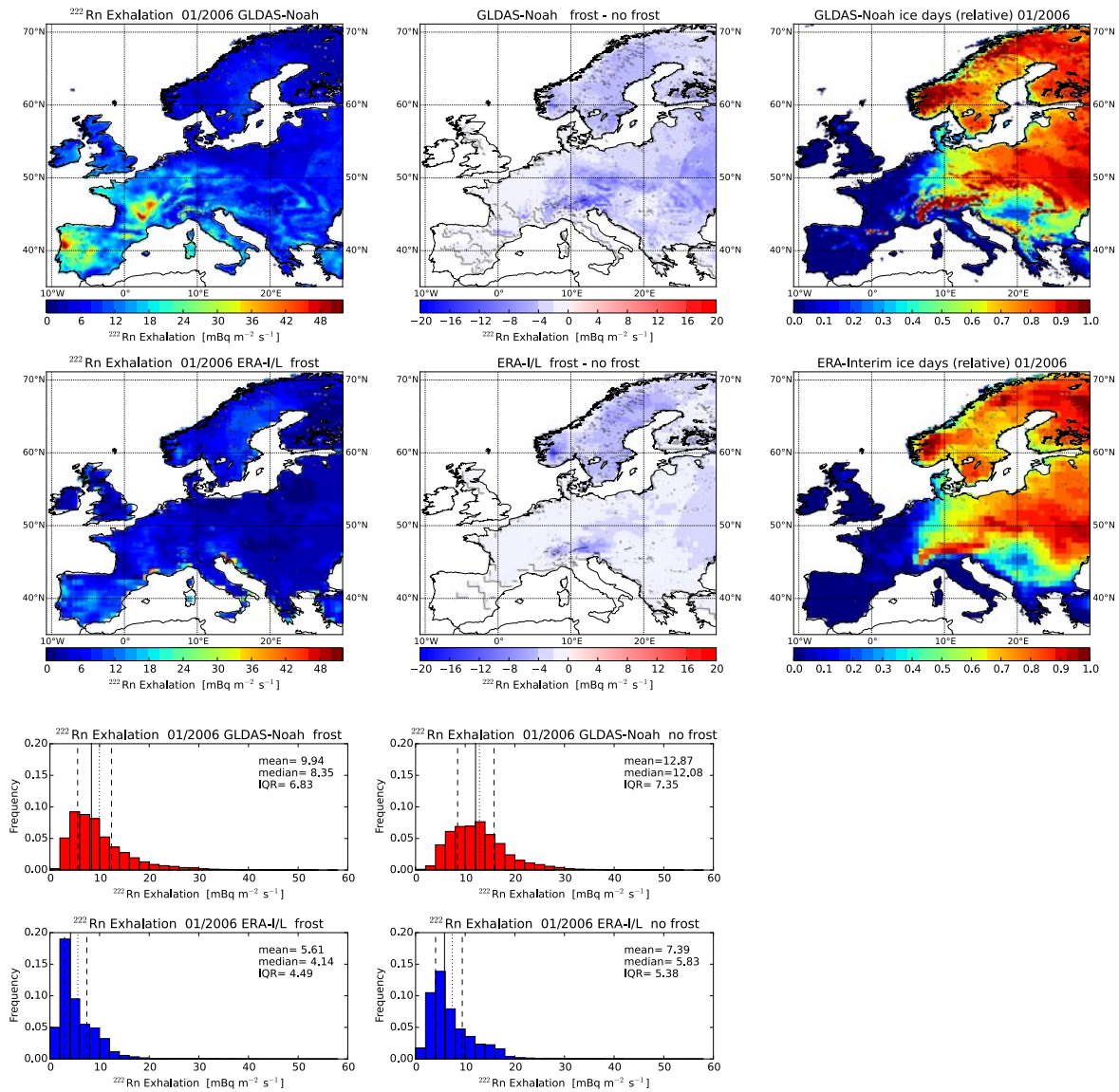


**Figure S3.**  $^{222}\text{Rn}$  exhalation rate in January 2006 taking into account the influence of frost on GLDAS-Noah-based (top row) or ERA-Interim/Land-based fluxes (middle row). Flux maps with a 50% reduction of the fluxes on ice days (left) and the difference compared to unreduced fluxes (middle) are shown. The right maps show the fraction of ice days in January 2006 in the meteorological reanalysis used in the respective soil model. Normalized frequency distributions with frost influence (left panels) and without (right panels) are shown in the bottom row.

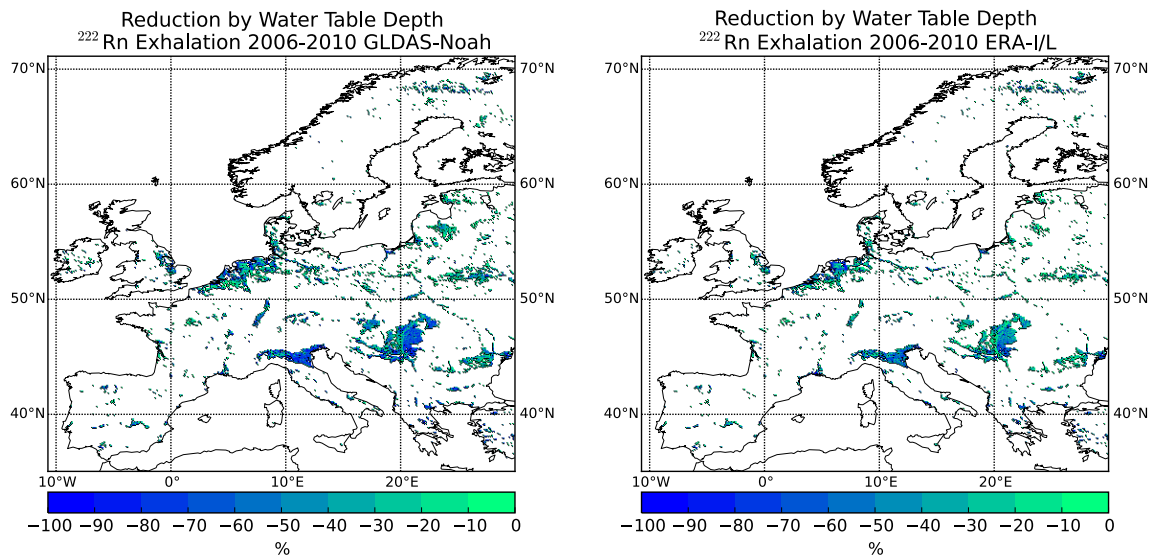


**Figure S4.** Influence of elevated water table on <sup>222</sup>Rn flux as percent change in individual pixels: left, based on GLDAS-Noah soil moisture model, right, based on ERA-I/L soil moisture model. Water table depth in Europe was taken from a hydrological model simulation by Miguez-Macho et al. (2008).

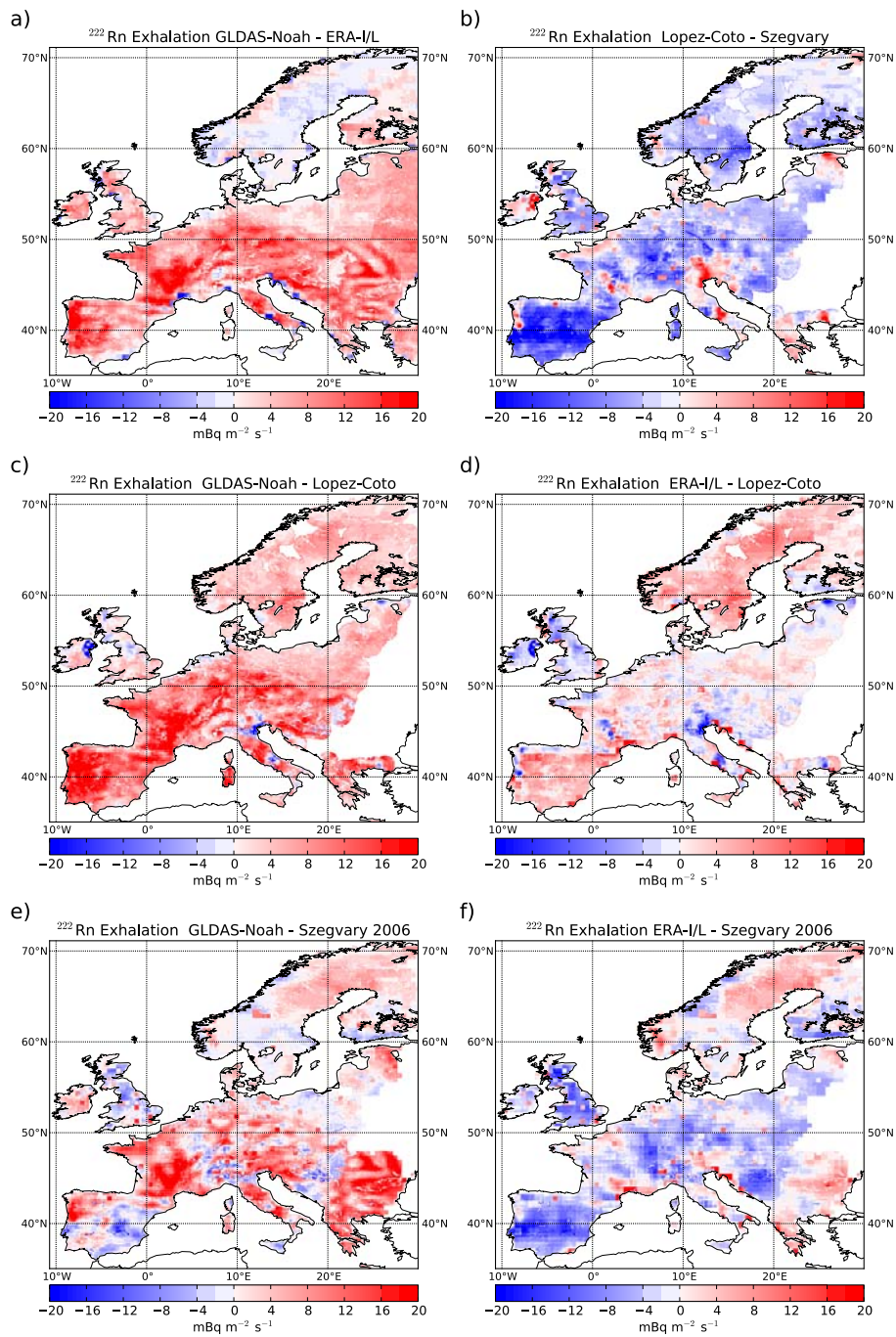


**Figure S5.** Differences in annual mean 2006 – 2010 climatologies of  $^{222}\text{Rn}$  exhalation rates between our maps based on GLDAS-Noah and ERA-Interim/Land soil moisture (upper left), between our maps and the López-Coto et al. (2013) 1957-2002 climatology (middle panels), and between our maps and the Szegvary et al. (2009) fluxes for the year 2006 only (lower panels). The difference between the López-Coto et al. (2013) 1957-2002 climatology and the Szegvary et al. (2009) fluxes for 2006 is shown in the upper right panel.



**Table S1.** Overview of episodic radon flux measurements in Europe from different publications. The date of measurement is indicated in the table, if it was available in the particular publication. The flux measurement data are shown in Figure 8, aggregated to monthly values.

Lat.	Long.	$j(^{222}\text{Rn})$ ( $\text{mBq m}^{-2} \text{s}^{-1}$ )	Date	Reference	Location
49.42	8.68	$14.44 \pm 0.98$	15.11.2011	Schmithüsen (2012)	Heidelberg (Germany)
49.42	8.68	$18.69 \pm 1.19$	15.11.2011	Schmithüsen (2012)	Heidelberg (Germany)
49.42	8.68	$19.15 \pm 1.22$	15.11.2011	Schmithüsen (2012)	Heidelberg (Germany)
49.42	8.68	$17.81 \pm 1.13$	24.11.2011	Schmithüsen (2012)	Heidelberg (Germany)
49.42	8.68	$16.29 \pm 0.97$	24.11.2011	Schmithüsen (2012)	Heidelberg (Germany)
49.42	8.68	$4.67 \pm 0.32$	24.11.2011	Schmithüsen (2012)	Heidelberg (Germany)
49.42	8.68	$12.49 \pm 0.73$	24.11.2011	Schmithüsen (2012)	Heidelberg (Germany)
49.42	8.68	$9.23 \pm 0.57$	02.12.2011	Schmithüsen (2012)	Heidelberg (Germany)
49.42	8.68	$13.03 \pm 0.80$	02.12.2011	Schmithüsen (2012)	Heidelberg (Germany)
49.42	8.68	$3.18 \pm 0.19$	09.12.2011	Schmithüsen (2012)	Heidelberg (Germany)
49.42	8.68	$3.34 \pm 0.21$	09.12.2011	Schmithüsen (2012)	Heidelberg (Germany)
49.42	8.68	$11.36 \pm 0.70$	14.12.2011	Schmithüsen (2012)	Heidelberg (Germany)
49.42	8.68	$13.65 \pm 0.83$	14.12.2011	Schmithüsen (2012)	Heidelberg (Germany)
49.42	8.68	$9.46 \pm 0.59$	13.01.2012	Schmithüsen (2012)	Heidelberg (Germany)
49.42	8.68	$4.90 \pm 0.31$	13.01.2012	Schmithüsen (2012)	Heidelberg (Germany)
49.42	8.68	$5.74 \pm 0.36$	16.01.2012	Schmithüsen (2012)	Heidelberg (Germany)
49.42	8.68	$6.32 \pm 0.39$	16.01.2012	Schmithüsen (2012)	Heidelberg (Germany)
49.42	8.68	$6.39 \pm 0.41$	24.01.2012	Schmithüsen (2012)	Heidelberg (Germany)
49.42	8.68	$4.78 \pm 0.32$	24.01.2012	Schmithüsen (2012)	Heidelberg (Germany)
49.42	8.68	$5.98 \pm 0.38$	08.03.2012	Schmithüsen (2012)	Heidelberg (Germany)
49.42	8.68	$6.88 \pm 0.43$	08.03.2012	Schmithüsen (2012)	Heidelberg (Germany)
49.42	8.68	$5.68 \pm 0.37$	08.03.2012	Schmithüsen (2012)	Heidelberg (Germany)
49.42	8.68	$5.52 \pm 0.34$	08.03.2012	Schmithüsen (2012)	Heidelberg (Germany)
49.42	8.68	$8.37 \pm 0.54$	20.03.2012	Schmithüsen (2012)	Heidelberg (Germany)
49.42	8.68	$5.22 \pm 0.31$	20.03.2012	Schmithüsen (2012)	Heidelberg (Germany)
49.42	8.68	$5.73 \pm 0.35$	20.03.2012	Schmithüsen (2012)	Heidelberg (Germany)
49.42	8.68	$9.24 \pm 0.55$	20.03.2012	Schmithüsen (2012)	Heidelberg (Germany)
49.42	8.68	$26.68 \pm 1.67$	16.05.2012	Schmithüsen (2012)	Heidelberg (Germany)
49.42	8.68	$22.30 \pm 1.39$	16.05.2012	Schmithüsen (2012)	Heidelberg (Germany)
49.42	8.68	$10.30 \pm 0.67$	16.05.2012	Schmithüsen (2012)	Heidelberg (Germany)
49.42	8.68	$8.94 \pm 0.55$	16.05.2012	Schmithüsen (2012)	Heidelberg (Germany)
49.42	8.68	$3.34 \pm 0.25$	22.05.2012	Schmithüsen (2012)	Heidelberg (Germany)
49.42	8.68	$15.65 \pm 0.98$	22.05.2012	Schmithüsen (2012)	Heidelberg (Germany)
49.42	8.68	$15.75 \pm 0.98$	29.05.2012	Schmithüsen (2012)	Heidelberg (Germany)
49.42	8.68	$17.57 \pm 1.09$	29.05.2012	Schmithüsen (2012)	Heidelberg (Germany)
49.42	8.68	$9.55 \pm 0.62$	05.06.2012	Schmithüsen (2012)	Heidelberg (Germany)



Lat.	Long.	$j(^{222}\text{Rn})$ (mBq m <sup>-2</sup> s <sup>-1</sup> )	Date	Reference	Location
49.42	8.68	13.51 ± 0.86	05.06.2012	Schmithüsen (2012)	Heidelberg (Germany)
49.42	8.68	30.01 ± 1.90	19.06.2012	Schmithüsen (2012)	Heidelberg (Germany)
49.42	8.68	4.19 ± 0.27	19.06.2012	Schmithüsen (2012)	Heidelberg (Germany)
49.42	8.68	17.35 ± 1.10	26.06.2012	Schmithüsen (2012)	Heidelberg (Germany)
49.42	8.68	18.51 ± 1.17	26.06.2012	Schmithüsen (2012)	Heidelberg (Germany)
49.42	8.68	5.49 ± 0.35	10.07.2012	Schmithüsen (2012)	Heidelberg (Germany)
49.42	8.68	16.49 ± 1.05	10.07.2012	Schmithüsen (2012)	Heidelberg (Germany)
49.42	8.68	5.53 ± 0.35	24.07.2012	Schmithüsen (2012)	Heidelberg (Germany)
49.42	8.68	18.71 ± 1.19	24.07.2012	Schmithüsen (2012)	Heidelberg (Germany)
49.42	8.68	13.93 ± 0.88	08.08.2012	Schmithüsen (2012)	Heidelberg (Germany)
49.42	8.68	11.96 ± 0.76	08.08.2012	Schmithüsen (2012)	Heidelberg (Germany)
49.42	8.68	5.46 ± 0.35	14.08.2012	Schmithüsen (2012)	Heidelberg (Germany)
49.42	8.68	13.78 ± 0.88	14.08.2012	Schmithüsen (2012)	Heidelberg (Germany)
49.42	8.66	29.57 ± 1.80	05.09.2012	Schwingshackl (2013)	Heidelberg (Germany)
49.42	8.66	40.22 ± 2.43	05.09.2012	Schwingshackl (2013)	Heidelberg (Germany)
49.42	8.66	15.66 ± 0.97	19.09.2012	Schwingshackl (2013)	Heidelberg (Germany)
49.42	8.66	20.07 ± 1.25	19.09.2012	Schwingshackl (2013)	Heidelberg (Germany)
49.42	8.66	24.18 ± 1.50	02.10.2012	Schwingshackl (2013)	Heidelberg (Germany)
49.42	8.66	38.71 ± 2.40	02.10.2012	Schwingshackl (2013)	Heidelberg (Germany)
49.42	8.66	10.03 ± 0.63	08.10.2012	Schwingshackl (2013)	Heidelberg (Germany)
49.42	8.66	19.92 ± 1.23	08.10.2012	Schwingshackl (2013)	Heidelberg (Germany)
49.42	8.66	6.28 ± 0.40	16.10.2012	Schwingshackl (2013)	Heidelberg (Germany)
49.42	8.66	23.33 ± 1.45	16.10.2012	Schwingshackl (2013)	Heidelberg (Germany)
49.42	8.66	24.68 ± 1.53	23.10.2012	Schwingshackl (2013)	Heidelberg (Germany)
49.42	8.66	24.24 ± 1.50	23.10.2012	Schwingshackl (2013)	Heidelberg (Germany)
49.42	8.66	5.77 ± 0.36	06.11.2012	Schwingshackl (2013)	Heidelberg (Germany)
49.42	8.66	16.29 ± 1.01	06.11.2012	Schwingshackl (2013)	Heidelberg (Germany)
49.42	8.66	15.47 ± 0.92	26.11.2012	Schwingshackl (2013)	Heidelberg (Germany)
49.42	8.66	20.89 ± 1.36	26.11.2012	Schwingshackl (2013)	Heidelberg (Germany)
49.42	8.66	12.05 ± 0.75	04.12.2012	Schwingshackl (2013)	Heidelberg (Germany)
49.42	8.66	34.01 ± 2.11	04.12.2012	Schwingshackl (2013)	Heidelberg (Germany)
49.42	8.66	27.28 ± 1.70	14.12.2012	Schwingshackl (2013)	Heidelberg (Germany)
49.42	8.66	28.48 ± 1.78	14.12.2012	Schwingshackl (2013)	Heidelberg (Germany)
49.42	8.66	18.48 ± 1.15	18.12.2012	Schwingshackl (2013)	Heidelberg (Germany)
49.42	8.66	17.65 ± 1.10	18.12.2012	Schwingshackl (2013)	Heidelberg (Germany)
49.42	8.66	20.71 ± 1.30	08.01.2013	Schwingshackl (2013)	Heidelberg (Germany)
49.42	8.66	17.57 ± 1.10	08.01.2013	Schwingshackl (2013)	Heidelberg (Germany)
49.42	8.66	4.62 ± 0.30	17.01.2013	Schwingshackl (2013)	Heidelberg (Germany)
49.42	8.66	15.29 ± 0.93	25.01.2013	Schwingshackl (2013)	Heidelberg (Germany)
49.42	8.66	18.63 ± 1.16	25.01.2013	Schwingshackl (2013)	Heidelberg (Germany)

Lat.	Long.	$j(^{222}\text{Rn})$ (mBq m <sup>-2</sup> s <sup>-1</sup> )	Date	Reference	Location
49.42	8.66	10.83 ± 0.69	15.02.2013	Schwingshackl (2013)	Heidelberg (Germany)
49.42	8.66	11.06 ± 0.70	15.02.2013	Schwingshackl (2013)	Heidelberg (Germany)
49.42	8.66	19.34 ± 1.21	07.03.2013	Schwingshackl (2013)	Heidelberg (Germany)
49.42	8.66	14.70 ± 0.92	07.03.2013	Schwingshackl (2013)	Heidelberg (Germany)
49.42	8.66	18.98 ± 1.57	23.07.2013	Schwingshackl (2013)	Heidelberg (Germany)
49.42	8.66	19.62 ± 1.32	23.07.2013	Schwingshackl (2013)	Heidelberg (Germany)
49.42	8.66	18.40 ± 1.51	04.10.2013	Schwingshackl (2013)	Heidelberg (Germany)
49.42	8.66	20.38 ± 1.35	04.10.2013	Schwingshackl (2013)	Heidelberg (Germany)
49.50	8.59	23.19 ± 1.84	17.07.2013	Schwingshackl (2013)	Heddesheim (Germany)
49.50	8.59	11.51 ± 0.90	17.07.2013	Schwingshackl (2013)	Heddesheim (Germany)
49.50	8.59	15.63 ± 1.25	20.08.2013	Schwingshackl (2013)	Heddesheim (Germany)
49.50	8.59	15.24 ± 1.19	20.08.2013	Schwingshackl (2013)	Heddesheim (Germany)
49.50	8.59	22.07 ± 1.77	27.08.2013	Schwingshackl (2013)	Heddesheim (Germany)
49.50	8.59	10.04 ± 0.82	27.08.2013	Schwingshackl (2013)	Heddesheim (Germany)
49.50	8.59	19.29 ± 1.54	02.09.2013	Schwingshackl (2013)	Heddesheim (Germany)
49.50	8.59	35.75 ± 2.77	02.09.2013	Schwingshackl (2013)	Heddesheim (Germany)
49.50	8.59	12.74 ± 1.02	24.09.2013	Schwingshackl (2013)	Heddesheim (Germany)
49.50	8.59	10.89 ± 0.86	24.09.2013	Schwingshackl (2013)	Heddesheim (Germany)
49.50	8.59	13.57 ± 1.10	30.09.2013	Schwingshackl (2013)	Heddesheim (Germany)
49.50	8.59	7.99 ± 0.64	30.09.2013	Schwingshackl (2013)	Heddesheim (Germany)
49.50	8.59	6.67 ± 0.54	08.10.2013	Schwingshackl (2013)	Heddesheim (Germany)
49.50	8.59	27.64 ± 2.15	08.10.2013	Schwingshackl (2013)	Heddesheim (Germany)
49.50	8.59	10.09 ± 0.81	14.10.2013	Schwingshackl (2013)	Heddesheim (Germany)
49.50	8.59	12.61 ± 0.99	14.10.2013	Schwingshackl (2013)	Heddesheim (Germany)
49.50	8.59	11.98 ± 0.97	05.11.2013	Schwingshackl (2013)	Heddesheim (Germany)
49.50	8.59	12.90 ± 1.02	05.11.2013	Schwingshackl (2013)	Heddesheim (Germany)
48.72	2.17	4.97 ± 0.52	10.07.2013	Schwingshackl (2013)	Gif-sur-Yvette (France)
48.72	2.17	7.29 ± 0.61	10.07.2013	Schwingshackl (2013)	Gif-sur-Yvette (France)
48.72	2.17	11.07 ± 1.06	10.07.2013	Schwingshackl (2013)	Gif-sur-Yvette (France)
48.72	2.17	11.93 ± 1.14	10.07.2013	Schwingshackl (2013)	Gif-sur-Yvette (France)
48.72	2.17	4.48 ± 0.47	10.07.2013	Schwingshackl (2013)	Gif-sur-Yvette (France)
48.72	2.17	9.71 ± 0.93	10.07.2013	Schwingshackl (2013)	Gif-sur-Yvette (France)
48.72	2.17	7.63 ± 0.69	10.07.2013	Schwingshackl (2013)	Gif-sur-Yvette (France)
48.72	2.17	5.93 ± 0.50	10.07.2013	Schwingshackl (2013)	Gif-sur-Yvette (France)
48.72	2.17	4.78 ± 0.40	10.07.2013	Schwingshackl (2013)	Gif-sur-Yvette (France)
48.72	2.17	8.14 ± 0.63	10.07.2013	Schwingshackl (2013)	Gif-sur-Yvette (France)
48.72	2.17	4.14 ± 0.35	10.07.2013	Schwingshackl (2013)	Gif-sur-Yvette (France)
48.72	2.17	4.43 ± 0.44	10.07.2013	Schwingshackl (2013)	Gif-sur-Yvette (France)
48.72	2.17	9.58 ± 0.75	06.08.2013	Schwingshackl (2013)	Gif-sur-Yvette (France)
48.72	2.17	8.91 ± 0.73	06.08.2013	Schwingshackl (2013)	Gif-sur-Yvette (France)

Lat.	Long.	$j(^{222}\text{Rn})$ (mBq m <sup>-2</sup> s <sup>-1</sup> )	Date	Reference	Location
48.72	2.17	10.26 ± 0.73	06.08.2013	Schwingshackl (2013)	Gif-sur-Yvette (France)
48.72	2.17	10.90 ± 0.81	06.08.2013	Schwingshackl (2013)	Gif-sur-Yvette (France)
48.72	2.17	7.89 ± 0.59	06.08.2013	Schwingshackl (2013)	Gif-sur-Yvette (France)
48.72	2.17	10.49 ± 0.74	06.08.2013	Schwingshackl (2013)	Gif-sur-Yvette (France)
48.72	2.17	8.37 ± 0.62	23.09.2013	Schwingshackl (2013)	Gif-sur-Yvette (France)
48.72	2.17	17.05 ± 1.19	23.09.2013	Schwingshackl (2013)	Gif-sur-Yvette (France)
48.72	2.17	12.46 ± 0.92	23.09.2013	Schwingshackl (2013)	Gif-sur-Yvette (France)
48.72	2.17	15.39 ± 1.08	23.09.2013	Schwingshackl (2013)	Gif-sur-Yvette (France)
48.72	2.17	5.71 ± 0.40	30.10.2013	Schwingshackl (2013)	Gif-sur-Yvette (France)
48.72	2.17	6.29 ± 0.46	30.10.2013	Schwingshackl (2013)	Gif-sur-Yvette (France)
48.72	2.17	4.25 ± 0.32	30.10.2013	Schwingshackl (2013)	Gif-sur-Yvette (France)
48.72	2.17	6.02 ± 0.42	30.10.2013	Schwingshackl (2013)	Gif-sur-Yvette (France)
48.72	2.17	4.63 ± 0.34	19.11.2013	Schwingshackl (2013)	Gif-sur-Yvette (France)
48.72	2.17	2.45 ± 0.20	19.11.2013	Schwingshackl (2013)	Gif-sur-Yvette (France)
48.72	2.17	3.82 ± 0.29	19.11.2013	Schwingshackl (2013)	Gif-sur-Yvette (France)
48.72	2.17	5.72 ± 0.43	19.11.2013	Schwingshackl (2013)	Gif-sur-Yvette (France)
48.72	2.17	5.98 ± 0.43	10.03.2014	Schwingshackl (2013)	Gif-sur-Yvette (France)
48.72	2.17	8.90 ± 0.66	10.03.2014	Schwingshackl (2013)	Gif-sur-Yvette (France)
48.72	2.17	6.41 ± 0.48	10.03.2014	Schwingshackl (2013)	Gif-sur-Yvette (France)
48.72	2.17	6.52 ± 0.47	10.03.2014	Schwingshackl (2013)	Gif-sur-Yvette (France)
48.72	2.17	8.39 ± 0.75	24.03.2014	Schwingshackl (2013)	Gif-sur-Yvette (France)
48.72	2.17	4.34 ± 0.41	24.03.2014	Schwingshackl (2013)	Gif-sur-Yvette (France)
48.72	2.17	5.83 ± 0.45	24.03.2014	Schwingshackl (2013)	Gif-sur-Yvette (France)
48.72	2.17	4.04 ± 0.34	24.03.2014	Schwingshackl (2013)	Gif-sur-Yvette (France)
48.72	2.17	5.64 ± 0.55	24.03.2014	Schwingshackl (2013)	Gif-sur-Yvette (France)
48.72	2.17	6.87 ± 0.51	24.03.2014	Schwingshackl (2013)	Gif-sur-Yvette (France)
48.52	5.25	30.07 ± 2.48	01.08.2013	Schwingshackl (2013)	Bure (France)
48.52	5.25	62.00 ± 5.31	01.08.2013	Schwingshackl (2013)	Bure (France)
48.52	5.25	32.29 ± 2.62	01.08.2013	Schwingshackl (2013)	Bure (France)
48.52	5.25	20.92 ± 1.56	01.08.2013	Schwingshackl (2013)	Bure (France)
48.52	5.25	76.16 ± 6.52	01.08.2013	Schwingshackl (2013)	Bure (France)
48.52	5.25	23.69 ± 1.77	01.08.2013	Schwingshackl (2013)	Bure (France)
48.52	5.25	13.49 ± 1.22	01.08.2013	Schwingshackl (2013)	Bure (France)
48.52	5.25	15.27 ± 1.37	01.08.2013	Schwingshackl (2013)	Bure (France)
48.52	5.25	54.77 ± 4.33	01.08.2013	Schwingshackl (2013)	Bure (France)
48.52	5.25	35.10 ± 2.64	01.08.2013	Schwingshackl (2013)	Bure (France)
48.52	5.25	13.02 ± 1.08	01.08.2013	Schwingshackl (2013)	Bure (France)
48.52	5.25	15.97 ± 1.08	19.08.2013	Schwingshackl (2013)	Bure (France)
48.52	5.25	20.72 ± 1.73	19.08.2013	Schwingshackl (2013)	Bure (France)
48.52	5.25	14.88 ± 1.01	19.08.2013	Schwingshackl (2013)	Bure (France)

Lat.	Long.	$j(^{222}\text{Rn})$ (mBq m <sup>-2</sup> s <sup>-1</sup> )	Date	Reference	Location
48.52	5.25	12.97 ± 1.09	19.08.2013	Schwingshackl (2013)	Bure (France)
48.52	5.25	13.46 ± 1.14	26.08.2013	Schwingshackl (2013)	Bure (France)
48.52	5.25	16.00 ± 1.34	26.08.2013	Schwingshackl (2013)	Bure (France)
48.52	5.25	15.88 ± 1.09	26.08.2013	Schwingshackl (2013)	Bure (France)
48.52	5.25	11.16 ± 0.84	26.08.2013	Schwingshackl (2013)	Bure (France)
48.52	5.25	18.81 ± 1.26	02.09.2013	Schwingshackl (2013)	Bure (France)
48.52	5.25	20.43 ± 1.37	02.09.2013	Schwingshackl (2013)	Bure (France)
48.52	5.25	14.91 ± 1.24	02.09.2013	Schwingshackl (2013)	Bure (France)
48.52	5.25	14.52 ± 1.08	23.09.2013	Schwingshackl (2013)	Bure (France)
48.52	5.25	14.32 ± 1.08	23.09.2013	Schwingshackl (2013)	Bure (France)
48.52	5.25	7.82 ± 0.71	23.09.2013	Schwingshackl (2013)	Bure (France)
48.52	5.25	7.99 ± 0.73	23.09.2013	Schwingshackl (2013)	Bure (France)
48.52	5.25	6.59 ± 0.60	04.03.2014	Schwingshackl (2013)	Bure (France)
48.52	5.25	12.56 ± 0.84	04.03.2014	Schwingshackl (2013)	Bure (France)
48.52	5.25	4.62 ± 0.39	04.03.2014	Schwingshackl (2013)	Bure (France)
48.52	5.25	9.14 ± 0.62	04.03.2014	Schwingshackl (2013)	Bure (France)
48.52	5.25	4.07 ± 0.35	04.03.2014	Schwingshackl (2013)	Bure (France)
48.52	5.25	17.66 ± 1.39	17.03.2014	Schwingshackl (2013)	Bure (France)
48.52	5.25	8.38 ± 0.81	17.03.2014	Schwingshackl (2013)	Bure (France)
48.52	5.25	8.10 ± 0.71	17.03.2014	Schwingshackl (2013)	Bure (France)
48.52	5.25	15.27 ± 1.07	17.03.2014	Schwingshackl (2013)	Bure (France)
48.52	5.25	16.01 ± 1.12	17.03.2014	Schwingshackl (2013)	Bure (France)
48.52	5.25	11.39 ± 1.02	17.03.2014	Schwingshackl (2013)	Bure (France)
51.42	-0.57	5.20 ± 0.45	16.09.2013	Schwingshackl (2013)	Egham (United Kingdom)
51.42	-0.57	4.36 ± 0.38	16.09.2013	Schwingshackl (2013)	Egham (United Kingdom)
51.42	-0.57	3.52 ± 0.38	16.09.2013	Schwingshackl (2013)	Egham (United Kingdom)
51.42	-0.57	3.12 ± 0.29	16.09.2013	Schwingshackl (2013)	Egham (United Kingdom)
51.42	-0.57	17.33 ± 2.34	16.09.2013	Schwingshackl (2013)	Egham (United Kingdom)
51.42	-0.57	2.96 ± 0.27	16.09.2013	Schwingshackl (2013)	Egham (United Kingdom)
51.42	-0.57	11.92 ± 1.62	16.09.2013	Schwingshackl (2013)	Egham (United Kingdom)
51.42	-0.57	10.45 ± 1.42	16.09.2013	Schwingshackl (2013)	Egham (United Kingdom)
51.42	-0.57	3.49 ± 0.28	16.09.2013	Schwingshackl (2013)	Egham (United Kingdom)
51.42	-0.57	8.59 ± 1.13	16.09.2013	Schwingshackl (2013)	Egham (United Kingdom)
51.42	-0.57	2.41 ± 0.25	16.09.2013	Schwingshackl (2013)	Egham (United Kingdom)
51.42	-0.57	4.00 ± 0.33	16.09.2013	Schwingshackl (2013)	Egham (United Kingdom)
51.10	10.92	24.45 ± 7.14	26.09.2003	Schell (2004)	Gebesee (Germany)
51.10	10.92	22.70 ± 3.50	20.10.2003	Schell (2004)	Gebesee (Germany)
51.10	10.92	21.91 ± 13.03	04.11.2003	Schell (2004)	Gebesee (Germany)
51.10	10.92	19.60 ± 14.52	14.01.2004	Schell (2004)	Gebesee (Germany)
51.10	10.92	20.08 ± 10.37	11.02.2004	Schell (2004)	Gebesee (Germany)

Lat.	Long.	$j(^{222}\text{Rn})$ (mBq m <sup>-2</sup> s <sup>-1</sup> )	Date	Reference	Location
51.10	10.92	21.11 ± 6.57	11.03.2004	Schell (2004)	Gebesee (Germany)
51.10	10.92	23.83 ± 2.70	15.04.2004	Schell (2004)	Gebesee (Germany)
51.10	10.92	22.55 ± 3.30	12.05.2004	Schell (2004)	Gebesee (Germany)
51.10	10.92	24.35 ± 5.74	19.07.2004	Schell (2004)	Gebesee (Germany)
51.10	10.92	27.92 ± 8.17	19.08.2004	Schell (2004)	Gebesee (Germany)
51.10	10.92	37.50 ± 12.74	15.09.2004	Schell (2004)	Gebesee (Germany)
36.72	-4.46	12.00 ± 8.00		Dueñas et al. (1997)	Málaga (Spain)
36.67	-4.47	25.00 ± 13.00		Dueñas et al. (1997)	Málaga (Spain)
36.69	-4.44	3.00 ± 1.60		Dueñas et al. (1997)	Málaga (Spain)
36.73	-4.46	10.00 ± 4.00		Dueñas et al. (1997)	Málaga (Spain)
40.45	-1.06	7.22 ± 1.63	July 2008	Grossi et al. (2011)	Teruel (Spain)
39.47	-0.97	11.32 ± 1.56	July 2008	Grossi et al. (2011)	Los Pedrones (Spain)
39.79	-3.54	15.76 ± 1.50	July 2008	Grossi et al. (2011)	Q. de la Orden (Spain)
40.58	-3.62	25.97 ± 5.99	July 2008	Grossi et al. (2011)	Madrif (Spain)
37.10	-6.70	1.36 ± 0.64		Grossi et al. (2012)	El Arenosillo (Spain)
48.72	2.16	7.40 ± 0.74	April 1958	Servant (1964)	Gif-sur-Yvette (France)
48.72	2.16	17.76 ± 0.74	May 1958	Servant (1964)	Gif-sur-Yvette (France)
48.72	2.16	22.20 ± 0.74	June 1958	Servant (1964)	Gif-sur-Yvette (France)
48.72	2.16	17.76 ± 0.74	July 1958	Servant (1964)	Gif-sur-Yvette (France)
48.72	2.16	17.02 ± 0.74	September 1958	Servant (1964)	Gif-sur-Yvette (France)
48.72	2.16	14.80 ± 0.74	October 1958	Servant (1964)	Gif-sur-Yvette (France)
48.72	2.16	11.84 ± 0.74	November 1958	Servant (1964)	Gif-sur-Yvette (France)
48.72	2.16	10.36 ± 0.74	December 1958	Servant (1964)	Gif-sur-Yvette (France)
48.72	2.16	9.25 ± 0.74	February 1959	Servant (1964)	Gif-sur-Yvette (France)
48.72	2.16	14.80 ± 0.74	March 1959	Servant (1964)	Gif-sur-Yvette (France)
48.72	2.16	13.69 ± 0.74	April 1959	Servant (1964)	Gif-sur-Yvette (France)
54.43	12.73	1.39 ± 0.83	April 1997	Schmidt (1999)	Zingst (Germany)
54.43	12.73	2.08 ± 0.19	August 1997	Schmidt (1999)	Zingst (Germany)
54.43	12.73	1.11	March 1998	Schmidt (1999)	Zingst (Germany)
54.43	12.73	1.25	July 1998	Schmidt (1999)	Zingst (Germany)
53.17	13.03	18.89 ± 3.47	May 1997	Schmidt (1999)	Neuglobsow (Germany)
53.17	13.03	17.22 ± 2.64	August 1997	Schmidt (1999)	Neuglobsow (Germany)
53.17	13.03	13.06 ± 3.33	March 1998	Schmidt (1999)	Neuglobsow (Germany)
53.17	13.03	18.19 ± 5.69	July 1998	Schmidt (1999)	Neuglobsow (Germany)
54.35	12.68	6.53	April 1997	Schmidt (1999)	Zingst (Germany)
54.35	12.68	8.89 ± 2.22	March 1998	Schmidt (1999)	Zingst (Germany)
54.35	12.68	8.89 ± 3.89	July 1998	Schmidt (1999)	Zingst (Germany)
53.75	13.12	10.83 ± 4.86	March 1998	Schmidt (1999)	Altenhagen (Germany)
53.75	13.12	4.03 ± 1.67	July 1998	Schmidt (1999)	Altenhagen (Germany)
53.39	6.36	1.04 ± 0.22	January	Manohar et al. (2015)	Lutjewad (Netherlands)

Lat.	Long.	$j(^{222}\text{Rn})$ ( $\text{mBq m}^{-2} \text{s}^{-1}$ )	Date	Reference	Location
53.39	6.36	$2.76 \pm 0.46$	February	Manohar et al. (2015)	Lutjewad (Netherlands)
53.39	6.36	$2.00 \pm 0.20$	March	Manohar et al. (2015)	Lutjewad (Netherlands)
53.39	6.36	$3.20 \pm 0.33$	April	Manohar et al. (2015)	Lutjewad (Netherlands)
53.39	6.36	$4.30 \pm 0.39$	May	Manohar et al. (2015)	Lutjewad (Netherlands)
53.39	6.36	$4.37 \pm 0.40$	June	Manohar et al. (2015)	Lutjewad (Netherlands)
53.39	6.36	$2.73 \pm 0.27$	July	Manohar et al. (2015)	Lutjewad (Netherlands)
53.39	6.36	$2.58 \pm 0.16$	August	Manohar et al. (2015)	Lutjewad (Netherlands)
53.39	6.36	$4.56 \pm 0.77$	September	Manohar et al. (2015)	Lutjewad (Netherlands)
53.39	6.36	$4.33 \pm 0.68$	October	Manohar et al. (2015)	Lutjewad (Netherlands)
53.39	6.36	$3.57 \pm 0.95$	November	Manohar et al. (2015)	Lutjewad (Netherlands)
53.39	6.36	$2.66 \pm 0.56$	December	Manohar et al. (2015)	Lutjewad (Netherlands)
43.50	-1.00	$4.58 \pm 0.89$	1990	Eckhardt (1990)	Dax-Sebastopol (France)
53.05	11.35	5.61	1990	Eckhardt (1990)	Gorleben (Germany)
49.52	8.52	$8.97 \pm 1.25$	1990	Eckhardt (1990)	Mannheim (Germany)
49.58	8.50	$10.75 \pm 1.67$	1990	Eckhardt (1990)	Mannheim (Germany)
49.27	8.60	$11.72 \pm 0.69$	1990	Eckhardt (1990)	St. Leon (Germany)
48.85	13.20	$4.17 \pm 1.11$	1990	Eckhardt (1990)	Deggendorf (Germany)
49.88	8.65	4.72	1990	Eckhardt (1990)	Darmstadt (Germany)
47.73	9.63	5.50	1990	Eckhardt (1990)	Ravensburg (Germany)
49.43	8.72	$5.50 \pm 0.33$	1990	Eckhardt (1990)	Strangwasem (Germany)
49.23	8.72	14.17	1990	Eckhardt (1990)	Östringen (Germany)
49.37	8.72	17.58	1990	Eckhardt (1990)	Leimen (Germany)
49.38	8.70	$36.39 \pm 13.42$	1990	Eckhardt (1990)	Heidelberg (Germany)
49.17	8.72	$23.00 \pm 1.67$	1993-1995	Schübler (1996)	Weiherbachtal (Germany)
51.85	6.62	$4.81 \pm 3.00$	1990	Eckhardt (1990)	Bocholt-Liedern (Germany)
49.35	8.65	22.31	1990	Eckhardt (1990)	Bruchhausen (Germany)
49.30	8.57	10.69	1990	Eckhardt (1990)	Reilingen (Germany)
47.05	8.30	$10.83 \pm 1.25$	1990	Eckhardt (1990)	Luzern (Switzerland)
49.38	8.57	13.97	1990	Eckhardt (1990)	Schwetzingen (Germany)
45.32	8.42	$8.56 \pm 0.89$	1990	Eckhardt (1990)	Vercelli (Italy)
49.20	7.95	26.39	1990	Eckhardt (1990)	Erfweiler (Germany)
49.27	8.87	$28.97 \pm 9.86$	1990	Eckhardt (1990)	Sinsheim (Germany)
49.38	8.82	29.44	1990	Eckhardt (1990)	Wiesenbach (Germany)
46.07	7.78	5.09		Eckhardt (1990)	Täsch (Switzerland)
52.25	21.00	7.18	1968	Pensko et al. (1968)	Warschau (Poland)
47.28	11.42	$12.31 \pm 3.80$	1935	Zeilinger (1935)	Innsbruck (Austria)
47.08	15.37	$14.63 \pm 5.37$	1935	Kosmath (1935)	Graz (Austria)
50.77	6.10	16.90	1970	Israel et al. (1970)	Aachen (Germany)
53.33	-6.25	27.41	1912	Smyth (1912)	Dublin (Ireland)
49.60	8.59	$7.20 \pm 0.72$	1984	Dörr (1984)	Hüttenfeld (Germany)

Lat.	Long.	$j(^{222}\text{Rn})$ (mBq m <sup>-2</sup> s <sup>-1</sup> )	Date	Reference	Location
49.53	8.62	19.01 ± 1.90	1984	Dörr (1984)	Muckensturm (Germany)
49.54	8.58	7.97 ± 0.80	1984	Dörr (1984)	Viernheim (Germany)
49.54	8.60	3.83 ± 0.38	1984	Dörr (1984)	Viernheim (Germany)
49.46	8.56	15.26 ± 1.53	1984	Dörr (1984)	Seckenheim (Germany)
49.35	8.65	5.09 ± 0.51	1984	Dörr (1984)	Sandhausen (Germany)
53.13	-8.45	4.10 ± 0.50	10.10.2000	Jutzi (2001)	Kylebrack (Ireland)
53.13	-8.45	5.84 ± 0.80	10.10.2000	Jutzi (2001)	Kylebrack (Ireland)
53.17	-8.37	16.38 ± 2.14	10.10.2000	Jutzi (2001)	Tynagh (Ireland)
53.17	-8.37	21.68 ± 2.80	10.10.2000	Jutzi (2001)	Tynagh (Ireland)
53.17	-8.83	17.32 ± 2.23	10.10.2000	Jutzi (2001)	Ardrahan (Ireland)
53.17	-8.83	8.22 ± 1.04	10.10.2000	Jutzi (2001)	Ardrahan (Ireland)
52.92	-9.25	1.28 ± 0.16	10.10.2000	Jutzi (2001)	Ennismon (Ireland)
52.92	-9.25	0.47 ± 0.21	10.10.2000	Jutzi (2001)	Ennismon (Ireland)
53.23	-8.25	13.80 ± 1.80	11.10.2000	Jutzi (2001)	Kiltomer (Ireland)
53.23	-8.25	5.46 ± 0.69	11.10.2000	Jutzi (2001)	Kiltomer (Ireland)
53.47	-8.17	2.55 ± 0.32	11.10.2000	Jutzi (2001)	Dysart (Ireland)
53.47	-8.17	3.37 ± 0.46	11.10.2000	Jutzi (2001)	Dysart (Ireland)
53.77	-8.08	4.30 ± 0.60	11.10.2000	Jutzi (2001)	Strokestown (Ireland)
53.77	-8.08	7.83 ± 1.10	11.10.2000	Jutzi (2001)	Strokestown (Ireland)
53.97	-7.85	4.67 ± 0.60	12.10.2000	Jutzi (2001)	Mohill (Ireland)
53.97	-7.85	5.36 ± 0.70	12.10.2000	Jutzi (2001)	Mohill (Ireland)
53.83	-7.05	0.49 ± 0.07	12.10.2000	Jutzi (2001)	Virginia (Ireland)
53.33	-6.88	4.68 ± 1.11	13.10.2000	Jutzi (2001)	Innfield (Ireland)
53.33	-6.88	1.78 ± 0.18	13.10.2000	Jutzi (2001)	Innfield (Ireland)
53.20	-7.38	8.22 ± 1.08	13.10.2000	Jutzi (2001)	Tullamore (Ireland)
53.20	-7.38	2.55 ± 0.35	13.10.2000	Jutzi (2001)	Tullamore (Ireland)
53.07	-7.97	8.27 ± 1.07	13.10.2000	Jutzi (2001)	Carrig (Ireland)
53.07	-7.97	9.94 ± 1.30	13.10.2000	Jutzi (2001)	Carrig (Ireland)
53.13	-8.45	2.09 ± 0.31	14.10.2000	Jutzi (2001)	Kylebrack (Ireland)
53.13	-8.45	3.97 ± 0.49	14.10.2000	Jutzi (2001)	Kylebrack (Ireland)
53.17	-8.37	3.78 ± 0.50	14.10.2000	Jutzi (2001)	Tynagh (Ireland)
53.17	-8.37	5.95 ± 0.80	14.10.2000	Jutzi (2001)	Tynagh (Ireland)
53.17	-8.83	18.53 ± 2.40	14.10.2000	Jutzi (2001)	Ardahan (Ireland)
53.17	-8.83	1.33 ± 0.20	14.10.2000	Jutzi (2001)	Ardahan (Ireland)
53.23	-8.37	2.92 ± 0.37	15.10.2000	Jutzi (2001)	Kiltomer (Ireland)
53.23	-8.37	5.46 ± 0.69	15.10.2000	Jutzi (2001)	Kiltomer (Ireland)
53.52	-8.68	1.84 ± 0.27	15.10.2000	Jutzi (2001)	Lerally (Ireland)
53.52	-8.68	1.29 ± 0.13	15.10.2000	Jutzi (2001)	Lerally (Ireland)
53.77	-8.08	9.69 ± 1.30	15.10.2000	Jutzi (2001)	Strokestown (Ireland)
53.77	-8.08	4.82 ± 0.65	15.10.2000	Jutzi (2001)	Strokestown (Ireland)

Lat.	Long.	$j(^{222}\text{Rn})$ (mBq m <sup>-2</sup> s <sup>-1</sup> )	Date	Reference	Location
52.83	-9.03	5.10 ± 0.70	16.10.2000	Jutzi (2001)	Ennis (Ireland)
52.83	-8.75	1.95 ± 0.20	16.10.2000	Jutzi (2001)	Tulla (Ireland)
52.42	-8.17	3.59 ± 1.62	17.10.2000	Jutzi (2001)	Tipperary (Ireland)
52.42	-8.17	4.46 ± 0.60	17.10.2000	Jutzi (2001)	Tipperary (Ireland)
52.42	-7.92	42.68 ± 0.20	17.10.2000	Jutzi (2001)	Cashel (Ireland)
52.42	-7.92	1.62 ± 0.20	17.10.2000	Jutzi (2001)	Cashel (Ireland)
52.08	-8.03	2.14 ± 0.29	18.10.2000	Jutzi (2001)	Lismore (Ireland)
52.08	-8.03	2.38 ± 2.41	18.10.2000	Jutzi (2001)	Lismore (Ireland)
47.54	7.58	18.33		Szegvary et al. (2007)	(Switzerland)
47.43	7.88	3.89		Szegvary et al. (2007)	(Switzerland)
46.51	6.67	25.28		Szegvary et al. (2007)	(Switzerland)
47.29	7.74	24.17		Szegvary et al. (2007)	(Switzerland)
46.93	7.42	23.33		Szegvary et al. (2007)	(Switzerland)
46.93	7.42	18.33		Szegvary et al. (2007)	(Switzerland)
46.33	6.92	10.28		Szegvary et al. (2007)	(Switzerland)
46.33	6.92	3.61		Szegvary et al. (2007)	(Switzerland)
46.30	7.84	13.89		Szegvary et al. (2007)	(Switzerland)
46.84	6.58	13.61		Szegvary et al. (2007)	(Switzerland)
47.08	6.79	18.61		Szegvary et al. (2007)	(Switzerland)
46.40	6.23	25.56		Szegvary et al. (2007)	(Switzerland)
46.81	9.84	5.00		Szegvary et al. (2007)	(Switzerland)
46.53	9.88	10.28		Szegvary et al. (2007)	(Switzerland)
46.34	10.07	27.22		Szegvary et al. (2007)	(Switzerland)
47.26	7.79	23.06		Szegvary et al. (2007)	(Switzerland)
46.50	8.31	16.94		Szegvary et al. (2007)	(Switzerland)
47.48	8.90	26.67		Szegvary et al. (2007)	(Switzerland)
47.43	9.40	12.22		Szegvary et al. (2007)	(Switzerland)
47.03	9.07	20.56		Szegvary et al. (2007)	(Switzerland)
47.13	9.52	10.83		Szegvary et al. (2007)	(Switzerland)
47.06	8.46	1.94		Szegvary et al. (2007)	(Switzerland)
47.59	7.64	30.28		Szegvary et al. (2007)	(Switzerland)
47.76	7.81	43.61		Szegvary et al. (2007)	(Germany)
47.66	8.00	8.33		Szegvary et al. (2007)	(Germany)
47.59	8.14	9.17		Szegvary et al. (2007)	(Germany)
47.56	7.95	16.11		Szegvary et al. (2007)	(Germany)
47.56	7.78	27.22		Szegvary et al. (2007)	(Germany)
47.65	7.82	24.72		Szegvary et al. (2007)	(Germany)
60.39	25.29	52.50		Szegvary et al. (2007)	(Finland)
60.46	26.22	23.33		Szegvary et al. (2007)	(Finland)
60.44	26.05	34.44		Szegvary et al. (2007)	(Finland)



Lat.	Long.	$j(^{222}\text{Rn})$ (mBq m <sup>-2</sup> s <sup>-1</sup> )	Date	Reference	Location
61.51	23.79	15.28		Szegvary et al. (2007)	(Finland)
61.27	24.04	16.67		Szegvary et al. (2007)	(Finland)
60.89	24.29	14.17		Szegvary et al. (2007)	(Finland)
60.45	22.37	37.22		Szegvary et al. (2007)	(Finland)
60.47	23.98	30.00		Szegvary et al. (2007)	(Finland)
66.14	28.14	3.33		Szegvary et al. (2007)	(Finland)
66.37	26.76	26.39		Szegvary et al. (2007)	(Finland)
66.51	25.79	13.61		Szegvary et al. (2007)	(Finland)
65.40	26.91	1.67		Szegvary et al. (2007)	(Finland)
65.95	26.47	1.67		Szegvary et al. (2007)	(Finland)
67.41	26.64	9.72		Szegvary et al. (2007)	(Finland)
66.72	27.33	0.56		Szegvary et al. (2007)	(Finland)
66.12	24.85	14.72		Szegvary et al. (2007)	(Finland)
47.71	17.67	8.06		Szegvary et al. (2007)	(Hungary)
47.56	18.41	30.00		Szegvary et al. (2007)	(Hungary)
47.94	19.14	22.22		Szegvary et al. (2007)	(Hungary)
48.10	19.54	12.22		Szegvary et al. (2007)	(Hungary)
48.05	19.79	13.06		Szegvary et al. (2007)	(Hungary)
47.10	17.89	21.94		Szegvary et al. (2007)	(Hungary)
47.35	17.47	6.94		Szegvary et al. (2007)	(Hungary)
47.73	20.27	6.39		Szegvary et al. (2007)	(Hungary)
48.10	20.77	30.83		Szegvary et al. (2007)	(Hungary)
48.23	20.26	20.28		Szegvary et al. (2007)	(Hungary)
47.76	18.61	13.89		Szegvary et al. (2007)	(Hungary)
47.55	18.80	14.44		Szegvary et al. (2007)	(Hungary)
55.92	-3.17	35.40		Robertson (2004)	Edinburgh (United Kingdom)
55.91	-3.22	17.20 ± 13.70		Robertson (2004)	Edinburgh (United Kingdom)
55.17	-2.05	1.00 ± 0.90		Robertson (2004)	Harwood (United Kingdom)
56.60	-3.80	9.70 ± 4.10		Robertson (2004)	Griffin (United Kingdom)

## References

- Dörr, H.: Die Untersuchung des Gas- und Wasserhaushalts in der ungesättigten Bodenzone mit Hilfe von Kohlendioxid- und Radon-222 Messungen, Ph.D. thesis, Institut für Umweltphysik, Heidelberg University, Germany, 1984.
- Dueñas, C., Fernández, M., Carretero, J., Liger, E., and Pérez, M.: Release of  $^{222}\text{Rn}$  from some soils, *Ann. Geophys.*, 15, 124–133, 1997.
- Eckhardt, K.: Messung des Radonflusses und seiner Abhängigkeit von der Bodenbeschaffenheit, Diplomarbeit, Institut für Umweltphysik, Heidelberg University, Germany, 1990.
- Grossi, C., Vargas, A., Camacho, A., López-Coto, I., Bolívar, J. P., Yu Xia, and Conen, F.: Inter-comparison of different direct and indirect methods to determine radon flux from soil, *Radiat. Meas.*, 46, 112-118, doi:10.1016/j.radmeas.2010.07.021, 2011.
- Grossi, C., Arnold, D., Adame, J. A. López-Coto, I., Bolivar, J. P., de la Morena, B.A. and Vargas, A.: Atmospheric  $^{222}\text{Rn}$  concentration and source term at El Arenosillo 100 m meteorological tower in Southwest Spain, *Radiat. Meas.*, 47, 149-162, doi: 10.1016/j.radmeas.2011.11.006, 2012.
- Hartmann, J. and Moosdorf, N.: The new global lithological map database GLiM: A representation of rock properties at the Earth surface, *Geochem. Geophys. Geosy.*, 13, Q12004, doi:10.1029/2012GC004370, 2012.
- Israel, H. and Horbert, M.: Tracing atmospheric eddy mass transfer by means of natural radioactivity, *J. Geophys. Res.*, 75, 3639-3649, 1970.
- Jutzi, S.: Verteilung der Boden-Radon Exhalation in Europa, Staatsexamensarbeit, Institut für Umweltphysik, Heidelberg University, Germany, 57pp., 2001.
- Kosmath, W.: Die Exhalation der Radiumemanation aus dem Erdboden und ihre Abhängigkeit von den meteorologischen Faktoren, *Gerlands Beiträge zur Geophysik*, 43, 258-279, 1935.
- López-Coto, J., Mas, J. L., and Bolivar, J. P.: A 40-year retrospective European radon flux inventory including climatological variability, *Atmos. Environ.*, 73, 22-33, doi: 10.1016/j.atmosenv.2013.02.043, 2013.
- Manohar, S. N., Meijer, H. A. J., Neubert, R. E. M., Kettner E., and Herber, M. A.: Radon flux measurements at atmospheric station Lutjewad – analysis of temporal trends and main drivers controlling the emissions, to be submitted.
- Miguez-Macho, G., Li, H., and Fan, Y.: Simulated Water Table and Soil Moisture Climatology Over North America, *Bull. Amer. Meteor. Soc.*, 89, 663-672, doi:10.1175/BAMS-89-5-663, 2008.
- Millington, R. J. and Quirk, J. P.: Transport in Porous media, Proceedings of the 7th International Congress of soil Science, Madison, Wisconsin, USA, 14-24 August 1960, 97-106, 1960.
- Moldrup, P., Kruse, C. W., Rolston, D. E., and Yamaguchi, T.: Modeling diffusion and reaction in soils: III. Predicting gas diffusivity from the Campbell soil-water retention model, *Soil Sci.*, 161, 366-375, 1996.

- Moldrup, P., Olesen, T., Yamaguchi, T., Schjønning, P., and Rolston, D. E.: Modeling diffusion and reaction in soils: IX. The Buckingham-Burdine-Campbell Equation for gas diffusivity in undisturbed soil, *Soil Sci.*, 164, 542-551, 1999.
- Pensko, J., Wardaszko, T., and Wochna M.: Natural atmospheric activity and its dependence of some geophysical factors, *Atompraxis*, 14, 255-358, 1968.
- Robertson, L. B.: Radon Emissions to the Atmosphere and their use as Atmospheric Tracers, Ph.D. thesis, University of Edinburgh, United Kingdom, 237 pp., 2004.
- Rogers, V.C. and Nielson, K. K.: Correlations for predicting air permeabilities and  $^{222}\text{Rn}$  diffusion coefficients of soils, *Health Phys.*, 61, 225-230, 1991.
- Salminen, R. (ed.): Geochemical Atlas of Europe. Part 1: Background Information, Methodology and Maps, Geological Survey of Finland, Espoo, Finland, 2005.
- Schell, S.:  $^{222}\text{Rn}$ -Profil-Messungen in Süd- und Ostdeutschland, Anwendung der Radon-Tracer-Methode zur Berechnung von  $\text{CO}_2$ - und  $\text{CH}_4$ -Flüssen, Diplomarbeit, Institut für Umweltphysik, Heidelberg University, Germany, 106 pp., 2004.
- Schmidt, M.: Messung und Bilanzierung anthropogener Treibhausgase in Deutschland, Ph.D. thesis, Heidelberg University, Germany, 112 pp., 1999.
- Schmithüsen, D.: Atmospheric and soil flux radon measurements in Heidelberg, Diplomarbeit, Institut für Umweltphysik, Heidelberg University, Germany, 66 pp. , 2012.
- Schüßler, W.: Effektive Parameter zur Bestimmung des Gasaustauschs zwischen Boden und Atmosphäre, Ph.D. thesis, Heidelberg University, Germany, 1996.
- Schwingshackl, C.: Experimental Validation of a Radon-222 Flux Map, Master Thesis, Institut für Umweltphysik, Heidelberg University, Germany, 100 pp., 2013.
- Servant, J.: Le radon et ses dérivés a vie courte dans la basse atmosphère, Ph.D. thesis, Université de Paris, France, 1964.
- Smyth, L. B.: On the supply of radium emanation from the soil to the atmosphere, *Philosophical Magazine Series 6*, 24, 632-637, doi:10.1080/14786441008637368, 1912.
- Szegvary, T., Leuenberger, M. C., and Conen, F.: Predicting terrestrial  $^{222}\text{Rn}$  flux using gamma dose rate as a proxy, *Atmos. Chem. Phys.*, 7, 2789–2795, doi:10.5194/acp-7-2789-2007, 2007.
- Szegvary, T., Conen, F., and Ciais, P.: European  $^{222}\text{Rn}$  inventory for applied atmospheric studies. *Atmos. Environ.*, 43, 1536-1539, doi:10.1016/j.atmosenv.2008.11.025, 2009.
- Zeilinger, P. R.: Über die Nachlieferung von Radium-Emanation aus dem Erdboden, *Terr. Magn. Atmos. Electr.*, 40, 281-294, doi:10.1029/TE040i003p00281, 1935.